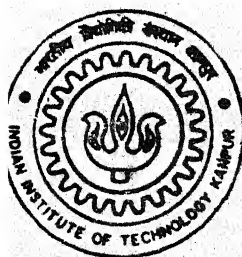


9810528

COMPUTER-AIDED DYNAMIC ANALYSIS OF FOUR-LINK MECHANISMS

by
RAVINDRA GARDAS



TH
ME/2000/M
G166c

DEPARTMENT OF MECHANICAL ENGINEERING
INDIAN INSTITUTE OF TECHNOLOGY KANPUR

January, 2000

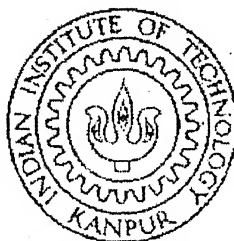
COMPUTER-AIDED DYNAMIC ANALYSIS OF FOUR-LINK MECHANISMS

028031

A Thesis Submitted
in partial Fulfillment of the Requirements
for the Degree of
Master of Technology

by

RAVINDRA GARDAS



to the

DEPARTMENT OF MECHANICAL ENGINEERING
INDIAN INSTITUTE OF TECHNOLOGY, KANPUR

January, 2000

15 MAY 2000 / ME
CENTRAL LIBRARY
I. I. T., KANPUR
A 130859

Th
ME / 2000 / M
G 166c

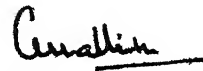


A130859

Dedicated
to
my mother.

CERTIFICATE

It is certified that the work contained in the thesis entitled, "**COMPUTER-AIDED DYNAMIC ANALYSIS OF FOUR-LINK MECHANISMS**", by **Ravindra Gardas**, has been carried out under my supervision and this work has not been submitted elsewhere for a degree.



Dr. A. K. Mallik

Professor

Department of Mechanical Engineering

Indian Institute of Technology, Kanpur.

Jan, 2000

Acknowledgments

I owe a deep debt of gratitude, respect and love to Mallik Sir, whose guidance and encouragement made me accomplish this work successfully. He is more than a Professor to me-He is a Teacher who taught me to understand knowledge in its correct perspective. I enjoyed the care and affection he showered on me. I learnt many things from him – Dynamics of Multibody System, Mechanisms and a positive attitude towards life. I pray to God for his health and hope for a continuing relationship with him.

I would like to thank Mr. Sachin Rasane, Milind Joshi, Anand Joshi, Ujwal Joshi and Girish Deshmukh helped me whenever I got stuck in the programming. I thank Amod, Ashish, Yogesh, Swapnil, Santosh, Vinayak, Sanjay and whole Ghati Mandal for their affection towards me. Deep thanks goes to Tularam without whose great help I would never have been able to write my report.

I wish to express my unbounded love for my mother and wife Rekha.

Ravindra Gardas

Abstract

Many software packages are available for design of mechanisms. Using computers, a designer can solve complex and practical problems rapidly and at the same time also test a vast spectrum of alternatives.

The main objective of the present thesis is to develop a software package for solving the problems on kinematic analysis, dynamic force analysis, dynamic motion analysis without friction and with friction of 4R, 3R-1P and 2R-2P mechanisms and balancing of 4R mechanism. The software informs the user the kind of problem it can handle, asks for input data, obtains the solution of the given problem. Computer programs have been developed using 'C' language.

List of Figures

Fig. No.	Description	Page
4R Mechanism		
2.2.1	Kinematic Analysis of a mechanism	5
2.3.1	Dynamic Force Analysis of a mechanism	7
2.3.2	Free-body diagram of the Crank for Force analysis	8
2.3.3	Diagram of the Crank for Acceleration analysis	9
2.3.4	Free-body diagram of the Coupler for Force analysis	10
2.3.5	Diagram of the Coupler for Acceleration analysis	11
2.3.6	Free-body diagram of the Follower for Force analysis	12
2.3.7	Diagram of the Follower for Acceleration analysis	13
2.4.1	Dynamic Motion Analysis of a mechanism without friction	17
2.4.2	Velocity diagram of a mechanism	19
2.4.3	Auxiliary Acceleration diagram of a mechanism	20
2.5.1	Balancing of a mechanism	22
2.5.2	Force balanced of a mechanism	24
2.5.3	Force and Moment balanced of a mechanism	26
2.6.1	Displacements of the Coupler and Follower Vs Crank Angle	29
2.6.2	Velocities of the Coupler and Follower Vs Crank Angle	29
2.6.3	Accelerations of the Coupler and Follower Vs Crank Angle	30
2.6.4	Required Turning Moment at the Crank Vs Crank Angle	32
2.6.5	Reaction at the hinge O_2 Vs Crank Angle	32
2.6.6	Reaction at the hinge A Vs Crank Angle	33
2.6.7	Reaction at the hinge B Vs Crank Angle	33
2.6.8	Reaction at the hinge O_4 Vs Crank Angle	34

2.6.9	Acceleration of the Crank Vs Crank Angle	36
2.6.10	Acceleration of the Coupler Vs Crank Angle	36
2.6.11	Acceleration of the follower Vs Crank Angle	37
2.6.12	Shaking Moment Vs Crank Angle	39
2.6.13	Required Turning Moment at the Crank after balancing Vs Crank Angle	39

3R-1P Mechanism

3.2.1	Kinematic Analysis of a mechanism	41
3.3.1	Dynamic Force Analysis of a mechanism	43
3.3.2	Free-body diagram of the Crank for Force analysis	44
3.3.3	Diagram of the Crank for Acceleration analysis	45
3.3.4	Free-body diagram of the Coupler for Force analysis	46
3.3.5	Diagram of the Coupler for Acceleration analysis	47
3.3.6	Free-body diagram of the Slider for Force analysis	48
3.4.1	Dynamic Motion Analysis of mechanism without friction	51
3.4.2	Velocity diagram of a mechanism	53
3.4.3	Auxiliary Acceleration diagram of a mechanism	54
3.4.4	Dynamic Motion Analysis of a mechanism with friction	56
3.4.5	Acceleration of the Crank Vs Power input of the system	58
3.5.1	Displacement of the Slider Vs Crank Angle	60
3.5.2	Displacement of the Coupler Vs Crank Angle	60
3.5.3	Velocities of the Slider and Coupler Vs Crank Angle	61
3.5.4	Accelerations of the Slider and Coupler Vs Crank Angle	61
3.5.5	Required Turning Moment at the Crank Vs Crank Angle	63
3.5.6	Reaction at the hinge O ₂ Vs Crank Angle	63
3.5.7	Reaction at the hinge A Vs Crank Angle	64
3.5.8	Reaction at the hinge B Vs Crank Angle	64
3.5.9	Acceleration of the Crank Vs Crank Angle	66
3.5.10	Acceleration of the Coupler Vs Crank Angle	66

3.5.11	Acceleration of the follower Vs Crank Angle	67
3.5.12	Acceleration of the Crank Vs Crank Angle	69
3.5.13	Acceleration of the Coupler Vs Crank Angle	69
3.5.14	Acceleration of the follower Vs Crank Angle	70

2R-2P Mechanism

4.2.1.1	Kinematic Analysis of a generalised 2r-2P mechanism	72
4.2.2.1	Kinematic Analysis of a Scotch-Yoke mechanism	74
4.3.1.1	Dynamic Force Analysis of a generalised 2r-2P mechanism	76
4.3.1.2	Free-body diagram of the Slider B for Force analysis	77
4.3.1.3	Free-body diagram of the Coupler for Force analysis	78
4.3.1.4	Diagram of the Coupler for Acceleration analysis	79
4.3.1.5	Free-body diagram of the Slider A for Force analysis	80
4.3.2.1	Dynamic Force Analysis of a Scotch-Yoke mechanism	83
4.3.2.2	Free-body diagram of the Crank for Force analysis	84
4.3.2.3	Diagram of the Crank for Acceleration analysis	85
4.3.2.4	Free-body diagram of the Slider for Force analysis	86
4.3.2.5	Free-body diagram of the Yoke for Force analysis	87
4.4.1	Dynamic Motion Analysis of a generalised 2r-2P mechanism without friction	90
4.4.2	Velocity diagram of a mechanism	92
4.4.3	Auxiliary Acceleration diagram of a mechanism	93
4.4.4	Dynamic Motion Analysis of a generalised 2r-2P mechanism with friction	95
4.4.5	Acceleration of the Slider B Vs Power input of the system	97
4.5.1	Velocity of the Coupler Vs Displacement of the Slider B	99
4.5.2	Velocity of the Slider A Vs Displacement of the Slider B	99
4.5.3	Acceleration of the Coupler Vs Displacement of the Slider B	100
4.5.4	Acceleration of the Slider A Vs Displacement of the Slider B	100
4.5.5	Displacements of the Slider and Yoke Vs Crank Angle	102

4.5.6	Velocities of the Slider and Yoke Vs Crank Angle	102
4.5.7	Accelerations of the Slider and Yoke Vs Crank Angle	103
4.5.8	Reaction at the hinge B Vs Displacement of the Slider B	105
4.5.9	Reaction at the hinge A Vs Displacement of the Slider B	105
4.5.10	Required Turning Moment at the Crank Vs Crank Angle	107
4.5.11	Reaction at the hinge O ₂ Vs Crank Angle	107
4.5.12	Reaction at the hinge A Vs Crank Angle	108
4.5.13	Acceleration of the Slider B Vs Displacement of the Slider B	110
4.5.14	Acceleration of the Coupler Vs Displacement of the Slider B	110
4.5.15	Acceleration of the Slider A Vs Displacement of the Slider B	111
4.5.16	Acceleration of the Slider B Vs Displacement of the Slider B	113
4.5.17	Acceleration of the Coupler Vs Displacement of the Slider B	113
4.5.18	Acceleration of the Slider A Vs Displacement of the Slider B	114

Contents

Certificate	i
Acknowledgments	ii
Abstract	iii
List of Figures	iv
1 Introduction	1
1.1 Introduction	1
1.2 Objectives and Scope of the present work	2
2 4R Mechanism	4
2.1 Introduction	4
2.2 Kinematic Analysis	5
2.3 Dynamic Force Analysis	7
2.4 Dynamic Motion Analysis without friction	17
2.5 Balancing	22
2.6 Numerical Examples and Results	28
3 3R-1P Mechanism	40
3.1 Introduction	40
3.2 Kinematic Analysis	40
3.3 Dynamic Force Analysis	43
3.4 Dynamic Motion Analysis	51
a) without friction	51
b) with friction	56
3.5 Numerical Examples and Results	59

4 2R-2P Mechanism	71
4.1 Introduction	71
4.2 Kinematic Analysis	72
1) A generalised 2R-2P mechanism	72
2) A Scotch-Yoke mechanism	74
4.3 Dynamic Force Analysis	76
1) A generalised 2R-2P mechanism	76
2) A Scotch-Yoke mechanism	83
4.4 Dynamic Motion Analysis of a generalised 2R-2P mechanism	90
a) without friction	90
b) with friction	95
4.5 Numerical Examples and Results	98
 5 Conclusion and Suggestions for Future Work	 115
5.1 Conclusion	115
5.2 Suggestions for Future Work	115

Bibliography

Chapter 1

Introduction

1.1 Introduction

Mechanisms have been and continue to be the basis of all machines. Simple machines, used since ancient times, are generally operated by either human or animal power. Some examples are a lever, a windlass, a screw, a wedge, and a pulley, and these are usually used to move large weights for building structures, for transporting water over small heights in irrigation systems or for military purposes in the throwing machines to toss projectiles of different kinds [1].

The study of mechanism involves their analysis as well as synthesis. Analysis is the study of motions and forces concerning different parts of an existing mechanism while synthesis involves the design of the different parts. In a mechanism, the various parts are so proportioned and related that the motion of one imparts requisite motions to the others and the parts are able to withstand the forces impressed upon them.

Analysis of mechanism involves kinematic and dynamic analysis. Kinematic analysis of a mechanism includes the determination of the position of all its driven members, the determination of linear and angular velocities and accelerations of these members as well as the investigation of motion of important points of this mechanism. Dynamic analysis of a mechanism includes force analysis and motion analysis. In dynamic force analysis, the motions of the driving members are given and our task is to determine the reaction forces in all kinematic pairs and the driving turning moment, whereas, in dynamic motion analysis, the acceleration behaviour of each member of a mechanism is to be determined for the prescribed input force and moment and instantaneous velocities.

Dynamic forces are associated with accelerating masses. As all machines have some accelerating parts, dynamic forces are always present when the machine is in operation. In situations where dynamic forces are dominant or comparable with magnitudes of external forces and operating speeds are high, dynamic analysis has to be carried out. The dynamic analysis of mechanisms is of fundamental importance for the design of large variety of mechanical systems used widely in industrial society: textile machinery, printing machineries, agricultural and public works machinery, suspensions etc. The analysis makes it possible to determine input forces, reactions in the pairs, tensions in the links, and also the temporal evolution of the position of the machine in function of the applied forces and the inertial characteristics of its links.

The 1950s saw the introduction of digital computers. The advent of computers in the field of engineering revolutionized the mechanism design. The speed and computational capabilities of computers rendered complex design calculations feasible and economical. One of the early contributions which used the computer for linkage synthesis and analysis was that of Freudenstein and Sandor. The graphical-based techniques suggested by Burmester in 1876 were reformulated for computer solution. This work formed the technical basis for the KINSYN and LINCAGES codes, which emerged in the 1970s.

The early 1970s saw a spurt in applications of the computer. Codes such as IMP, developed by Sheth and J. Uicker at the University of Wisconsin, and DRAM and ADAMS, developed at the University of Michigan by D. Smith, N. Orlandea and M. Chace, had early roots in this decade [2].

During the last 30 years, many packages have been developed for mechanism design. Commercially available packages for analysis and synthesis of mechanisms are IMP-UM, MCADA, DADS, MEDUSA, VECNET, DYMACE and many others.

1.2 Objectives and Scope of the Present Work

The objective of this work is to develop a computer software, which can solve the problems on kinematic analysis, dynamic force and motion analysis of 4R, 3R-1P, 2R-2P mechanisms and balancing of 4R mechanism.

In chapter 2, a 4R mechanism is considered. The kinematic analysis, dynamic force analysis, dynamic motion analysis without friction and balancing of this mechanism are discussed. Numerical example and results are given at the end of the chapter.

In chapter 3, a 3R-1P mechanism is considered. The kinematic analysis, dynamic force analysis, dynamic motion analysis without friction and with friction of this mechanism are discussed. Numerical example and results are included at the end of the chapter.

In chapter 4, a 2R-2P mechanism is considered. The kinematic analysis and dynamic force analysis of a generalised 2R-2P mechanism and Scotch-Yoke mechanism, dynamic motion analysis without friction and with friction of a generalised 2R-2P mechanism are discussed. Numerical example and results are also given at the end of the chapter.

The main conclusion of the present work is summarized in chapter 5. Some directions for future work are also mentioned therein.

To meet the computational requirements, 'C' language on Unix platform was selected as the programming language.

The development of the package and hence the thesis has been done with the aim that the computer should accept performance specifications of the linkage in the user's terms. The package should be useful in both academic institutions and industry. This package will supplement an earlier package developed at I. I. T. Kanpur for kinematic synthesis of planar four and six-link mechanisms.

Chapter 2

4R Mechanism

2.1 Introduction

A 4R mechanism is the most fundamental of the plane kinematic linkages. It is a much preferred mechanical device for the mechanization and control of motion due to its simplicity and versatility. Basically it consists of four rigid links which are connected in the form of a quadrilateral by four pin-joints. A link that makes complete revolutions is the crank, the link opposite to the fixed link is the coupler and the fourth link a lever or rocker if oscillates or an another crank, if rotates[3].

The crank-rocker mechanism, with properly adjusted links, is used as part of the feed mechanism of shaping machines; the double-crank mechanism, with opposite links equal in length, appears in rope-making machinery and is also used in the coupling of locomotive wheels; and the double-rocker mechanism, with equal rockers, is employed in the steering linkage of automobiles [4].

In this chapter we are going to discuss the dynamic force and motion analysis of 4R mechanism and force and shaking moment balancing. In *dynamic force analysis* we calculate the forces on various members of a mechanism for a known input motion which is usually determined by experimentation or analytical prediction based on *kinematic analysis* whereas for *dynamic motion analysis* we calculate the accelerations of various links of a mechanism for a given forces on the mechanism [5]. In balancing we calculate the counterweights for force balance and moment of inertia of counterweight for shaking moment balance [6].

2.2 Kinematic Analysis

A 4R mechanism for *kinematic analysis* is shown in fig 2.2.1. Link 2 (O_2A) is the input crank, link 3 (AB) is the coupler and link 4 (O_4B) is the follower [5].

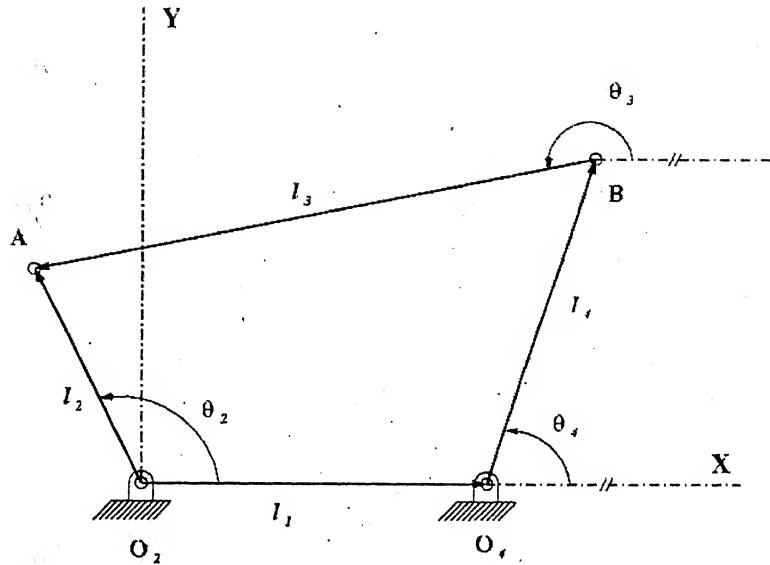


Figure 2.2.1 : Kinematic Analysis of a 4R Mechanism

Using the symbols explained in fig. 2.2.1,

The governing loop-closure equation is,

$$\vec{l}_1 + \vec{l}_4 + \vec{l}_3 = \vec{l}_2 \quad (2.2.1)$$

or $\vec{l}_1 + \vec{l}_4 + \vec{l}_3 - \vec{l}_2 = 0$

or $l_1 + l_4 e^{i\theta_4} + l_3 e^{i\theta_3} - l_2 e^{i\theta_2} = 0$.

Equating the real and imaginary parts of the above equation separately to zero, we get,

$$l_1 + l_4 \cos\theta_4 + l_3 \cos\theta_3 - l_2 \cos\theta_2 = 0$$

and $l_4 \sin\theta_4 + l_3 \sin\theta_3 - l_2 \sin\theta_2 = 0$.

From the above equations, we get,

$$\theta_4 = 2 \tan^{-1} \left(\frac{a \pm \sqrt{a^2 + b^2 - c^2}}{b + c} \right) \quad (2.2.1)$$

$$\text{and } \theta_3 = 2 \tan^{-1} \left(\frac{a \mp \sqrt{a^2 + b^2 - c'^2}}{b + c'} \right). \quad (2.2.2)$$

where,

$$a = \sin \theta_2, b = \cos \theta_2 - \frac{l_1}{l_2}$$

$$c = -\left(\frac{l_1}{l_4}\right) \cos \theta_2 + \left(\frac{l_1^2 + l_2^2 + l_4^2 - l_3^2}{2l_2 l_4}\right)$$

$$\text{and } c' = -\left(\frac{l_1}{l_3}\right) \cos \theta_2 + \left(\frac{l_1^2 + l_2^2 + l_3^2 - l_4^2}{2l_2 l_3}\right).$$

Differentiating equations (2.2.2) and (2.2.3) w. r. t. time, we get,

$$\dot{\theta}_4 = \frac{l_2 \sin(\theta_2 - \theta_3)}{l_4 \sin(\theta_4 - \theta_3)} \dot{\theta}_2 \quad (2.2.3)$$

$$\text{and } \dot{\theta}_3 = \frac{l_2 \sin(\theta_2 - \theta_4)}{l_3 \sin(\theta_3 - \theta_4)} \dot{\theta}_2 \quad (2.2.4)$$

Again differentiating equations (2.2.4) and (2.2.5) w. r. t. time, we get,

$$\ddot{\theta}_4 = \frac{l_2 \ddot{\theta}_2 \sin(\theta_2 - \theta_3) + l_2 \dot{\theta}_2^2 \cos(\theta_2 - \theta_3) - l_3 \dot{\theta}_3^2 - l_4 \dot{\theta}_4^2 \cos(\theta_4 - \theta_3)}{l_4 \sin(\theta_4 - \theta_3)} \quad (2.2.5)$$

$$\text{and } \ddot{\theta}_3 = \frac{l_2 \ddot{\theta}_2 \sin(\theta_2 - \theta_4) + l_2 \dot{\theta}_2^2 \cos(\theta_2 - \theta_4) - l_4 \dot{\theta}_4^2 - l_3 \dot{\theta}_3^2 \cos(\theta_3 - \theta_4)}{l_3 \sin(\theta_3 - \theta_4)} \quad (2.2.6)$$

2.3 Dynamic Force Analysis

In *dynamic force analysis*, the motion is usually known either by experimentation or analytical predictions based on *kinematic analysis*, the driving torque and the reactions in various hinges i.e., M_2 and $P_{O_2}, P_A, P_B, P_{O_4}$ are to be determined. Figure 2.3.1 shows a 4R mechanism [5]. The kinematic pairs are assumed to be frictionless.

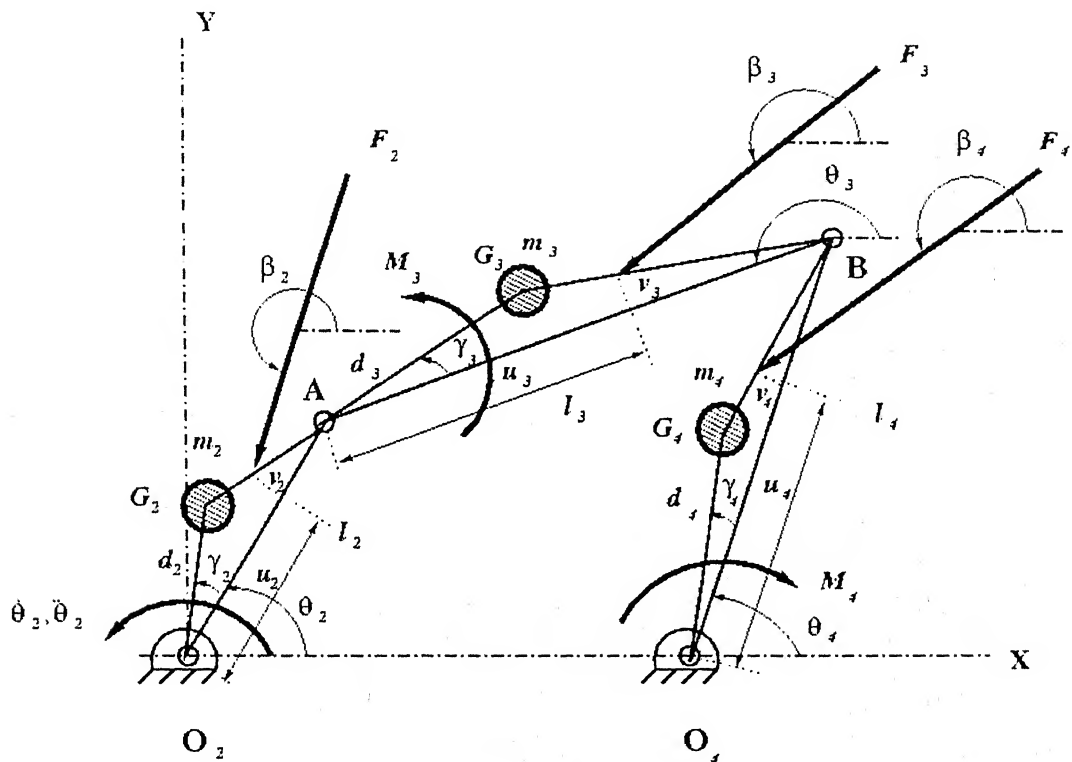


Figure 2.3.1 : Dynamic Force Analysis of a 4R Mechanism

In fig.2.3.1,

m_j = mass of the j -th link where $j = 2, 3, 4$.

G_j = location of the C.G. of the j -th link.

d_j = distance of G_j from a kinematic pair as indicated in fig. 2.3.1.

F_j = external force acting on the j -th link at an angle of β_j to the X -axis at a point with local coordination (u_j, v_j) .

$F_{j,x}$ = X -component of F_j .

$F_{j,y}$ = Y-component of F_j

M_j = external moment on j -th link.

$P_{K,x}$ = force exerted at the hinge K in the x -direction where $K = B, A$

$P_{K,y}$ = force exerted at the hinge K in the y -direction.

k_j = centroidal radius of gyration of the j -th link.

$P_{ij,x}$ = force exerted on the j -th link by the i -th link in the x -direction where

$i = 1, 2, 3, 4$.

$P_{ij,y}$ = force exerted on the j -th link by the i -th link in the y -direction.

The dynamic equations for each link can be obtained as discussed below :-

1. Crank:-

Refer to fig.2.3.2 as the free-body-diagram of the crank,

with $i = 1, 3$, $j = 2$, $K = O_2$, A.

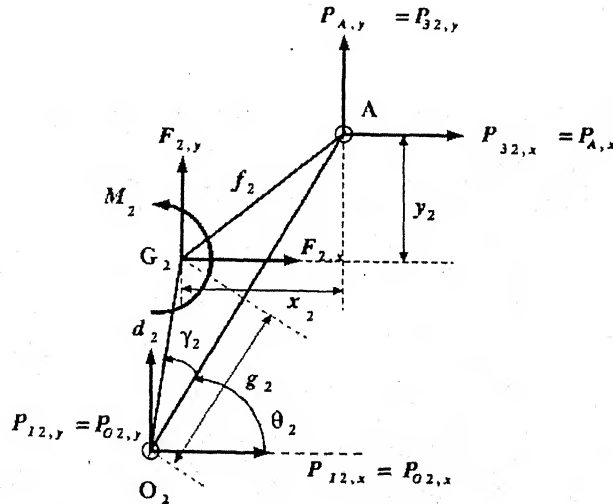


Figure 2.3.2 : Free-Body-Diagram of the Crank for Force Analysis.

From fig. 2.3.2,

$$x_2 = d_2 \sin \gamma_2 \sin \theta_2 + (l_2 - g_2) \cos \theta_2$$

and
$$y_2 = (l_2 - g_2) \sin \theta_2 - d_2 \sin \gamma_2 \cos \theta_2 .$$

Equations of motion for the crank are,

$$\begin{Bmatrix} F_{2,x} \\ F_{2,y} \\ M_2 \end{Bmatrix} + \begin{bmatrix} 1 & 0 & 1 & 0 \\ 0 & 1 & 0 & 1 \\ d_2 \sin(\theta_2 + \gamma_2) & -d_2 \cos(\theta_2 + \gamma_2) & -y_2 & x_2 \end{bmatrix} \begin{Bmatrix} P_{o2,x} \\ P_{o2,y} \\ P_{A,x} \\ P_{A,y} \end{Bmatrix} = m_2 \begin{Bmatrix} a_{G2,x} \\ a_{G2,y} \\ \ddot{\theta}_2 k_2^2 \end{Bmatrix} \quad (2.3.1)$$

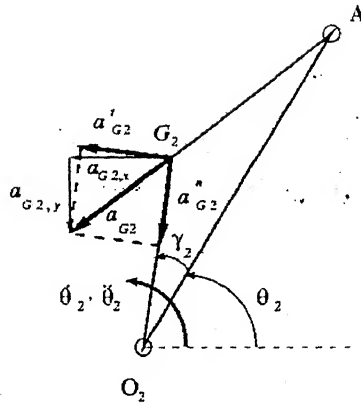


Figure 2.3.3 : Diagram of the Crank for Acceleration Analysis

Various components of acceleration of G_2 are explained in fig. 2.3.3 and the superscripts n, t refer to normal and tangential components, respectively.

From fig. 2.3.3,

$$a_{G2,x} = a_{G2}^n \cos(\theta_2 + \gamma_2) + a_{G2}^t \sin(\theta_2 + \gamma_2) \quad (2.3.2)$$

$$\text{and } a_{G2,y} = a_{G2}^n \sin(\theta_2 + \gamma_2) - a_{G2}^t \cos(\theta_2 + \gamma_2) \quad (2.3.3)$$

where $a_{G2}^n = d_2 \dot{\theta}_2^2$, $a_{G2}^t = d_2 \ddot{\theta}_2$.

Using equations (2.3.2) and (2.3.3), the right hand side of equation (2.3.1) turns out as,

$$m_2 \begin{Bmatrix} a_{G2,x} \\ a_{G2,y} \\ \ddot{\theta}_2 k_2^2 \end{Bmatrix} = m_2 \begin{Bmatrix} d_2 \ddot{\theta}_2^2 \cos(\theta_2 + \gamma_2) \\ d_2 \ddot{\theta}_2^2 \sin(\theta_2 + \gamma_2) \\ 0 \end{Bmatrix} + m_2 \begin{bmatrix} d_2 \sin(\theta_2 + \gamma_2) & 0 & 0 \\ -d_2 \cos(\theta_2 + \gamma_2) & 0 & 0 \\ k_2^2 & 0 & 0 \end{bmatrix} \begin{Bmatrix} \ddot{\theta}_2 \\ \ddot{\theta}_3 \\ \ddot{\theta}_4 \end{Bmatrix} \quad (2.3.4)$$

2. Coupler:-

Refer to fig.2.3.4 as the free-body-diagram of the coupler,

with $j = 3$, $K = A, B$.

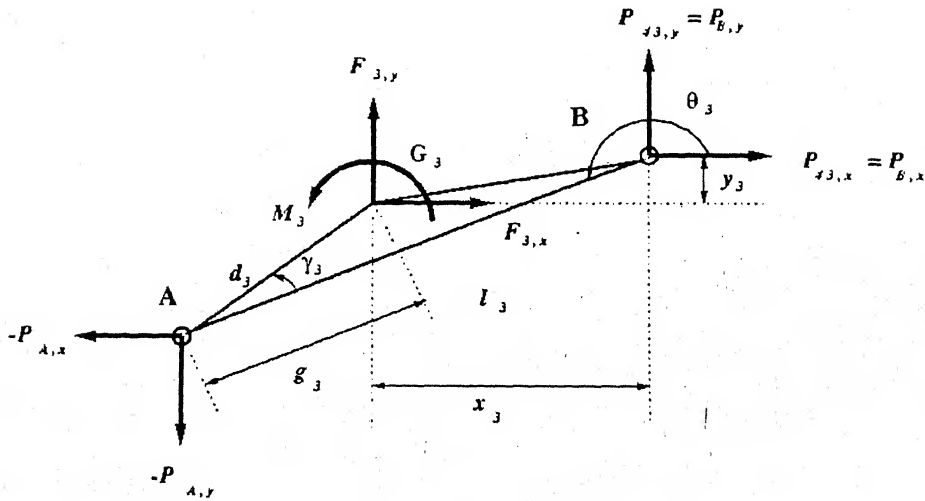


Figure 2.3.4 : Free-Body-Diagram of the Coupler for Force Analysis.

From the fig 2.3.4,

$$x_3 = d_3 \sin \gamma_3 \sin(\theta_3 - \pi) + (l_3 - g_3) \cos(\theta_3 - \pi)$$

and $y_3 = (l_3 - g_3) \sin(\theta_3 - \pi) - d_3 \sin \gamma_3 \cos(\theta_3 - \pi).$

Equations of motion for the coupler are,

$$\begin{Bmatrix} F_{3,x} \\ F_{3,y} \\ M_3 \end{Bmatrix} + \begin{bmatrix} -1 & 0 & 1 & 0 \\ 0 & -1 & 0 & 1 \\ -d_3 \sin(\theta_3 + \gamma_3 - \pi) & d_3 \cos(\theta_3 + \gamma_3 - \pi) & -y_3 & x_3 \end{bmatrix} \begin{Bmatrix} P_{1,x} \\ P_{1,y} \\ P_{B,x} \\ P_{B,y} \end{Bmatrix} = m_3 \begin{Bmatrix} a_{G3,x} \\ a_{G3,y} \\ \dot{\theta}_3 k_3^2 \end{Bmatrix} \quad (2.3.1)$$

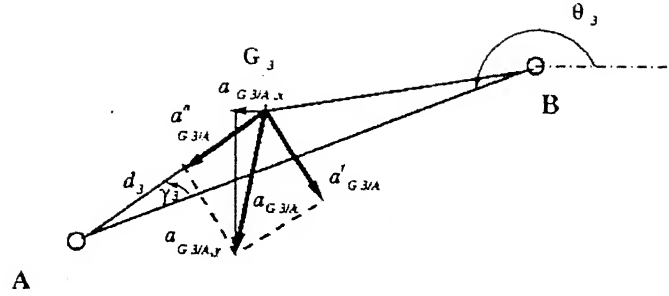


Figure 2.3.5 : Diagram of the Coupler for Acceleration Analysis

Various components of acceleration of G_3 are explained in fig. 2.3.5 and the superscripts n, t refer to normal and tangential components, respectively.

From the fig. 2.3.5,

$$a_{G3,x} = a_{A,x} + a_{G3/A,x} \quad (2.3.2)$$

$$\text{and } a_{G3,y} = a_{A,y} + a_{G3/A,y} \quad (2.3.3)$$

$$\text{where, } a_{A,x} = l_2 \dot{\theta}_2^2 \cos(\theta_2 + \gamma_2) + l_2 \ddot{\theta}_2 \sin(\theta_2 + \gamma_2)$$

$$\text{and } a_{A,y} = l_2 \dot{\theta}_2^2 \sin(\theta_2 + \gamma_2) - l_2 \ddot{\theta}_2 \cos(\theta_2 + \gamma_2).$$

$$a_{G3/A,x} = a_{G3/A}^n \cos(\theta_3 + \gamma_3 - \pi) - a_{G3/A}^t \sin(\theta_3 + \gamma_3 - \pi)$$

$$\text{and } a_{G3/A,y} = a_{G3/A}^n \sin(\theta_3 + \gamma_3 - \pi) + a_{G3/A}^t \cos(\theta_3 + \gamma_3 - \pi).$$

$$a_{G3+A}^n = d_3 \dot{\theta}_3^2 \quad , \quad a_{G3+A}^t = -d_3 \ddot{\theta}_3 \quad .$$

Using equations (2.3.6) and (2.3.7), the right hand side of equation (2.3.5) turns out as,

$$m_3 \begin{Bmatrix} a_{G3,\lambda} \\ a_{G3,\nu} \\ \ddot{\theta}_3 k_3^2 \end{Bmatrix} = m_3 \begin{Bmatrix} l_2 \ddot{\theta}_2^2 \cos(\theta_2 + \gamma_2) + d_3 \ddot{\theta}_3^2 \cos(\theta_3 + \gamma_3 - \pi) \\ l_2 \ddot{\theta}_2^2 \sin(\theta_2 + \gamma_2) - d_3 \ddot{\theta}_3^2 \sin(\theta_3 + \gamma_3 - \pi) \\ 0 \end{Bmatrix} + m_3 \begin{bmatrix} l_2 \sin(\theta_2 + \gamma_2) & -d_3 \sin(\theta_3 + \gamma_3 - \pi) & 0 \\ -l_2 \cos(\theta_2 + \gamma_2) & -d_3 \cos(\theta_3 + \gamma_3 - \pi) & 0 \\ 0 & k_3^2 & 0 \end{bmatrix} \begin{Bmatrix} \ddot{\theta}_2 \\ \ddot{\theta}_3 \\ \ddot{\theta}_4 \end{Bmatrix} \quad (2.3.1)$$

1. Follower: -

Refer to fig.2.3.6 as the free-body-diagram of the follower,

with $j = 4$, $K = O_4$, B.

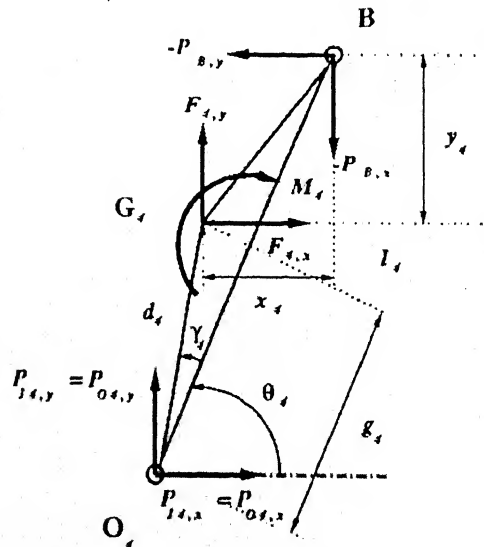


Figure 2.3.1 : Free-Body-Diagram of the Follower for Force Analysis.

From fig. 2.3.6,

$$x_4 = d_4 \sin \gamma_4 \sin \theta_4 + (l_4 - g_4) \cos \theta_4$$

$$\text{and } y_4 = (l_4 - g_4) \sin \theta_4 - d_4 \sin \gamma_4 \cos \theta_4.$$

Equations of motion for the follower are,

$$\begin{Bmatrix} F_{4,x} \\ F_{4,y} \\ M_4 \end{Bmatrix} + \begin{bmatrix} -1 & 0 & 1 & 0 \\ 0 & -1 & 0 & 1 \\ -y_4 & x_4 & -d_4 \sin(\theta_4 + \gamma_4) & d_4 \cos(\theta_4 + \gamma_4) \end{bmatrix} \begin{Bmatrix} P_{B,x} \\ P_{B,y} \\ P_{O_4,x} \\ P_{O_4,y} \end{Bmatrix} = m_4 \begin{Bmatrix} a_{G_4,x} \\ a_{G_4,y} \\ \ddot{\theta}_4 k_4^2 \end{Bmatrix} \quad (2.3.1)$$

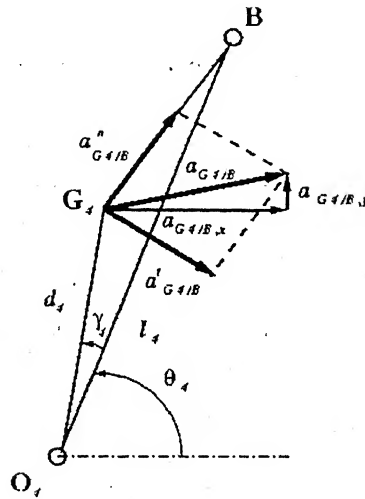


Figure 2.3.7 : Diagram of the Follower for Acceleration Analysis

Various components of acceleration of G_4 are explained in fig. 2.3.7 and the superscripts n, t refer to normal and tangential components, respectively.

From the fig. 2.3.7,

$$a_{G_4,x} = a_{B,x} + a_{G_4/B,x} \quad (2.3.2)$$

$$\text{and } a_{G_4,y} = a_{B,y} + a_{G_4/B,y} \quad (2.3.3)$$

where,

$$a_{B,x} = l_2 \dot{\theta}_2^2 \cos(\theta_2 + \gamma_2) + l_2 \ddot{\theta}_2 \sin(\theta_2 + \gamma_2) + l_3 \dot{\theta}_3^2 \cos(\theta_3 + \gamma_3 - \pi) + l_3 \ddot{\theta}_3 \sin(\theta_3 + \gamma_3 - \pi)$$

and $a_{A,y} = l_2 \dot{\theta}_2^2 \sin(\theta_2 + \gamma_2) - l_2 \ddot{\theta}_2 \cos(\theta_2 + \gamma_2) - l_3 \dot{\theta}_3^2 \sin(\theta_3 + \gamma_3 - \pi) + l_3 \ddot{\theta}_3 \cos(\theta_3 + \gamma_3 - \pi)$

$$a_{G^4 B, x} = a_{G^4 B}'' \cos(\theta_4 + \gamma_4) + a_{G^4 B}' \sin(\theta_4 + \gamma_4)$$

and $a_{G^4 B, y} = a_{G^4 B}'' \sin(\theta_4 + \gamma_4) - a_{G^4 B}' \cos(\theta_4 + \gamma_4).$

$$a_{G^4 B}'' = f_4 \dot{\theta}_4^2, \quad a_{G^4 B}' = f_4 \ddot{\theta}_4.$$

Using equations (2.3.10) and (2.3.11), the right hand side of equation (2.3.9) turns out as,

$$m_4 \begin{Bmatrix} a_{G^4, x} \\ a_{G^4, y} \\ \ddot{\theta}_4 k_4^2 \end{Bmatrix} = m_4 \begin{Bmatrix} l_2 \dot{\theta}_2^2 \cos(\theta_2 + \gamma_2) + l_3 \dot{\theta}_3^2 \cos(\theta_3 + \gamma_3 - \pi) + f_4 \dot{\theta}_4^2 \cos(\theta_4 + \gamma_4) \\ l_2 \dot{\theta}_2^2 \sin(\theta_2 + \gamma_2) - l_3 \dot{\theta}_3^2 \sin(\theta_3 + \gamma_3 - \pi) + f_4 \dot{\theta}_4^2 \sin(\theta_4 + \gamma_4) \\ 0 \end{Bmatrix} + m_4 \begin{bmatrix} l_2 \sin(\theta_2 + \gamma_2) & l_3 \sin(\theta_3 + \gamma_3 - \pi) & f_4 \sin(\theta_4 + \gamma_4) \\ -l_2 \cos(\theta_2 + \gamma_2) & l_3 \cos(\theta_3 + \gamma_3 - \pi) & -f_4 \cos(\theta_4 + \gamma_4) \\ 0 & k_3^2 & 0 \end{bmatrix} \begin{Bmatrix} \ddot{\theta}_2 \\ \ddot{\theta}_3 \\ \ddot{\theta}_4 \end{Bmatrix} \quad (2.3.12)$$

Combining all equations (2.3.1), (2.3.5) and (2.3.9) one can finally write,

$$\{F\} + [Q]\{P\} = \{H\} \quad (2.3.13)$$

where ,

$$\{F\} = \begin{Bmatrix} F_{2,x} \\ F_{2,y} \\ M_2 \\ F_{3,x} \\ F_{3,y} \\ M_3 \\ F_{4,x} \\ F_{4,y} \\ M_4 \end{Bmatrix}$$

$$[Q] = \begin{bmatrix} 1 & 0 & 1 & 0 & 0 & 0 & 0 & 0 \\ 0 & 1 & 0 & 1 & 0 & 0 & 0 & 0 \\ d_2 \sin(\theta_2 + \gamma_2) & -d_2 \cos(\theta_2 + \gamma_2) & -y_2 & x_2 & 0 & 0 & 0 & 0 \\ 0 & 0 & -1 & 0 & 1 & 0 & 0 & 0 \\ 0 & 0 & 0 & -1 & 0 & 1 & 0 & 0 \\ 0 & 0 & -d_1 \sin(\theta_1 + \gamma_1 - \pi) & d_1 \cos(\theta_1 + \gamma_1 - \pi) & -y_1 & x_1 & 0 & 0 \\ 0 & 0 & 0 & 0 & -1 & 0 & 1 & 0 \\ 0 & 0 & 0 & 0 & 0 & -1 & 0 & 1 \\ 0 & 0 & 0 & 0 & y_4 & -x_4 & d_4 \sin(\theta_4 + \gamma_4) & -d_4 \cos(\theta_4 + \gamma_4) \end{bmatrix}$$

$$\{P\} = \begin{Bmatrix} P_{O2,x} \\ P_{O2,y} \\ P_{A,x} \\ P_{A,y} \\ P_{B,x} \\ P_{B,y} \\ P_{O4,x} \\ P_{O4,y} \end{Bmatrix}$$

$$\{H\} = \begin{Bmatrix} m_2 \begin{Bmatrix} a_{G2,x} \\ a_{G2,y} \\ \ddot{\theta}_2 k_2^2 \end{Bmatrix} \\ m_3 \begin{Bmatrix} a_{G3,x} \\ a_{G3,y} \\ \ddot{\theta}_3 k_3^2 \end{Bmatrix} \\ m_4 \begin{Bmatrix} a_{G4,x} \\ a_{G4,y} \\ \ddot{\theta}_4 k_4^2 \end{Bmatrix} \end{Bmatrix}$$

But from equations (2.3.4), (2.3.8) and (2.3.12),

$$\{H\} = \{U\} + [\lambda]\{\ddot{\theta}\} \quad (2.3.14)$$

where,

$$\{U\} = \left\{ \begin{array}{c} m_2 \begin{bmatrix} d_2 \dot{\theta}_2^2 \cos(\theta_2 + \gamma_2) \\ d_2 \dot{\theta}_2^2 \sin(\theta_2 + \gamma_2) \\ 0 \end{bmatrix} \\ m_3 \begin{bmatrix} l_2 \dot{\theta}_2^2 \cos(\theta_2 + \gamma_2) + d_3 \dot{\theta}_3^2 \cos(\theta_3 + \gamma_3 - \pi) \\ l_2 \dot{\theta}_2^2 \sin(\theta_2 + \gamma_2) - d_3 \dot{\theta}_3^2 \sin(\theta_3 + \gamma_3 - \pi) \\ 0 \end{bmatrix} \\ m_4 \begin{bmatrix} l_2 \dot{\theta}_2^2 \cos(\theta_2 + \gamma_2) + l_3 \dot{\theta}_3^2 \cos(\theta_3 + \gamma_3 - \pi) + f_4 \dot{\theta}_4^2 \cos(\theta_4 + \gamma_4) \\ l_2 \dot{\theta}_2^2 \sin(\theta_2 + \gamma_2) - l_3 \dot{\theta}_3^2 \sin(\theta_3 + \gamma_3 - \pi) + f_4 \dot{\theta}_4^2 \sin(\theta_4 + \gamma_4) \\ 0 \end{bmatrix} \end{array} \right\}$$

$$[\lambda] = \left[\begin{array}{ccc} m_2 \begin{bmatrix} d_2 \sin(\theta_2 + \gamma_2) & 0 & 0 \\ -d_2 \cos(\theta_2 + \gamma_2) & 0 & 0 \\ k_2^2 & 0 & 0 \end{bmatrix} & & \\ m_3 \begin{bmatrix} l_2 \sin(\theta_2 + \gamma_2) & d_3 \sin(\theta_3 + \gamma_3 - \pi) & 0 \\ -l_2 \cos(\theta_2 + \gamma_2) & d_3 \cos(\theta_3 + \gamma_3 - \pi) & 0 \\ 0 & k_3^2 & 0 \end{bmatrix} & & \\ m_4 \begin{bmatrix} l_2 \sin(\theta_2 + \gamma_2) & l_3 \sin(\theta_3 + \gamma_3 - \pi) & f_4 \sin(\theta_4 + \gamma_4) \\ -l_2 \cos(\theta_2 + \gamma_2) & l_3 \cos(\theta_3 + \gamma_3 - \pi) & -f_4 \cos(\theta_4 + \gamma_4) \\ 0 & 0 & k_4^2 \end{bmatrix} & & \end{array} \right]$$

$$\{\ddot{\theta}\} = \begin{Bmatrix} \ddot{\theta}_2 \\ \ddot{\theta}_3 \\ \ddot{\theta}_4 \end{Bmatrix}$$

From equation (2.3.13) we can evaluate the driving torque and the hinge reactions i.e., M_2 and P_{O2} , P_A , P_B , P_{O4} for the given motion and external forces.

2.4 Dynamic Motion Analysis

In *dynamic motion analysis*, the acceleration behaviour of each member of a mechanism is to be determined for prescribed input force and moment and instantaneous velocity [5]. The *Rate-of-change-of-energy Method* is used for the motion analysis. It is based directly on the instantaneous energy balance [7]. Figure 2.4.1 shows a 4R mechanism. The kinematic pairs are assumed to be frictionless.

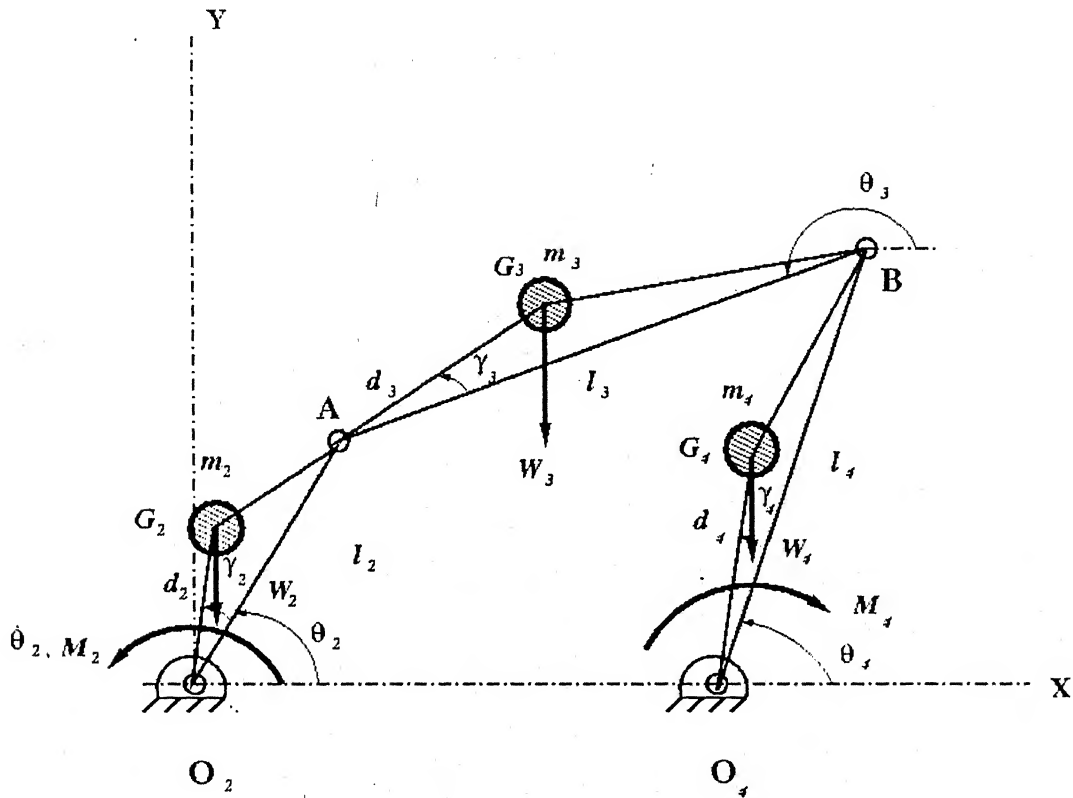


Figure 2.4.1 : Dynamic Motion Analysis of a 4R Mechanism.

In fig.2.4.1,

m_j = mass of the j -th link where $j = 2,3,4$.

G_j = location of the C.G. of the j -th link.

d_j = distance of G_j from a kinematic pair as indicated in fig. 2.4.1.

M_j = external moment on j -th link

W_j = weight of the j -th link.

k_j = centroidal radius of gyration of the j -th link.

The total K.E. of a mechanism can be expressed as,

$$T = \frac{1}{2} \sum^r J_o \omega^2 + \frac{1}{2} \sum^s m V^2 + \frac{1}{2} \sum^f m V_G^2 + \frac{1}{2} \sum^f J_G \omega^2 . \quad (2.4.1)$$

where, r , s , and f refer to rotating, sliding, and floating links; J_o is the moment of inertia of a rotating link about an axis passing through the hinge; V_G the velocity of the C.G. of a floating link; and J_G the moment of inertia of the floating link about the axis passing through the C.G [5].

The time rate of change of the total kinetic energy of the mechanism is equal to the power input of the force system acting on it [7].

It is expressed mathematically by,

$$\sum \dot{P} = \frac{dT}{dt} = \sum^r J_o \omega \alpha + \sum^s m V_a + \sum^f m V_G (a_G)_t + \sum^f J_G \omega \alpha . \quad (2.4.2)$$

where, $(a_G)_t$ is the tangential component of the acceleration of G , i.e., the component of a_G in the direction of V_G

From Goodman transformation equations (J. Hirschhorn [7], pp.123) in the form applicable to mechanisms with a rotating input link,

$$\alpha_l = \alpha_{i''} + \frac{\omega_l}{\omega_i} \alpha_i \quad (2.4.3)$$

$$(a_G)_t = (a_{G''})_t + \frac{v_G}{\omega_i} \alpha_i \quad (2.4.4)$$

where, α_l = angular acceleration of the link l .

α_i = angular acceleration of the input link i .

$\alpha_{i''}$ = angular acceleration of the link l obtained from an auxiliary acceleration analysis based on actual velocities but with zero input accelerations.

ω_l = angular velocity of the link l .

ω_i = angular velocity of the input link i .

$(a_G)_t$ = component of acceleration a_G in the direction of v_G .

$(a_G)_{t'}$ = component of acceleration a_G in the direction of v_G from the auxiliary acceleration diagram.

The method of solution involves the construction of the velocity diagram and of the auxiliary acceleration diagram, based on the actual velocities and an arbitrarily assumed zero input acceleration.

The velocity diagram is constructed as shown in fig.2.4.2,

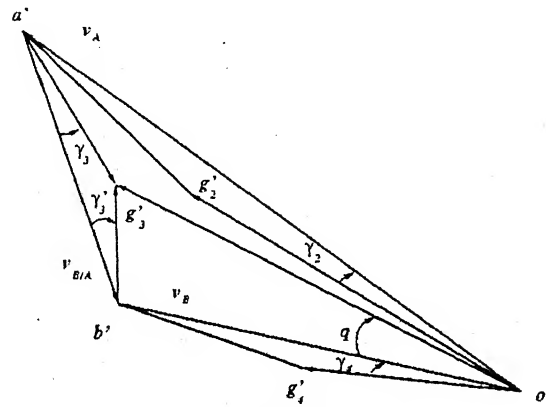


Figure 2.4. 2 : Velocity Diagram of a 4R Mechanism.

From equations (2.2.2), (2.2.3), (2.2.4) and (2.2.5),

$$\theta_4 = 2 \tan^{-1} \left(\frac{a \pm \sqrt{a^2 + b^2 - c^2}}{b + c} \right)$$

$$\theta_3 = 2 \tan^{-1} \left(\frac{a \mp \sqrt{a^2 + b^2 - c'^2}}{b + c'} \right)$$

$$\dot{\theta}_4 = \frac{l_2 \sin(\theta_2 - \theta_3)}{l_4 \sin(\theta_4 - \theta_3)} \dot{\theta}_2$$

and $\dot{\theta}_3 = \frac{l_2 \sin(\theta_2 - \theta_4)}{l_3 \sin(\theta_3 - \theta_4)} \dot{\theta}_2$

From fig. 2.4.2,

$$v_{G2} = \frac{v_A}{\cos \gamma_2} \left(\frac{g_2}{l_2} \right)$$

$$v_{G3} = \overline{o'g'_3} = \overline{o'h'} + \overline{h'g'_3}$$

$$\therefore v_{G3} = \sqrt{v_B^2 + (h'g'_3)^2 - 2v_B h'g'_3 \cos(\pi + \theta_3 - \theta_4 - \gamma'_3)}$$

The auxiliary acceleration diagram is constructed as shown in fig. 2.4.3,

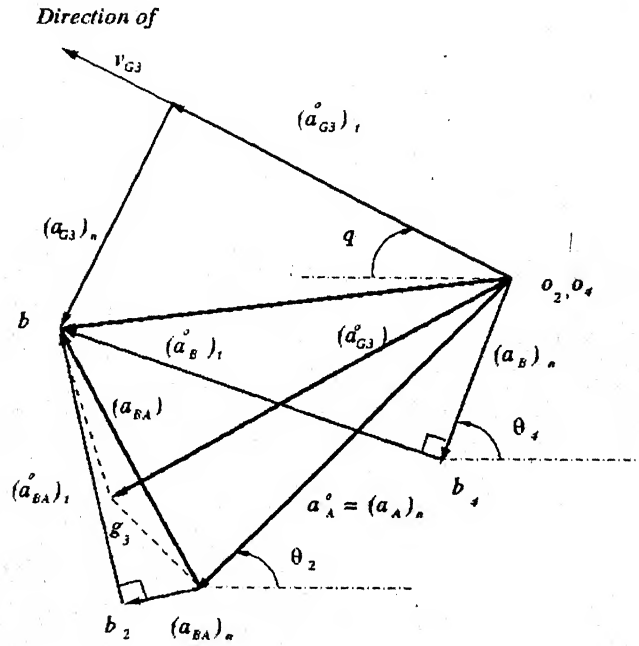


Figure 2.4.3 : Auxiliary Acceleration Diagram of a 4R Mechanism.

From fig. 2.4.3,

$$(a_A)_n = l_2 \omega_2^2$$

$$\overline{O_4 b} = \overline{O_4 b_4} + \overline{b_4 b}$$

$$\overline{ab_2} = l_3 \theta_3^2$$

$$\overline{ab} = \overline{ab_2} + \overline{b_2 b}$$

$$\therefore (a_{BA})_t = \overline{b_2 b} = \overline{ab} - \overline{ab_2}$$

$$\alpha_3'' = \frac{(a_{B,1}'')_t}{l_3}$$

But from the Goodman transformation equations (2.4.3) and (2.4.4), with $i=2$, yield:

Link 2:

$$\alpha_2 = \alpha_{2''} + \frac{\omega_2}{\omega_2} \alpha_2 = \alpha_2 \quad (2.4.5)$$

Link 3:

$$\alpha_3 = \alpha_{3''} + \frac{\omega_3}{\omega_2} \alpha_2 \quad (2.4.6)$$

$$(a_{G3})_t = (a_{G3}'')_t + \frac{v_{G3}}{\omega_2} \alpha_2 \quad (2.4.7)$$

Link 4:

$$\alpha_4 = \alpha_{4''} + \frac{\omega_4}{\omega_2} \alpha_2 \quad (2.4.8)$$

The corresponding time rates of change of kinetic energy are:

For link 2: $J_{O2} \omega_2 \alpha_2$

For link 3: $m_3 v_{G3} (a_{G3})_t + J_{G3} \omega_3 \alpha_3$

For link 4: $J_{O4} \omega_4 \alpha_4$

Equation (2.4.2) becomes,

$$\frac{dT}{dt} = J_{O2} \omega_2 \alpha_2 + m_3 v_{G3} (a_{G3})_t + J_{G3} \omega_3 \alpha_3 + J_{O4} \omega_4 \alpha_4 \quad (2.4.9)$$

The power input of the force system in the phase considered is,

$$\sum \dot{\mathcal{P}} = M_2 \omega_2 + M_4 \omega_4 + (W_2)_t v_{G2} + (W_3)_t v_{G3} + (W_4)_t v_{G4} \quad (2.4.10)$$

α_2 can be evaluated by equating equations (2.4.9) and (2.4.10).

From equations (2.4.6) and (2.4.8), we can evaluate the value of α_3 and α_4 .

2.5 Balancing

In order to fully force balance linked mechanisms, it must be possible to make the total center of mass of such mechanisms stationary. This is usually accomplished with the help of appropriately chosen counterweights. The total elimination of the shaking moment on the ground in such fully force balanced mechanisms is generally only possible by the introduction of counter-rotating disks and, possibly, by giving the floating links the shape of physical pendulum [8].

1) Force Balancing

When completely force balanced, the vector sum of the forces acting on the frame is zero. This is accomplished by making the total center of mass for the mechanism stationary [6]. Figure 2.5.1 shows a 4R mechanism

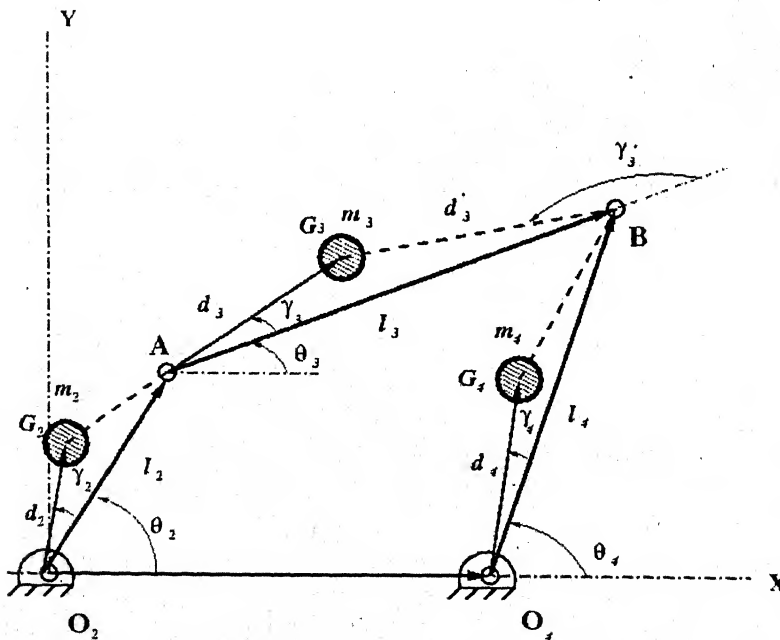


Figure 2.5.1 : Force Balancing of a 4R Mechanism.

In fig.2.5.1,

m_j = mass of the j -th link where $j = 2,3,4$.

G_j = location of the C.G. of the j -th link.

d_j = distance of G_j from a kinematic pair as indicated in fig. 2.5.1.

Let G be the center of mass for the system of moving links and let \mathbf{d}_G define the position of G with respect to origin O_2 .

$$M = \sum_{j=2}^4 m_j \quad (2.5.1)$$

where M is the total moving mass of the system.

$$M\mathbf{d}_G = \sum_{j=2}^4 m_j \mathbf{d}_j \quad (2.5.2)$$

where \mathbf{d}_j is the vector from the tail of the link vector l_j to the center of mass of the j -th link.

From fig. 2.5.1,

$$\mathbf{d}_2 = d_2 e^{i(\theta_2 + \gamma_2)}$$

$$\mathbf{d}_3 = d_3 e^{i(\theta_3 + \gamma_3)} + l_2 e^{i\theta_2}$$

$$\mathbf{d}_4 = d_4 e^{i(\theta_4 + \gamma_4)} + l_1.$$

Upon substitution of above equations, with rearrangements, equation (2.5.2) becomes,

$$M\mathbf{d}_G = m_2 d_2 e^{i(\theta_2 + \gamma_2)} + m_3 (d_3 e^{i(\theta_3 + \gamma_3)} + l_2 e^{i\theta_2}) + m_4 (d_4 e^{i(\theta_4 + \gamma_4)} + l_1). \quad (2.5.3)$$

the governing loop closure equation is,

$$\bar{l}_2 + \bar{l}_3 = \bar{l}_1 + \bar{l}_4$$

$$\text{or } \bar{l}_2 + \bar{l}_3 - \bar{l}_1 - \bar{l}_4 = 0$$

$$l_2 e^{i\theta_2} + l_3 e^{i\theta_3} - l_4 e^{i\theta_4} - l_1 = 0$$

$$\text{or } e^{i\theta_3} = \frac{1}{l_3} (l_4 e^{i\theta_4} + l_1 - l_2 e^{i\theta_2}).$$

Substitution of the above equation into equation (2.5.3) gives,

$$\begin{aligned} M\mathbf{d}_G = & \left[m_2 d_2 e^{i\gamma_2} + m_3 l_2 - m_3 d_3 \frac{l_2}{l_3} e^{i\gamma_3} \right] e^{i\theta_2} + \left[m_4 d_4 e^{i\gamma_4} + m_3 d_3 \frac{l_4}{l_3} e^{i\gamma_3} \right] e^{i\theta_4} \\ & + \left[m_4 l_1 + m_3 d_3 \frac{l_1}{l_3} e^{i\gamma_3} \right] \end{aligned} \quad (2.5.4)$$

which is of the form

$$M\mathbf{d}_G = \mathbf{A}e^{i\theta_2} + \mathbf{B}e^{i\theta_4} + \mathbf{C}.$$

If $\mathbf{A} = \mathbf{B} = 0$,

$M\mathbf{d}_G$ is constant, meeting the criterion required for complete force balance.

When $\mathbf{A} = 0$, we obtain

$$m_2 d_2 = m_3 d'_3 \frac{l_2}{l_3} \quad (2.5.5)$$

$$\text{and } \gamma_2 = \gamma'_3. \quad (2.5.6)$$

When $\mathbf{B} = 0$, we obtain

$$m_4 d_4 = m_3 d_3 \frac{l_4}{l_3} \quad (2.5.7)$$

$$\text{and } \gamma_4 = \gamma_3 + \pi. \quad (2.5.8)$$

Since the center of mass of the entire mechanism is kept stationary, full force balance is maintained by adding counter-weights regardless of variation in input speed.

Figure 2.5.2 shows the counter-weights and its position for 4R mechanism.

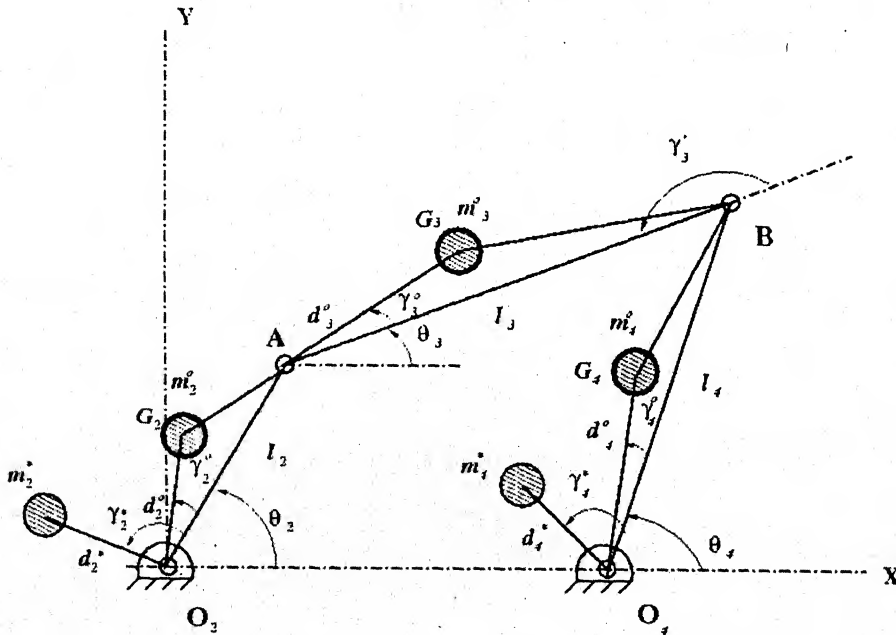


Figure 2.5.1 : Force Balanced 4R mechanism.

There are two constraints on the selection of counter-weight position and mass:

Constraint 1:

$$m_j d_j e^{i\gamma_j} = m_j^o d_j^o e^{i\gamma_j^o} + m_j^* d_j^* e^{i\gamma_j^*}$$

$$\text{or } m_j^* d_j^* = \sqrt{(m_j d_j)^2 + (m_j^o d_j^o)^2 - 2m_j d_j m_j^o d_j^o \cos(\gamma_j - \gamma_j^o)} \quad (2.5.9)$$

$$\text{and } \gamma_j^* = \tan^{-1} \left(\frac{m_j d_j \sin \gamma_j - m_j^o d_j^o \sin \gamma_j^o}{m_j d_j \cos \gamma_j - m_j^o d_j^o \cos \gamma_j^o} \right) \quad (2.5.10)$$

where

m_j, d_j, γ_j are the parameters obtained from the equations (2.5.5), (2.5.6), (2.5.7)

and (2.5.8)

m_j^o, d_j^o, γ_j^o are the parameters for the unbalanced linkage

m_j^*, d_j^*, γ_j^* are the parameters for the counter-weights.

Constraint 2:

$$m_j = m_j^o + m_j^* \quad (2.5.11)$$

required only in cases when both fixed pivot links are chosen to receive counter-weights.

2) Shaking Moment Balancing

Balancing of force ensures a zero vector sum of the inertial forces acting on the fixed link supports but will not provide zero forces at individual supports. The resultant of these forces results in a pure time-varying couple known as the shaking moment. Hence it is desirable for complete balancing of linkages, that both force and shaking moments be reduced to zero [9].

Figure 2.5.3 shows a 4R mechanism for shaking moment balancing.

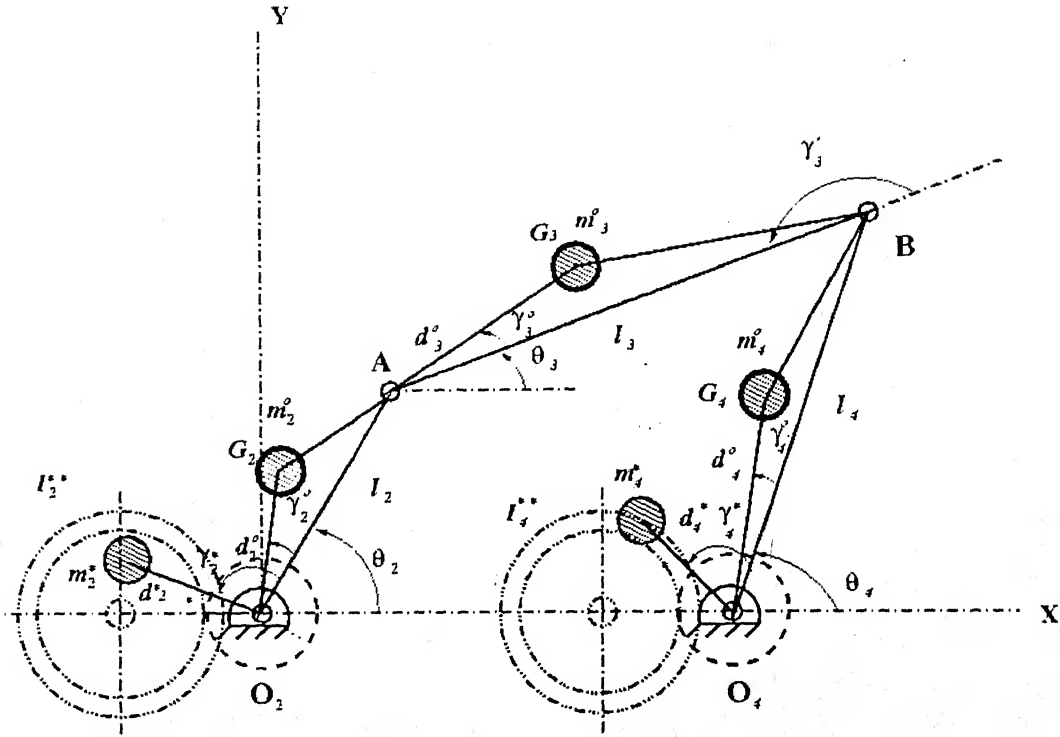


Figure 2.5.2 : Shaking Moment Balancing of 4R Mechanism.

Shaking moment of a force balanced 4R mechanism is given as [6],

$$M_s = \sum_{j=2}^4 K_j \ddot{\theta}_j + K(\tau_2 \ddot{\theta}_2 + \dot{\tau}_2 \dot{\theta}_2), \quad (2.5.12)$$

where,

$$K_j = -m_j(k_j^2 + d_j^2 - l_j d_j \cos \gamma_j)$$

$$K = -2m_3 l_2 d_2 \sin \gamma_3$$

$$\tau_2 = \sin(\theta_2 - \theta_3)$$

$$\dot{\tau}_2 = (\dot{\theta}_2 - \dot{\theta}_3) \cos(\theta_2 - \theta_3)$$

If we add the effects of two inertia counterweights I_2^{**} and I_4^{**} geared to the input and output links as shown in fig. 2.5.3.

Then equation (2.5.12) becomes,

$$M_s = \sum_{j=2}^4 K_j \ddot{\theta}_j + K(\tau_2 \ddot{\theta}_2 + \dot{\tau}_2 \dot{\theta}_2) + I_2^{**} \ddot{\theta}_2 + I_4^{**} \ddot{\theta}_4, \quad (2.5.12)$$

The shaking moment can therefore be made to reduce partially if

$$I_2^{**} = -K_2 - K\tau_2 = m_2(k_2^2 + d_2^2 - l_2 d_2 \cos \gamma_2) + 2m_3 l_2 d_2 \sin \gamma_3 \sin(\theta_2 - \theta_3)$$

$$I_4^{**} = -K_4 = m_4(k_4^2 + d_4^2 - l_4 d_4 \cos \gamma_4)$$

Partial shaking moment will be,

$$M_s = \sum K_3 \ddot{\theta}_3 + K(\dot{\tau}_2 \dot{\theta}_2), \quad (2.5.14)$$

Full shaking moment balance can be achieved if,

- (i) the center of mass of the coupler lies on the line connecting the hinges A and B i.e., $\gamma_3 = 0$ or $K = 0$, and
- (ii) $K_3 = 0$ or $k_3^2 = d_3(l_3 - d_3)$ i.e. coupler is a physical pendulum with $l_3 = 2d_3$.

• Effect of Moment Balance on Input Torque

The added counterweights I_2^{**} and I_4^{**} effectively double the inertial contributions of the input and output links. The input torque itself is not doubled, however. The input torque of the linkage is given by [10],

$$M_{in} = \frac{1}{\theta_2} \sum_{j=2}^4 m_j (\dot{d}_{Gj} \ddot{\theta}_j + k_j^2 \dot{\theta}_j \ddot{\theta}_j) \quad (2.5.13)$$

where,

\dot{d}_{Gj} is the velocity of center of mass G_j

\ddot{d}_{Gj} is the acceleration of center of mass G_j .

From the above equation we can evaluate the required turning moment at the crank.

2.6 Numerical Examples and Results

Computer programs in C language have been developed for solving the problems. This section illustrates some examples giving the results generated by those programs.

a) Kinematic Analysis

Example: -

A 4R mechanism having crank length, $l_2 = 76.2$ mm, coupler length, $l_3 = 305$ mm, follower length, $l_4 = 152$ mm, fixed length, $l_1 = 254$ mm and rotates at a speed of 100 rad/sec and an acceleration of 25 rad/sec². Determine the following when the crank angle varies from 0° to 360°.

- 1) Displacements of the coupler and slider
- 2) Velocities of the coupler and slider
- 3) Accelerations of the coupler and slider.

The following sample results are shown as: -

- 1) Displacement of the coupler and follower (fig.2.6.1)
- 2) Velocity of the coupler and follower (fig.2.6.2)
- 3) Acceleration of the coupler and follower (fig.2.6.3)

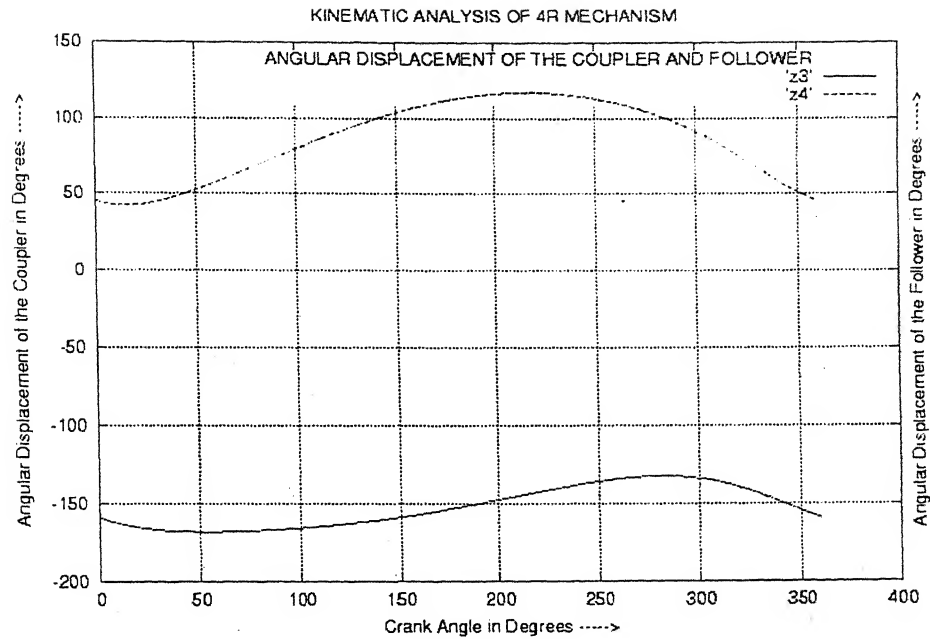


Figure 2.6.1 : Displacements of the Coupler and Follower Vs Crank Angle.

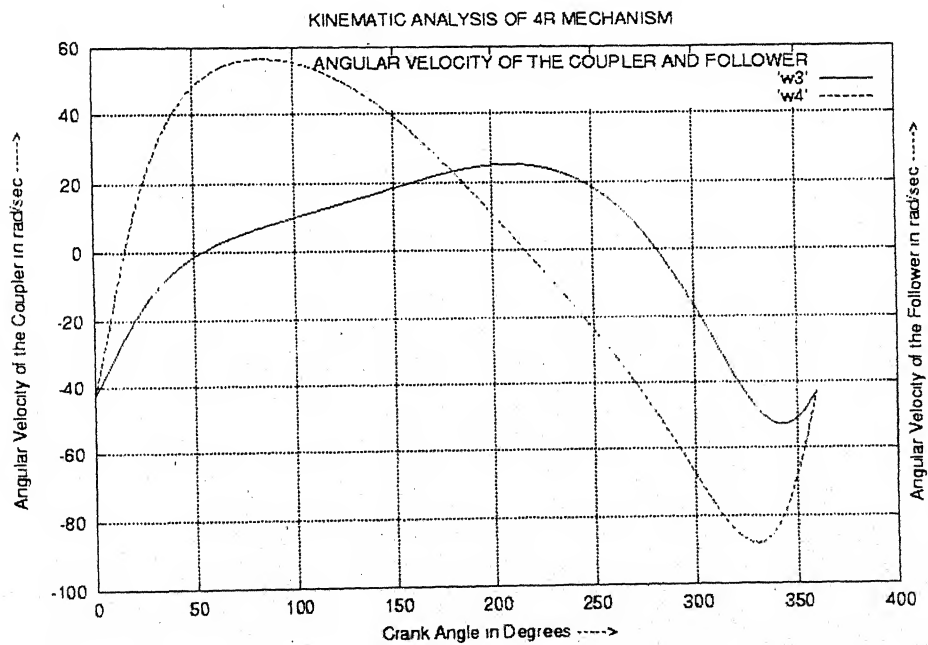


Figure 2.6.2 : Velocities of the Coupler and Follower Vs Crank Angle.

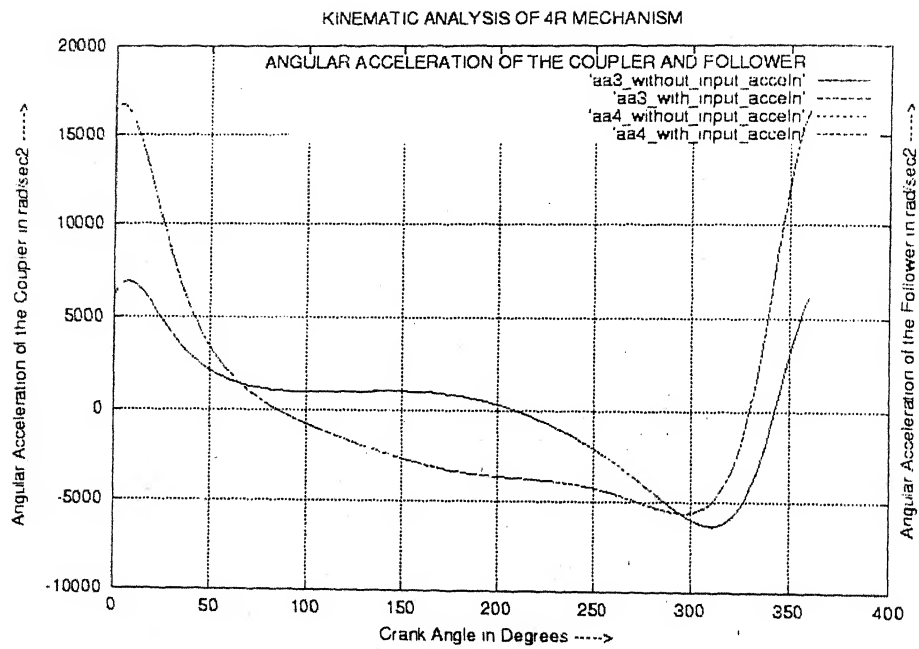


Figure 2.6.3 : Accelerations of the Coupler and Follower Vs Crank Angle.

b) Dynamic Force Analysis

Example: -

A 4R mechanism having crank length, $l_2 = 76.2$ mm, coupler length, $l_3 = 305$ mm, follower length, $l_4 = 152$ mm, fixed distance, $l_1 = 254$ mm and rotates at a speed of 100 rad/sec and an acceleration of 25 rad/sec^2 . Crank is having the following data: $g_2 = 25.4$ mm, $\gamma_2 = 15^\circ$, $m_2 = 0.125$ kg, $k_2 = 23$ mm, $F_2 = 5$ N, $\beta_2 = 10^\circ$. Coupler is having the following data: $g_3 = 102$ mm, $\gamma_3 = 14^\circ$, $m_3 = 0.25$ kg, $k_3 = 114$ mm, $F_3 = 10$ N, $\beta_3 = 20^\circ$, $M_3 = 2.5$ N-m. Follower is having the following data: $g_4 = 102$ mm, $\gamma_4 = 15^\circ$, $m_4 = 0.125$ kg, $k_4 = 73$ mm, $F_4 = 10$ N, $\beta_4 = 10^\circ$, $M_4 = 2.5$ N-m. Determine the following when the crank angle varies from 0° to 360° .

- 1) Required turning moment at the crank, M_2 .
- 2) Reaction at the hinge O_2 , P_{O_2} .
- 3) Reaction at the hinge A, P_A .
- 4) Reaction at the hinge B, P_B .
- 5) Reaction at the hinge O_4 , P_{O_4} .

Results are shown as: -

- 1) Required turning moment at the crank i.e. M_2 (fig.2.6.4).
- 2) Reaction at the hinge O_2 i.e., P_{O_2} (fig.2.6.5)
- 3) Reaction at the hinge A i.e., P_A (fig.2.6.6)
- 4) Reaction at the hinge B i.e., P_B (fig.2.6.7)
- 5) Reaction at the hinge O_4 i.e., P_{O_4} (fig.2.6.8)

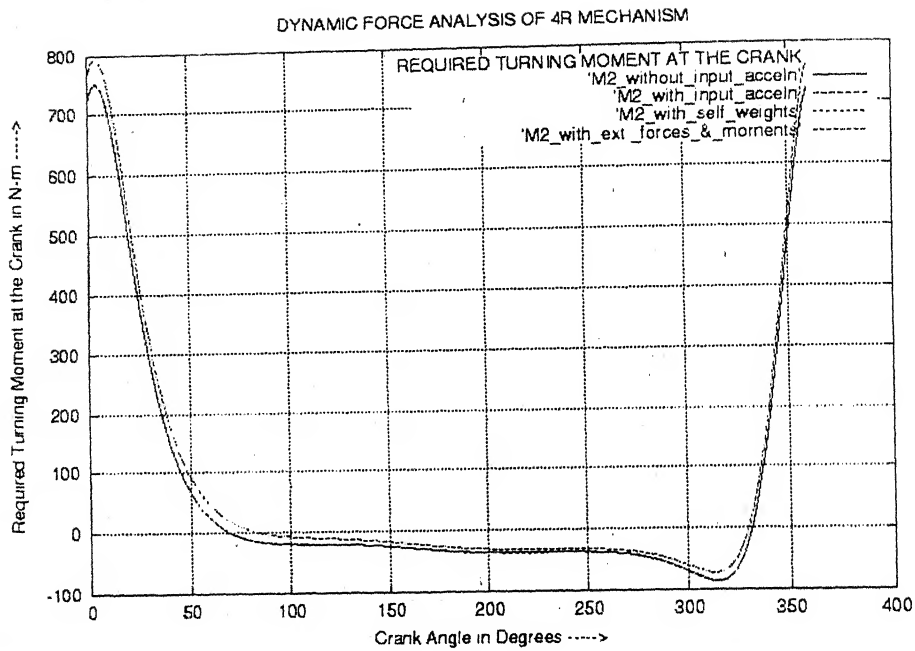


Figure 2.6.4 : Required Turning Moment at the Crank Vs Crank Angle.

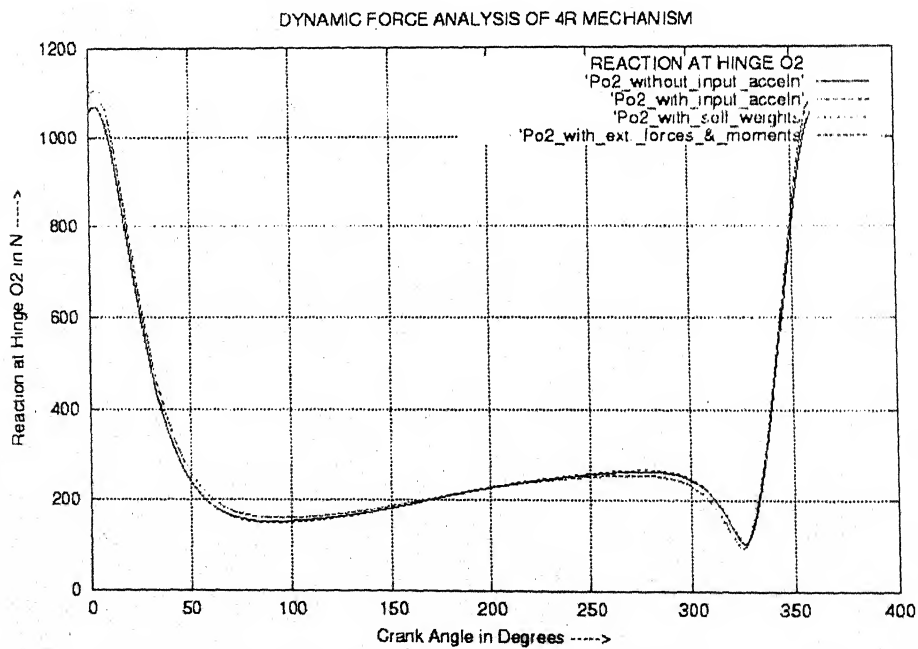


Figure 2.6.5 : Reaction at the hinge O₂ Vs Crank Angle.

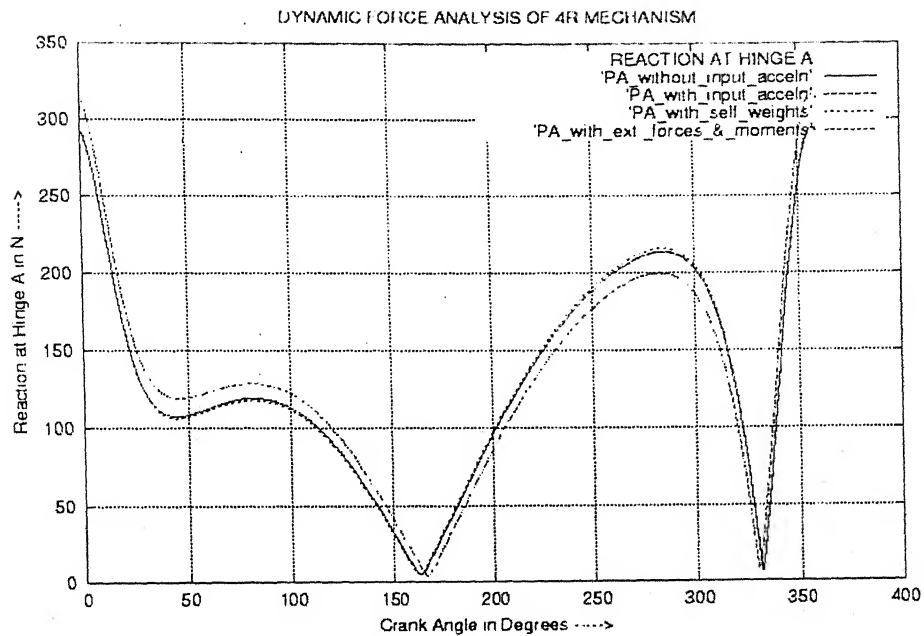


Figure 2.6.6 : Reaction at the hinge A Vs Crank Angle.

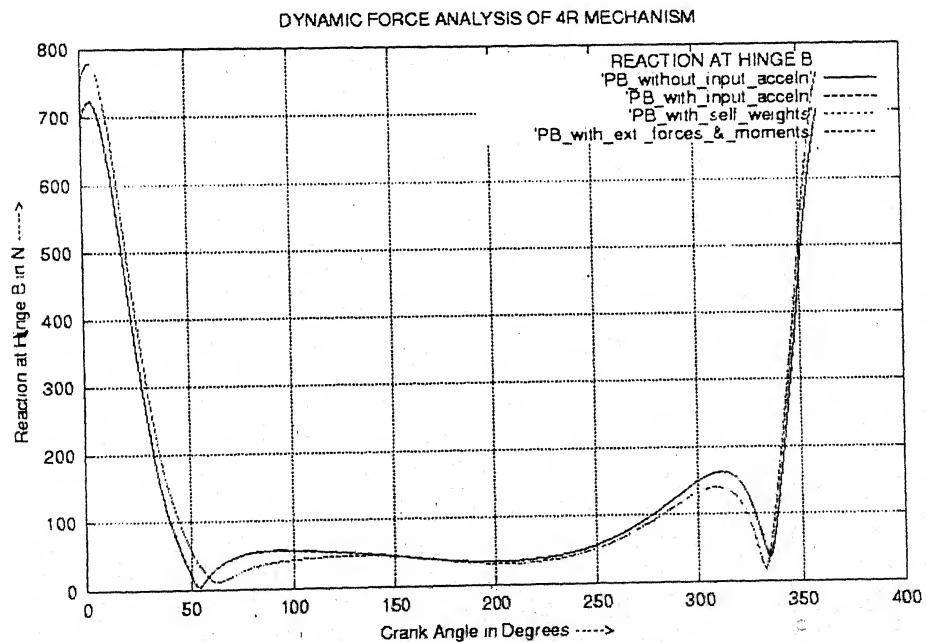


Figure 2.6.7 : Reaction at the hinge B Vs Crank Angle.

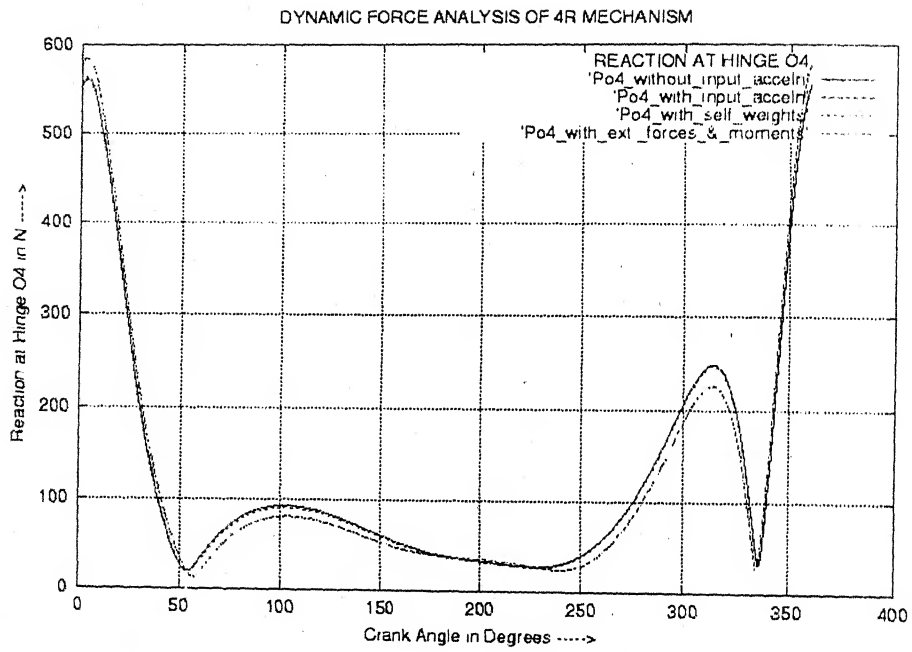


Figure 2.6.8 : Reaction at the hinge O_4 Vs Crank Angle.

c) Dynamic motion analysis

Example: -

A 4R mechanism having crank length, $l_2 = 76.2$ mm, coupler length, $l_3 = 305$ mm, follower length, $l_4 = 152$ mm, fixed length, $l_1 = 254$ mm and rotates at a speed of 100 rad/sec. Crank is having the following data: $g_2 = 25.4$ mm, $\gamma_2 = 15^\circ$, $m_2 = 0.125$ kg, $k_2 = 23$ mm, $M_2 = 0.5$ N-m. Coupler is having the following data: $g_3 = 102$ mm, $\gamma_3 = 14^\circ$, $m_3 = 0.25$ kg, $k_3 = 114$ mm. Follower is having the following data: $m_4 = 0.125$ kg, $g_4 = 102$ mm, $\gamma_4 = 15^\circ$, $k_4 = 73$ mm, $M_4 = 0.5$ N-m. Determine the following when the crank angle varies from 0° to 360° .

- 1) Acceleration of the crank.
- 2) Acceleration of the coupler.
- 3) Acceleration of the slider.

Results are shown as: -

- 1) Acceleration of the crank (fig.2.6.9)
- 2) Acceleration of the coupler (fig.2.6.10)
- 3) Acceleration of the follower (fig.2.6.11)

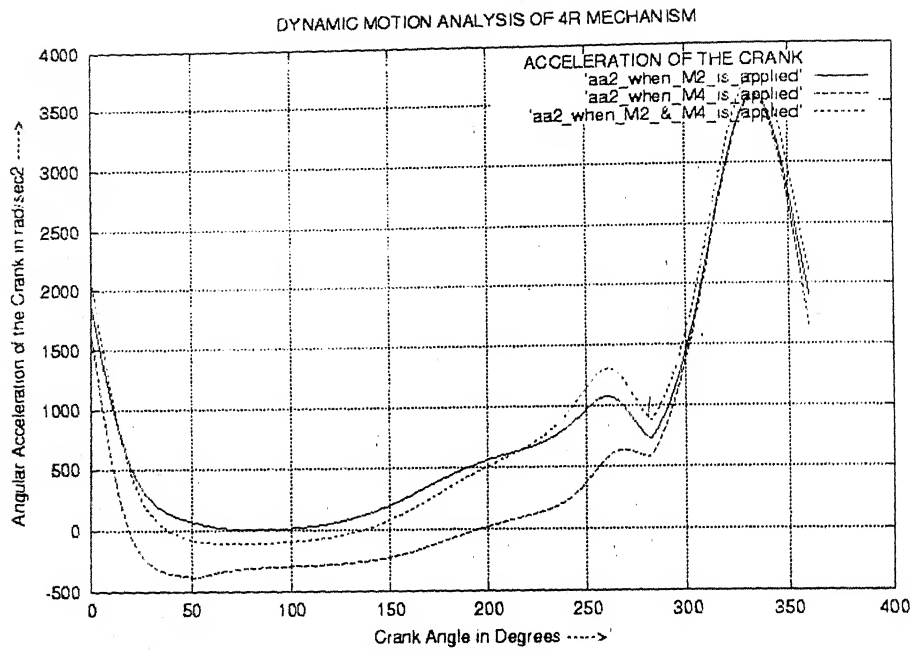


Figure 2.6.9 : Acceleration of the Crank Vs Crank Angle.

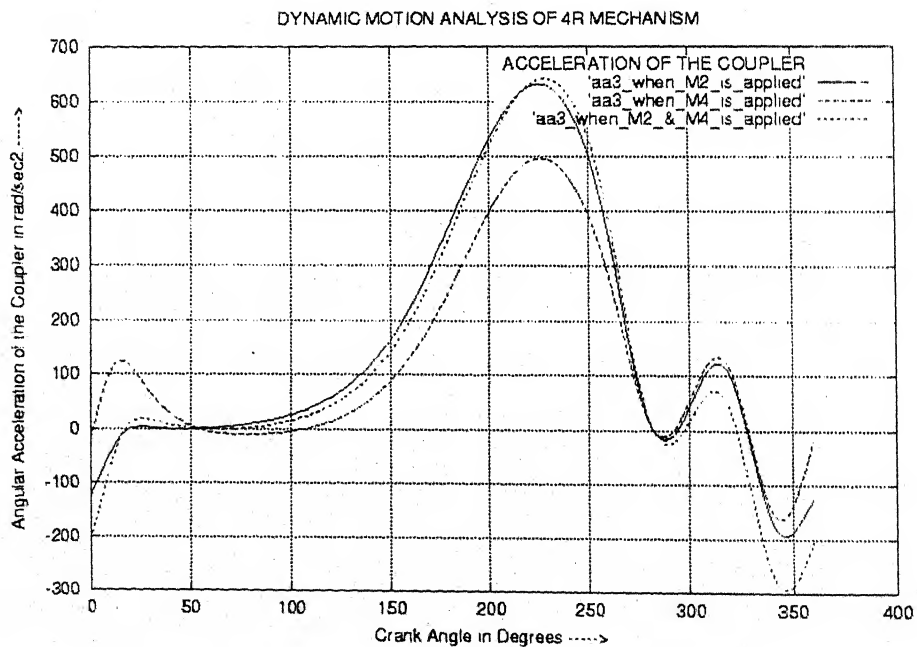


Figure 2.6.10 : Acceleration of the Coupler Vs Crank Angle.

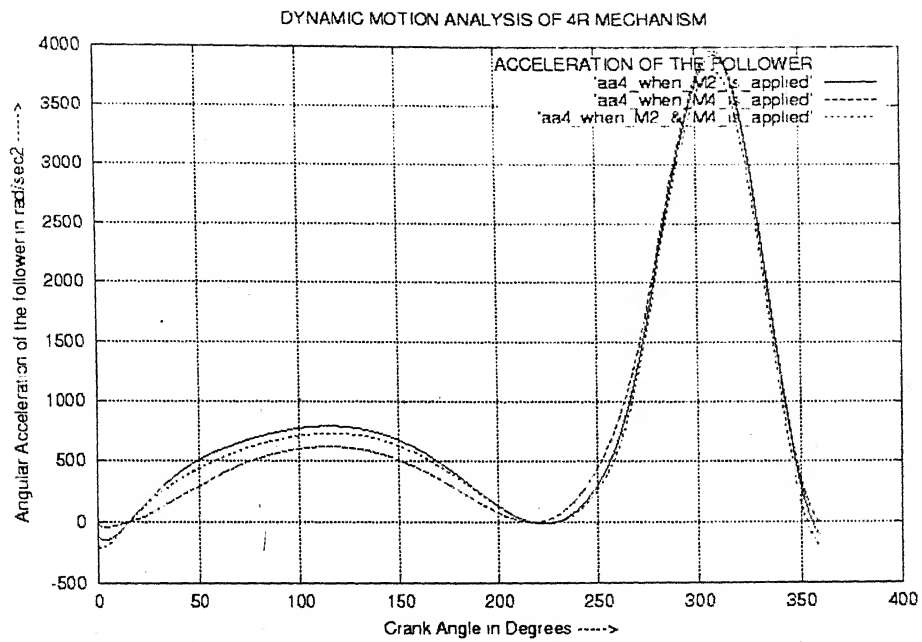


Figure 2.6.11 : Acceleration of the Follower Vs Crank Angle.

d) Balancing

Example: -

A 4R mechanism having crank length, $l_2 = 76.2$ mm, coupler length, $l_3 = 305$ mm, follower length, $l_4 = 152$ mm, fixed length, $l_1 = 254$ mm and rotates at a speed of 100 rad/sec and an acceleration of 25 rad/sec^2 . Crank is having the following data: $g_2 = 25.4$ mm, $\gamma_2 = 15^\circ$, $m_2 = 0.125$ kg, $k_2 = 23$ mm, Coupler is having the following data: $g_3 = 102$ mm, $\gamma_3 = 14^\circ$, $m_3 = 0.25$ kg, $k_3 = 114$ mm. Follower is having the following data: $m_4 = 0.125$ kg, $g_4 = 102$ mm, $\gamma_4 = 15^\circ$, $k_4 = 73$ mm. Determine the following when crank angle varies from 0° to 360° .

- 1) Counterweights and its position i.e. $m_2^* d_2^*$, $m_4^* d_4^*$ and γ_2^* , γ_4^* .
- 2) Moment of inertia of counterweights for shaking moment balance i.e. I_2^{**} and I_4^{**} .
- 3) Shaking moment before and after moment balance i.e. complete shaking moment and partial shaking moment.
- 4) Required input turning moment after force and shaking moment balance.

Results are shown as: -

- 1) Counterweights and its position and its moment of inertia i.e. $m_2^* d_2^*$, $m_4^* d_4^*$, γ_2^* , γ_4^* , I_2^{**} and I_4^{**} (table 2.6.1)
- 2) Shaking moment before and after moment balance (fig.2.6.12)
- 3) Required input turning moment after force and shaking moment balance (fig.2.6.13)

Table 2.6.1

$m_2^* d_2^*$ in kg-m	$m_4^* d_4^*$ in kg-m	γ_2^* in Degrees	γ_4^* in Degrees	I_2^{**} in kg-m ²	I_4^{**} in kg-m ²
0.0044	0.0072	168.6691°	190.3510°	0.0003	0.0007

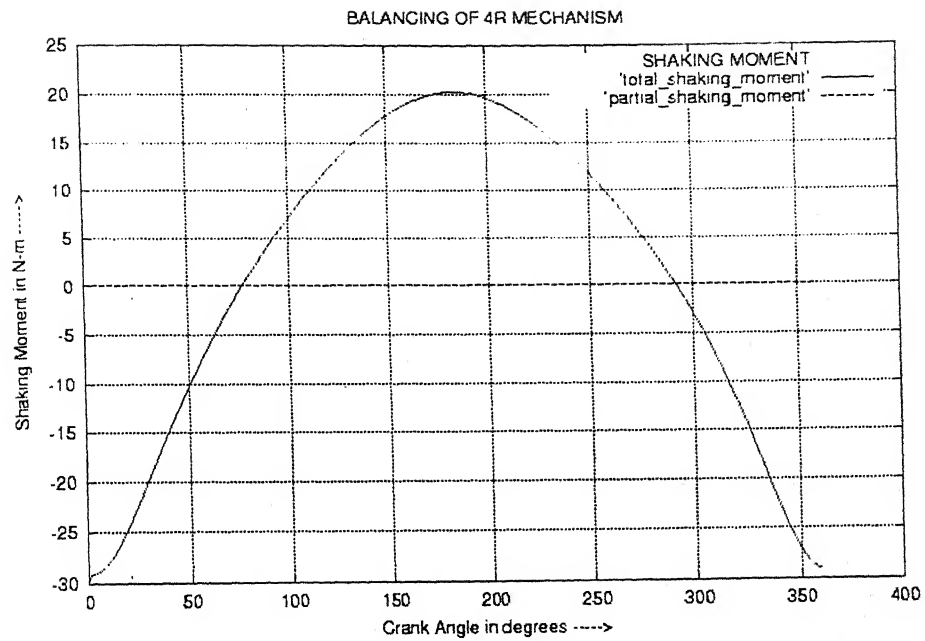


Figure 2.6.12 : Shaking Moment Vs Crank Angle.

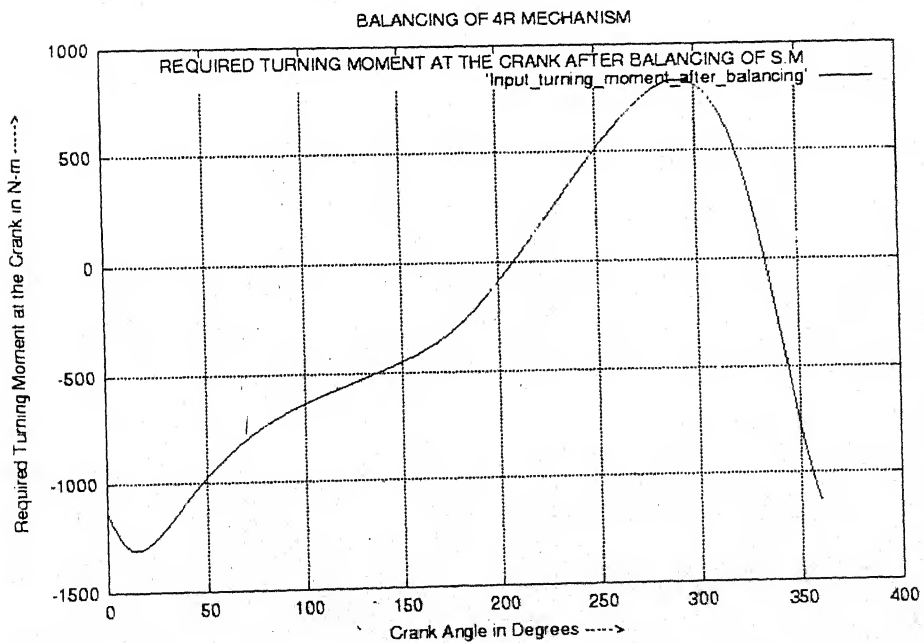


Figure 2.6.13 : Required Turning Moment at the Crank Vs Crank Angle.

Chapter 3

3R-1P Mechanism

3.1 Introduction

The 3R-1P mechanism is perhaps the most important single mechanism in engineering, being basic to the vast majority of internal – combustion engines, steam engines, compressors, pumps, mechanical presses and punches, and a host of other machines. The 3R-1P mechanism converts the reciprocating motion of a slider into a rotary motion of the crank or vice-versa [7].

The geometry of the 3R-1P mechanism and the position of the mechanism at any instant in time, the relationship between the slider force and the slider displacement, and the speed of the crank, all affect the forces acting on various parts of the mechanism.

In this chapter we are going to discuss the dynamic force and motion analysis of 3R-1P mechanism. In *dynamic force analysis* we calculate the forces on various members of a mechanism for a known input motion which is usually determined by experimentation or analytical prediction based on *kinematic analysis* whereas for *dynamic motion analysis* we calculate the motion of various links of a mechanism for a given forces on the mechanism [5].

3.2 Kinematic Analysis

A 3R-1P mechanism for *kinematic analysis* is shown in fig. 3.2.1. Link 2 ($O_2 A$) is the input crank, link 3 (AB) is the coupler, link 4 at B is the slider and l_1 is the offset distance [11].

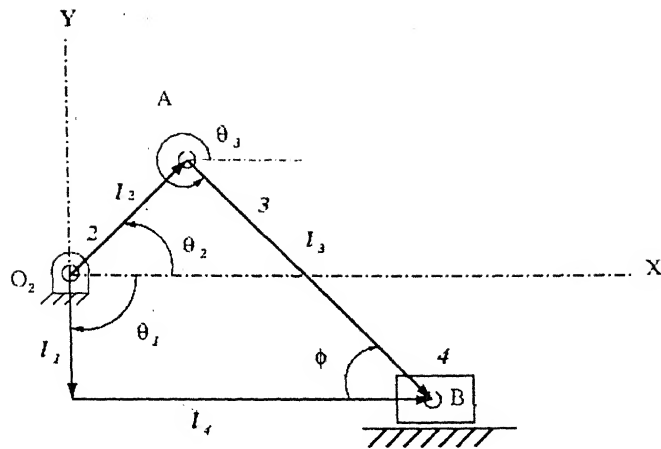


Figure 3.2.1 : Kinematic Analysis of 3R-1P Mechanism.

Using the symbols explained in fig. 3.2.1,
the governing loop-closure equation is given by,

$$\vec{l}_1 + \vec{l}_4 = \vec{l}_2 + \vec{l}_3 \quad (3.2.1)$$

or $\vec{l}_1 - \vec{l}_2 - \vec{l}_3 + \vec{l}_4 = 0$

or $l_1 e^{i\theta_1} - l_2 e^{i\theta_2} - l_3 e^{i\theta_3} + l_4 = 0.$

Equating the real and imaginary parts of the above equation separately to zero, we get,

$$l_1 \cos\theta_1 - l_2 \cos\theta_2 - l_3 \cos\theta_3 + l_4 = 0$$

and $l_1 \sin\theta_1 - l_2 \sin\theta_2 - l_3 \sin\theta_3 = 0.$

By putting $\theta_1 = -\pi/2$, we get,

$$\theta_3 = -\sin^{-1}\left(\frac{l_1 + l_2 \sin\theta_2}{l_3}\right) \quad (3.2.2)$$

and $l_4 = l_2 \cos \theta_2 + l_3 \cos \theta_3.$ (3.2.3)

Differentiating equations (3.2.2) and (3.2.3) with respect to time,

$$\dot{\theta}_3 = -\dot{\theta}_2 \left(\frac{l_2 \cos \theta_2}{l_3 \cos \theta_3} \right) \quad (3.2.4)$$

and $\dot{l}_4 = -l_3 \dot{\theta}_3 \sin \theta_3 - l_2 \dot{\theta}_2 \sin \theta_2.$ (3.2.5)

Again differentiating equations (3.2.4) and (3.2.5) with respect to time,

$$\ddot{\theta}_3 = \left(\frac{l_3 \dot{\theta}_3^2 \sin \theta_3 + l_2 \dot{\theta}_2^2 \sin \theta_2 - l_3 \ddot{\theta}_2 \cos \theta_2}{l_3 \cos \theta_3} \right) \quad (3.2.6)$$

and $\ddot{l}_4 = -l_3 \ddot{\theta}_3 \sin \theta_3 - l_3 \dot{\theta}_3^2 \cos \theta_3 - l_2 \ddot{\theta}_2 \sin \theta_2 - l_2 \dot{\theta}_2^2 \cos \theta_2.$ (3.2.7)

3.3 Dynamic Force Analysis

In *dynamic force analysis*, the motion is usually known either by experimentation or analytical predictions based on *kinematic analysis*, the driving torque and the reaction in kinematic pairs are to be determined. Also we can calculate F_4 for a given torque M_2 [5]. Figure 3.3.1 shows an offset 3r-1p mechanism. The kinematic pairs are assumed to be frictionless.

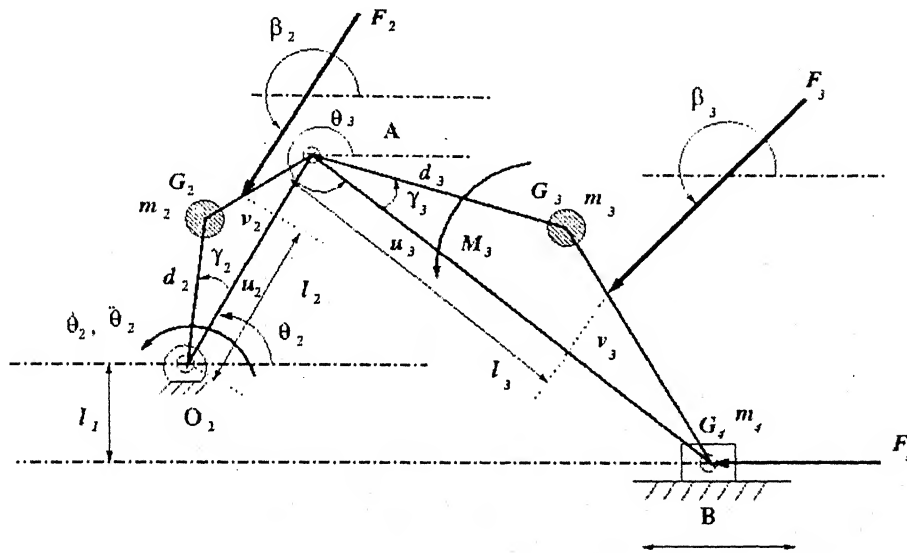


Figure 3.3.1 : Dynamic Force Analysis of 3R-1P Mechanism.

In fig.3.3.1,

m_j = mass of the j -th link where $j = 2, 3, 4$

G_j = location of the C.G. of the j -th link.

d_j = distance of G_j from a kinematic pair as indicated in fig. 3.3.1

F_j = external force acting on the j -th link at an angle of β_j to the X -axis at a point with local coordination (u_j, v_j) .

$F_{j,x}$ = X -component of F_j .

$F_{j,y}$ = Y -component of F_j

M_j = external moment on j -th link.

$P_{K,x}$ = force exerted at the hinge K in the x -direction where $K = A, B$

$P_{K,y}$ = force exerted at the hinge K in the y -direction.

k_j = centroidal radius of gyration of the j -th link.

$P_{ij,x}$ = force exerted on the j -th link by the i -th link in the x -direction

$P_{ij,y}$ = force exerted on the j -th link by the i -th link in the y -direction.

where, $i = 1, 2, 3, 4$

The dynamic equations for each link can be obtained as discussed below :-

1. Crank:-

Refer to fig.3.3.2 as the free-body-diagram of the crank,

with $i = 1, 3$, $j = 2$, $K = O_2, A$.

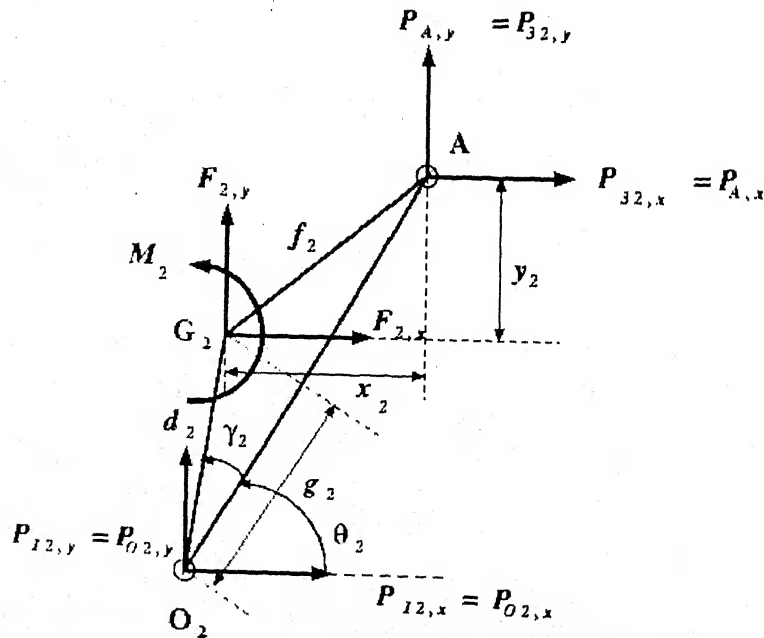


Figure 3.3.2 : Free-Body-Diagram of the Crank for Force Analysis.

From fig. 3.3.2,

$$x_2 = d_2 \sin \gamma_2 \sin \theta_2 + (l_2 - g_2) \cos \theta_2$$

and $y_2 = (l_2 - g_2) \sin \theta_2 - d_2 \sin \gamma_2 \cos \theta_2 .$

Equations of motion for the crank are,

$$\begin{Bmatrix} F_{2,x} \\ F_{2,y} \\ M_2 \end{Bmatrix} + \begin{bmatrix} 1 & 0 & 1 & 0 \\ 0 & 1 & 0 & 1 \\ d_2 \sin(\theta_2 + \gamma_2) & -d_2 \cos(\theta_2 + \gamma_2) & -y_2 & x_2 \end{bmatrix} \begin{Bmatrix} P_{O_2,x} \\ P_{O_2,y} \\ P_{A,x} \\ P_{A,y} \end{Bmatrix} = m_2 \begin{Bmatrix} a_{G2,x} \\ a_{G2,y} \\ \ddot{\theta}_2 k_2^2 \end{Bmatrix} \quad (3.3.1)$$

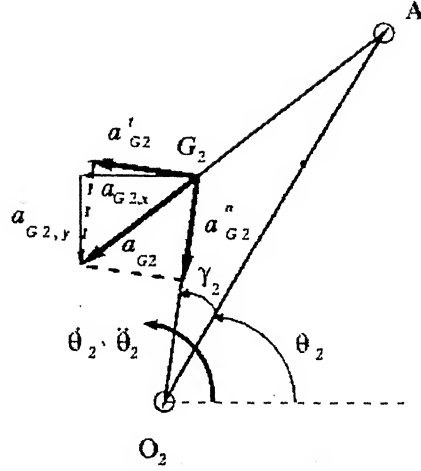


Figure 3.3.3 : Diagram of the Crank for Acceleration Analysis.

Various components of acceleration of G_2 are explained in fig. 3.3.3 and the superscripts n , t refer to normal and tangential components, respectively.

From fig. 3.3.3,

$$a_{G2,x} = a_{G2}'' \cos(\theta_2 + \gamma_2) + a_{G2}' \sin(\theta_2 + \gamma_2) \quad (3.3.2)$$

$$\text{and } a_{G2,y} = a_{G2}'' \sin(\theta_2 + \gamma_2) - a_{G2}' \cos(\theta_2 + \gamma_2) \quad (3.3.3)$$

where $a_{G2}'' = d_2 \dot{\theta}_2^2$, $a_{G2}' = d_2 \ddot{\theta}_2$.

Using equations (3.3.2) and (3.3.3), the right hand side of equation (3.3.1) turns out as,

$$m_2 \begin{Bmatrix} a_{G2,x} \\ a_{G2,y} \\ \ddot{\theta}_2 k_2^2 \end{Bmatrix} = m_2 \begin{Bmatrix} d_2 \dot{\theta}_2^2 \cos(\theta_2 + \gamma_2) \\ d_2 \dot{\theta}_2^2 \sin(\theta_2 + \gamma_2) \\ 0 \end{Bmatrix} + m_2 \begin{bmatrix} d_2 \sin(\theta_2 + \gamma_2) & 0 & 0 \\ -d_2 \cos(\theta_2 + \gamma_2) & 0 & 0 \\ k_2^2 & 0 & 0 \end{bmatrix} \begin{Bmatrix} \ddot{\theta}_2 \\ \ddot{\theta}_3 \\ \ddot{l}_4 \end{Bmatrix} \quad (3.3.4)$$

2. Coupler:-

Refer to fig.3.3.4 as the free-body-diagram of the coupler, with $j = 3, K = A, B$.

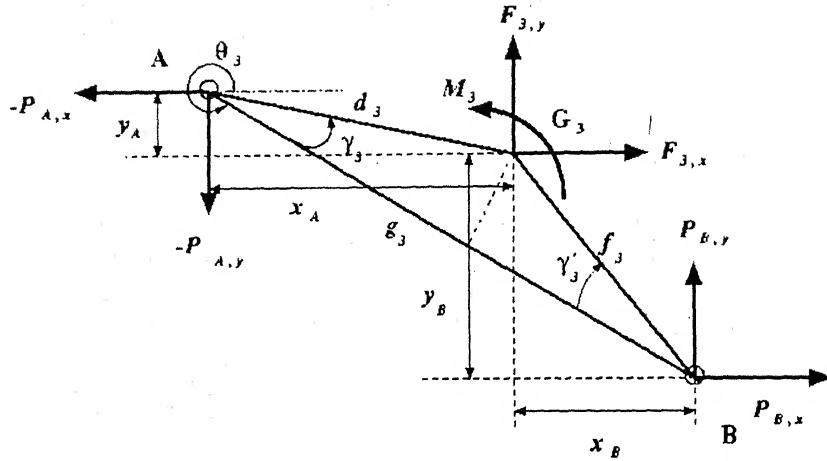


Figure 3.3.4 : Free-Body-Diagram of the Coupler for Force Analysis.

From fig. 3.3.4,

$$x_A = d_3 \sin(\theta_3 + \gamma_3 - 3\pi/2)$$

$$y_A = d_3 \cos(\theta_3 + \gamma_3 - 3\pi/2)$$

$$x_B = f_3 \cos(\gamma'_3 - \theta_3 + 4\pi)$$

and $y_B = f_3 \sin(\gamma'_3 - \theta_3 + 4\pi).$

Equations of motion for the coupler are,

$$\begin{Bmatrix} F_{3,x} \\ F_{3,y} \\ M_3 \end{Bmatrix} + \begin{bmatrix} -1 & 0 & 1 & 0 \\ 0 & -1 & 0 & 1 \\ y_A & x_A & y_B & x_B \end{bmatrix} \begin{Bmatrix} P_{A,x} \\ P_{A,y} \\ P_{B,x} \\ P_{B,y} \end{Bmatrix} = m_3 \begin{Bmatrix} a_{G3,x} \\ a_{G3,y} \\ \ddot{\theta}_3 k_3^2 \end{Bmatrix} \quad (3.3.5)$$

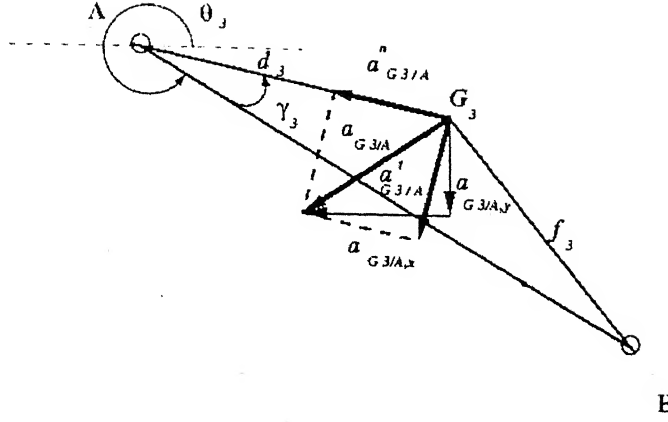


Figure 3.3.5 : Diagram of the Coupler for Acceleration Analysis.

From fig. 3.3.5,

$$a_{G3,x} = a_{A,x} + a_{G3/A,x} \quad (3.3.1)$$

$$\text{and } a_{G3,y} = a_{A,y} + a_{G3/A,y} \quad (3.3.2)$$

$$\text{where } a_{A,x} = l_2 \dot{\theta}_2^2 \cos(\theta_2 + \gamma_2) + l_2 \ddot{\theta}_2 \sin(\theta_2 + \gamma_2)$$

$$\text{and } a_{A,y} = l_2 \dot{\theta}_2^2 \sin(\theta_2 + \gamma_2) - l_2 \ddot{\theta}_2 \cos(\theta_2 + \gamma_2)$$

$$a_{G3/A,x} = a''_{G3/A} \cos(2\pi - \theta_3 - \gamma_3) + a'_{G3/A} \sin(2\pi - \theta_3 - \gamma_3)$$

$$\text{and } a_{G3/A,y} = -a''_{G3/A} \sin(2\pi - \theta_3 - \gamma_3) + a'_{G3/A} \cos(2\pi - \theta_3 - \gamma_3)$$

$$a''_{G3/A} = d_3 \dot{\theta}_3^2 \quad , \quad a'_{G3/A} = d_3 \ddot{\theta}_3$$

Using equations (3.3.6) and (3.3.7), the right hand side of equation (3.3.5) turns out as,

$$m_3 \begin{Bmatrix} a_{G3,x} \\ a_{G3,y} \\ \ddot{\theta}_3 k_3^2 \end{Bmatrix} = m_3 \begin{Bmatrix} l_2 \dot{\theta}_2^2 \cos(\theta_2 + \gamma_2) + d_3 \dot{\theta}_3^2 \cos(2\pi - \theta_3 - \gamma_3) \\ l_2 \dot{\theta}_2^2 \sin(\theta_2 + \gamma_2) - d_3 \dot{\theta}_3^2 \sin(2\pi - \theta_3 - \gamma_3) \\ 0 \end{Bmatrix}$$

$$+ m_3 \begin{bmatrix} l_2 \sin(\theta_2 + \gamma_2) & d_3 \sin(2\pi - \theta_3 - \gamma_3) & 0 \\ -l_2 \cos(\theta_2 + \gamma_2) & d_3 \cos(2\pi - \theta_3 - \gamma_3) & 0 \\ 0 & k_3^2 & 0 \end{bmatrix} \begin{Bmatrix} \ddot{\theta}_2 \\ \ddot{\theta}_3 \\ \ddot{l}_4 \end{Bmatrix} \quad (3.3.8)$$

3. Slider:-

Refer to fig.3.3.6 as the free-body-diagram of the slider,

with $j = 4, K = B$.

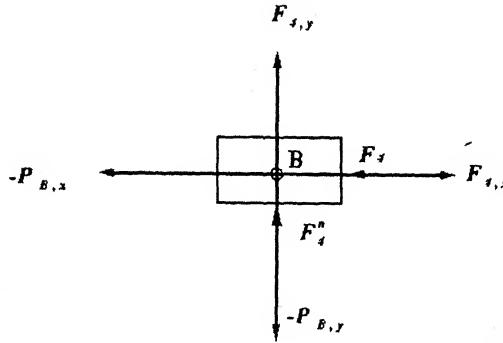


Figure 3.3.6 : Free-Body-Diagram of the Slider for Force Analysis.

Equations of motion for the slider are,

$$F_{4,x} - P_{B,x} = m_4 a_{G4,x} \quad (3.3.9)$$

$$F_{4,y} - P_{B,y} = m_4 a_{G4,y} = 0$$

and $F_{4,y} = F_4''$.

Combining all equations (3.3.1), (3.3.5) and (3.3.9) one can write,

$$\{F\} + [Q]\{P\} = \{H\} \quad (3.3.10)$$

where ,

$$\{F\} = \begin{Bmatrix} F_{2,x} \\ F_{2,y} \\ M_2 \\ F_{3,x} \\ F_{3,y} \\ M_3 \\ F_{4,x} \end{Bmatrix}$$

$$[Q] = \begin{bmatrix} 1 & 0 & 1 & 0 & 0 & 0 \\ 0 & 1 & 0 & 1 & 0 & 0 \\ d_2 \sin(\theta_2 + \gamma_2) & -d_2 \cos(\theta_2 + \gamma_2) & -y_2 & x_2 & 0 & 0 \\ 0 & 0 & -1 & 0 & 1 & 0 \\ 0 & 0 & 0 & -1 & 0 & 1 \\ 0 & 0 & y_A & x_A & y_B & x_B \\ 0 & 0 & 0 & 0 & -1 & 0 \end{bmatrix}$$

$$\{P\} = \begin{Bmatrix} P_{O2,x} \\ P_{O2,y} \\ P_{A,x} \\ P_{A,y} \\ P_{B,x} \\ P_{B,y} \end{Bmatrix}$$

But from equations (3.3.4), (3.3.8) and (3.3.9),

$$\{H\} = \{U\} + [\lambda] \ddot{\theta}, \quad (3.3.11)$$

where,

$$\{U\} = \begin{Bmatrix} m_2 d_2 \dot{\theta}_2^2 \cos(\theta_2 + \gamma_2) \\ m_2 d_2 \dot{\theta}_2^2 \sin(\theta_2 + \gamma_2) \\ 0 \\ m_3 l_2 \dot{\theta}_2^2 \cos(\theta_2 + \gamma_2) + m_3 d_3 \dot{\theta}_3^2 \cos(2\pi - \theta_3 - \gamma_3) \\ m_3 l_2 \dot{\theta}_2^2 \sin(\theta_2 + \gamma_2) - m_3 d_3 \dot{\theta}_3^2 \sin(2\pi - \theta_3 - \gamma_3) \\ 0 \\ 0 \end{Bmatrix}$$

$$[\lambda] = \begin{bmatrix} m_2 \begin{bmatrix} d_2 \sin(\theta_2 + \gamma_2) & 0 & 0 \\ -d_2 \cos(\theta_2 + \gamma_2) & 0 & 0 \\ k_2^2 & 0 & 0 \end{bmatrix} \\ m_3 \begin{bmatrix} l_2 \sin(\theta_2 + \gamma_2) & d_3 \sin(\theta_3 + \gamma_3) & 0 \\ -l_2 \cos(\theta_2 + \gamma_2) & d_3 \cos(\theta_3 + \gamma_3) & 0 \\ 0 & k_3^2 & 0 \end{bmatrix} \\ m_4 \begin{bmatrix} 0 & 0 & 1 \end{bmatrix} \end{bmatrix}$$

$$\{\ddot{\theta}\} = \begin{Bmatrix} \ddot{\theta}_2 \\ \ddot{\theta}_3 \\ \ddot{l}_4 \end{Bmatrix}$$

From the above equation (3.3.10) we can evaluate the driving torque and the hinge reactions i.e. M_2 and P_{O2}, P_A, P_B, P_{O4} for the given motion and external forces. Also we can evaluate F_4 for a given torque M_2 .

3.4 Dynamic Motion Analysis

In *dynamic motion analysis*, the motion behaviour of each member of a mechanism is to be determined for prescribed input force and moment and instantaneous velocities. The *Rate-of-change-of-energy Method* is used for the motion analysis. It is based directly on the instantaneous energy balance [5].

a) Dynamic Motion Analysis without friction

Figure 3.4.1 shows a 3R-1P Mechanism. The kinematic pairs are assumed to be frictionless.

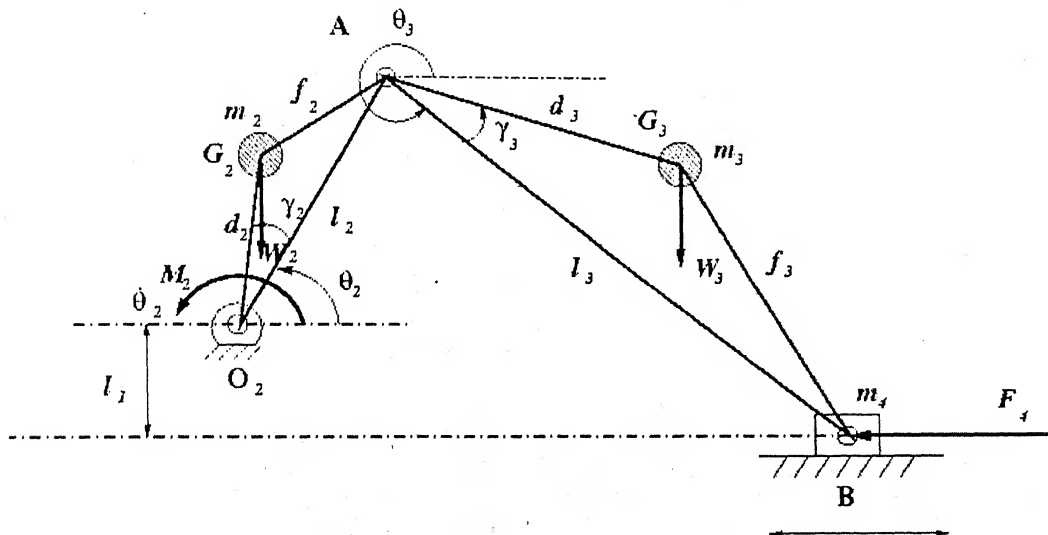


Figure 3.4.1 : Dynamic Motion Analysis of 3R-1P Mechanism without friction.

In fig.3.4.1,

m_j = mass of the j -th link where $j = 2, 3, 4$

G_j = location of the C.G. of the j -th link.

d_j = distance of G_j from a kinematic pair as indicated in fig. 3.4.1

k_j = centroidal radius of gyration of the j -th link.

W_j = weight of the j -th link.

The total K.E. of a mechanism can be expressed as,

$$T = \frac{1}{2} \sum^r J_o \omega^2 + \frac{1}{2} \sum^s m V^2 + \frac{1}{2} \sum^f m V_G^2 + \frac{1}{2} \sum^f J_G \omega^2 \quad (3.4.1)$$

The time rate of change of the total kinetic energy of the mechanism is equal to the power input of the force system acting on it.

It is expressed mathematically by,

$$\frac{dT}{dt} = \sum^r J_o \omega \alpha + \sum^s m V_a + \sum^f m V_G (a_G)_i + \sum^f J_G \omega \alpha \quad (3.4.2)$$

From Goodman transformation equations (J.Hirschhorn [4], p.123) in the form applicable to mechanisms with a rotating input link,

$$\alpha_l = \alpha_{l''} + \frac{\omega_l}{\omega_i} \alpha_i \quad (3.4.3)$$

$$(a_G)_l = (a_{G''})_l + \frac{v_G}{\omega_i} \alpha_i \quad (3.4.4)$$

where, α_l = angular acceleration of the link l .

α_i = angular acceleration of the input link i .

$\alpha_{l''}$ = angular acceleration of the link l obtained from an auxiliary acceleration analysis based on actual velocities but with zero input acceleration.

ω_l = angular velocity of the link l .

ω_i = angular velocity of the input link i .

$(a_G)_l$ = component of acceleration a_G in the direction of v_G .

$(a_{G''})_l$ = component of acceleration a_G in the direction of v_G from an auxiliary acceleration diagram.

The method of solution involves the construction of the velocity diagram and of an auxiliary acceleration diagram, based on the actual velocities and an arbitrarily assumed zero input acceleration.

The velocity diagram is constructed as shown in fig. 3.4.2,

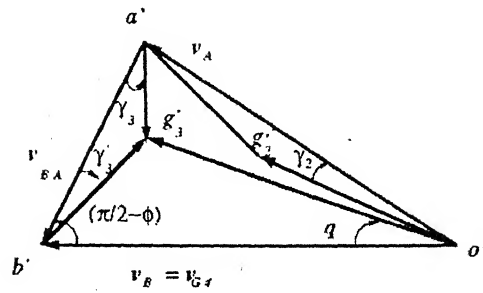


Figure 3.4.2 : Velocity diagram of 3R-1P Mechanism.

From the equation (3.2.2), (3.2.4) and (3.2.5),

$$\theta_3 = -\sin^{-1}\left(\frac{l_1 + l_2 \sin \theta_2}{l_3}\right)$$

$$\dot{\theta}_3 = \omega_3 = -\dot{\theta}_2 \left(\frac{l_2 \cos \theta_2}{l_3 \cos \theta_3} \right)$$

and $\dot{l}_4 = v_{G4} = -l_3 \dot{\theta}_3 \sin \theta_3 - l_2 \dot{\theta}_2 \sin \theta_2$

From fig. 3.4.2,

$$v_{G2} = \frac{v_A}{\cos \gamma_2} \left(\frac{g_2}{l_2} \right) \quad (3.4.5)$$

$$v_{G3} = \overline{o'g'_3} = \overline{o'h'} + \overline{h'g'_3}$$

$$\therefore v_{G3} = \sqrt{v_B^2 + (b'g'_3)^2 - 2v_B b'g'_3 \cos(\pi/2 - \phi - \gamma'_3)} \quad (3.4.6)$$

The auxiliary acceleration diagram is constructed as shown in fig. 3.4.3,

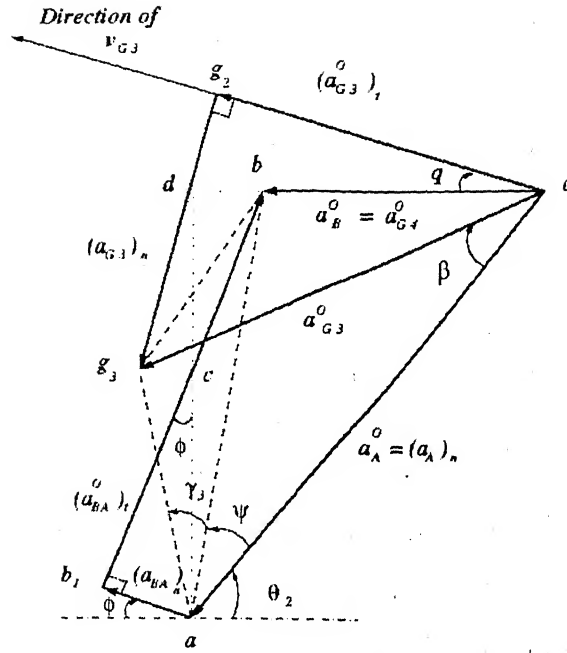


Figure3.4.3 : Acceleration diagram of 3R-1P Mechanism.

From fig.3.4.3,

$$(a_A)_n = l_2 \omega_2^2$$

$$a_{G3}^o = \overline{og_3} = \overline{oa} + \overline{ag_3}$$

$$\therefore a_{G3}^o = \sqrt{(a_A)_n^2 + (ag_3)^2 - 2(a_A)_n(ag_3)\cos(\psi + \gamma_3)} \quad (3.4.7)$$

$$(a_{G3}^o)_t = \overline{og_2} = \overline{og_3} - \overline{g_2g_3}$$

$$\therefore (a_{G3}^o)_t = \sqrt{(a_{G3}^o)^2 + (a_{G3})_n^2 - 2(a_{G3}^o)(a_{G3})_n \cos(\pi/2 + \beta - q - \theta_2)} \quad (3.4.8)$$

$$(a_{BA}^o)_t = \overline{h_1c} + \overline{bc}$$

$$\therefore (a_{BA}^o)_t = \left(\frac{(a_A)_n \sin \theta_2 - (a_{BA})_n \sin \phi \cos \phi}{\cos \phi} \right) \quad (3.4.9)$$

$$\alpha_{3^o} = \frac{(a_{BA}^o)_t}{l_3} \quad (3.4.10)$$

But from the Goodman transformation equations (3.4.3) and (3.4.4), with $i=2$, yield:

Link 2:

$$\alpha_2 = \alpha_{2''} + \frac{\omega_2}{\omega_2} \alpha_2 = \alpha_2 \quad (3.4.11)$$

Link 3:

$$\alpha_3 = \alpha_{3''} + \frac{\omega_3}{\omega_2} \alpha_2 \quad (3.4.12)$$

$$(a_{G3})_t = (a_{G3}^o)_t + \frac{v_{G3}}{\omega_2} \alpha_2 \quad (3.4.13)$$

Link 4:

$$a_4 = a_B^o + \frac{v_4}{\omega_2} \alpha_2 \quad (4.4.13)$$

The corresponding time rates of change of kinetic energy are:

For link 2: $J_{O2} \omega_2 \alpha_2$

For link 3: $m_3 v_{G3} (a_{G3})_t + J_{G3} \omega_3 \alpha_3$

For link 4: $m_4 v_4 a_4$

\therefore The equation (3.4.2) becomes,

$$\frac{dT}{dt} = J_{O2} \omega_2 \alpha_2 + m_3 v_{G3} (a_{G3})_t + J_{G3} \omega_3 \alpha_3 + m_4 v_4 a_4 \quad (3.4.14)$$

The power input of the force system in the phase considered is,

$$\sum \dot{W} = F_4 v_4 + (W_3)_t v_{G3} + (W_2)_t v_{G2} + M_2 \omega_2 \quad (3.4.15)$$

α_2 can be evaluated by equating the equation (3.4.15) and (3.4.16).

From the equation (3.4.12) and (3.4.14), we can evaluate the value of α_3 and a_4 .

b) Dynamic motion Analysis with friction

The effect of friction in hinged joints is negligibly small, whereas that of sliding connections may be quite appreciable. Consideration of friction is thus complicated by a feedback effect: while the friction forces are a function of the accelerations, they themselves affect the accelerations by virtue of their power input, which is equal to the negative product of the force magnitude and the relative speed of the moving parts [7]. Figure 3.4.4 shows a 3R-1P Mechanism.

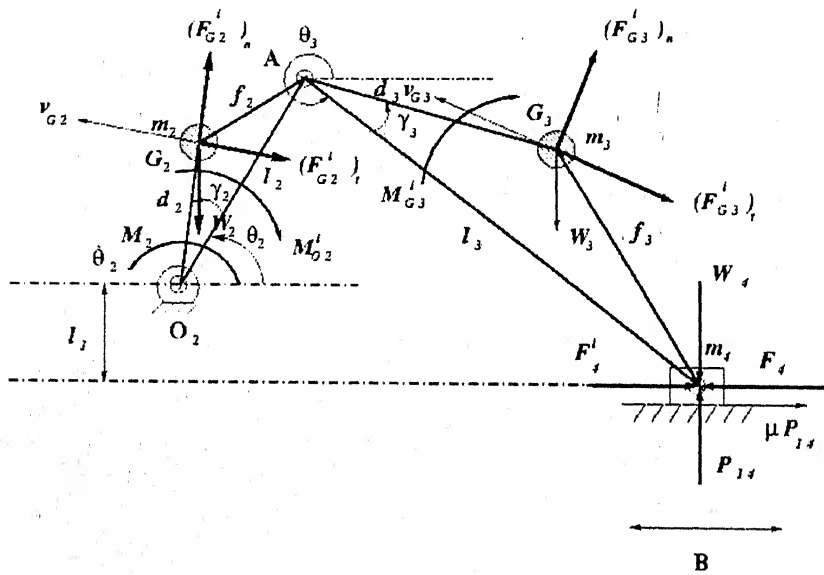


Figure 3.4.4 : Dynamic Motion Analysis of 3R-1P Mechanism with friction.

In fig.3.4.4,

m_j = mass of the j -th link where $j = 2, 3, 4$

G_j = location of the C.G. of the j -th link.

d_j = distance of G_j from a kinematic pair as indicated in fig. 3.4.4

k_j = centroidal radius of gyration of the j -th link.

W_j = weight of the j -th link.

M_{Gj}^i = inertial turning moment of the j -th link

F_{Gj}^i = inertial force of the j -th link.

$(F_{Gj}^i)_n$ = normal component of inertial force of the j -th link.

$(F_{Gj}^i)_t$ = component of inertial force in the direction of v_{Gj} of the j -th link.

P_{ij} = normal force exerted on the j -th link by the i -th link.

where, superscript i represents the inertia ,

$j = 2, 3, 4$. $K = O_2, A, B$.

From the equations (3.4.15) and (3.4.16),

$$\frac{dT}{dt} = J_{O_2} \omega_2 \alpha_2 + m_3 v_{G3} (a_{G3})_t + J_{G3} \omega_3 \alpha_3 + m_4 v_4 a_4$$

$$\sum \wp = F_4 v_4 + (W_3)_t v_{G3} + M_2 \omega_2$$

After equating these equations,

$$\alpha_2 = f(\sum \wp) \quad (3.4.16)$$

Since the static loads and the normal components of the inertia forces are independent of the input acceleration, while the inertia torques and tangential components of the inertia forces are linear functions of it, P_{14} and the frictional power loss $\Delta \sum \wp$ are also linear functions of α_2 ,

$$\therefore \Delta \sum \wp = f(\alpha_2) \quad (3.4.17)$$

The normal side reaction P_{14} is determined by considering the equilibrium of the subassembly consisting of the coupler and the slider and taking moment about A as shown in fig.3.4.4.

$$\therefore \Delta \sum \wp = -\mu P_{14} v_4 \quad (3.4.18)$$

The power input of the force system in the phase considered without friction is,

$$\sum \wp_{ph} = F_4 v_4 + (W_3)_t v_{G3} + (W_2)_t v_{G2} + M_2 \omega_2 \quad (3.4.19)$$

$$\therefore \alpha_2 = f(\sum \phi_{ph} + \Delta \sum \phi) \quad (3.4.20)$$

By plotting the equations ,

$$\alpha_2 = f(\sum \phi) \quad (1)$$

and

$$\alpha_2 = f(\sum \phi_{ph} + \Delta \sum \phi) \quad (2)$$

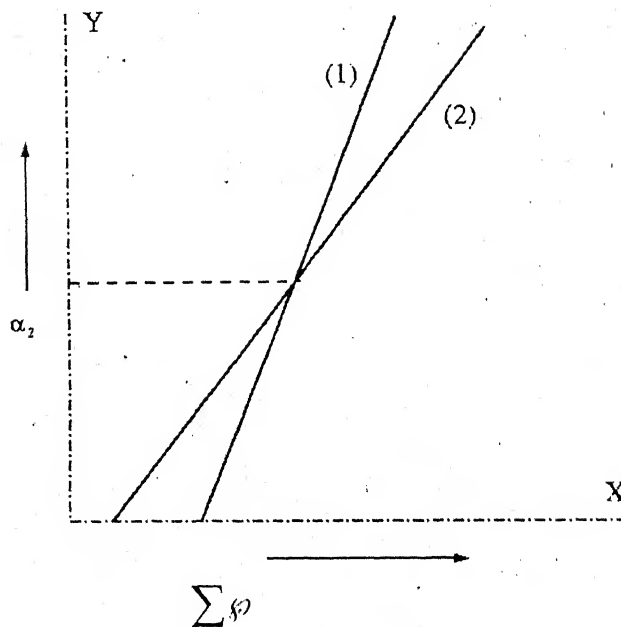


Figure 3.4.5: Acceleration of the Crank Vs Power input of the system.

α_2 is obtained graphically, at the intersection of two lines, as shown in fig. 3.4.5.

3.5 Numerical Examples and Results

Computer programs in C language have been developed for solving the problems. This section illustrates some examples giving the results generated by those programs.

a) Kinematic Analysis

Example: -

A 3R-1P mechanism having crank length, $l_2 = 76.2$ mm, coupler length, $l_3 = 305$ mm, offset distance, $l_1 = 10$ mm and rotates at a speed of 100 rad/sec and an acceleration of 25 rad/sec². Determine the following when the crank angle varies from 0° to 360°.

- 1) Displacements of the coupler and slider
- 2) Velocities of the coupler and slider
- 3) Accelerations of the coupler and slider.

The following sample results are shown: -

- 1) Displacement of the slider (fig.3.5.1)
- 2) Angular displacement of the coupler (fig.3.5.2)
- 3) Velocity of the slider and coupler (fig.3.5.3)
- 4) Acceleration of the slider and coupler (fig.3.5.4)

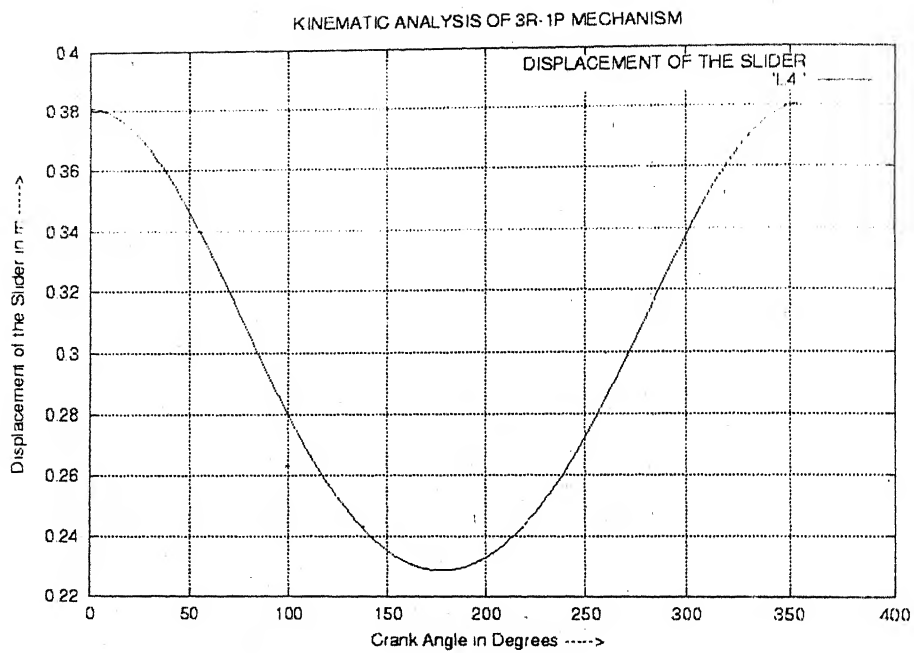


Figure 3.5.1 : Displacement of the Slider Vs Crank Angle.

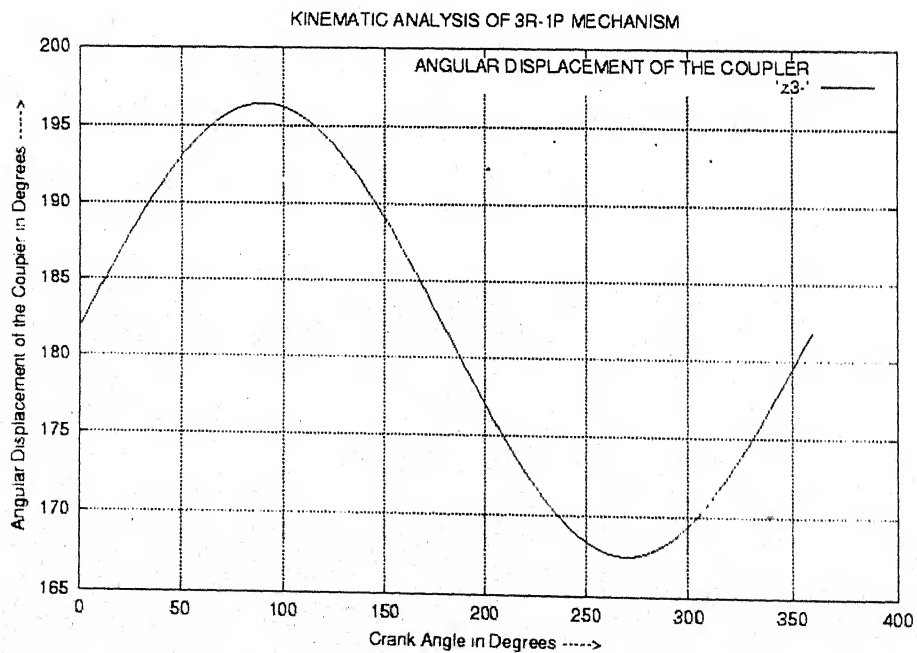


Figure 3.5.2 : Displacement of the Coupler Vs Crank Angle.

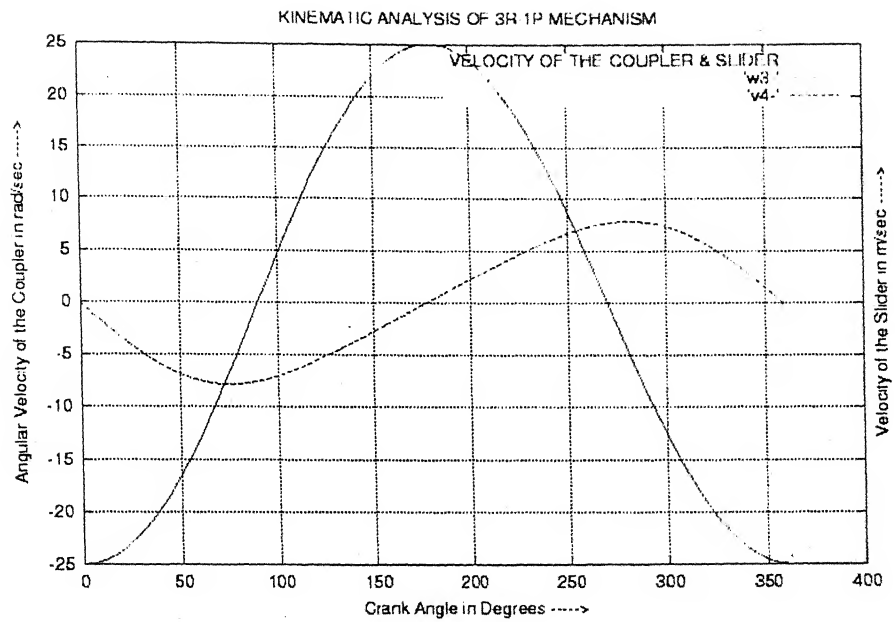


Figure 3.5.3 : Velocity of the Slider and Coupler Vs Crank Angle.

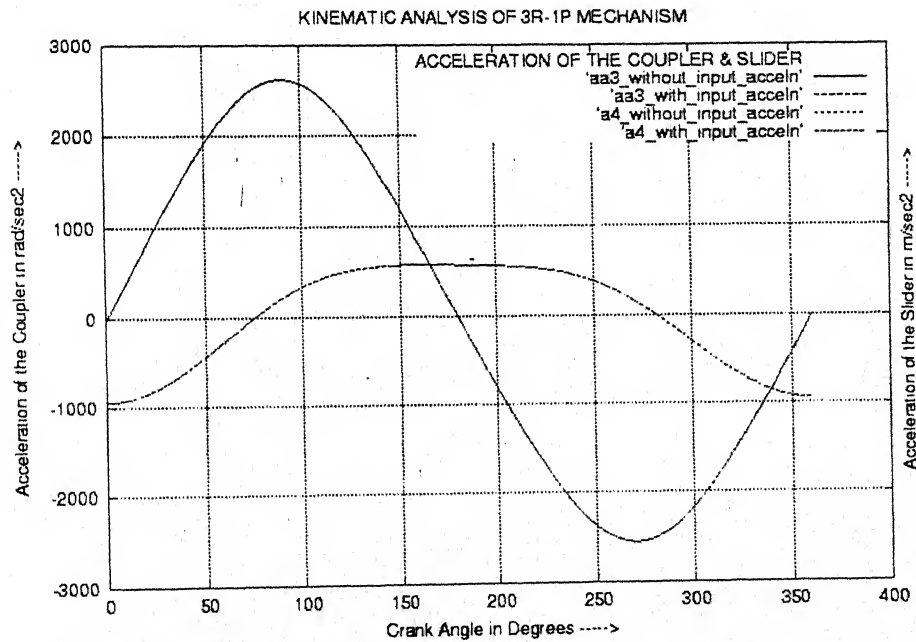


Figure 3.5.4 : Acceleration of the Slider and Coupler Vs Crank Angle.

b) Dynamic Force Analysis

Example: -

A 3R-1P mechanism having crank length, $l_2 = 76.2$ mm, coupler length, $l_3 = 305$ mm, offset distance, $l_1 = 10$ mm and rotates at a speed of 100 rad/sec and an acceleration of 25 rad/sec^2 . Crank is having the following data: $g_2 = 25.4$ mm, $\gamma_2 = 15^\circ$, $m_2 = 0.125$ kg, $k_2 = 23$ mm, $F_2 = 2$ N, $\beta_2 = 10^\circ$. Coupler is having the following data: $g_3 = 102$ mm, $\gamma_3 = 14^\circ$, $m_3 = 0.25$ kg, $k_3 = 114$ mm, $F_3 = 4$ N, $\beta_3 = 20^\circ$, $M_3 = 0.5$ N-m. Slider is having the following data: $m_4 = 0.125$ kg, $F_4 = 5$ N. Determine the following when crank angle varies from 0° to 360° .

- 1) Required turning moment at the crank, M_2 .
- 2) Reaction at the hinge O_2 , P_{O_2} .
- 3) Reaction at the hinge A, P_A .
- 4) Reaction at the hinge B, P_B .

The following sample results are shown: -

- 1) Required turning moment at the crank i.e. M_2 (fig.3.5.5)
- 2) Reaction at the hinge O_2 i.e. P_{O_2} (fig.3.5.6)
- 3) Reaction at the hinge A i.e. P_A (fig.3.5.7)
- 4) Reaction at the hinge B i.e. P_B (fig.3.5.8)

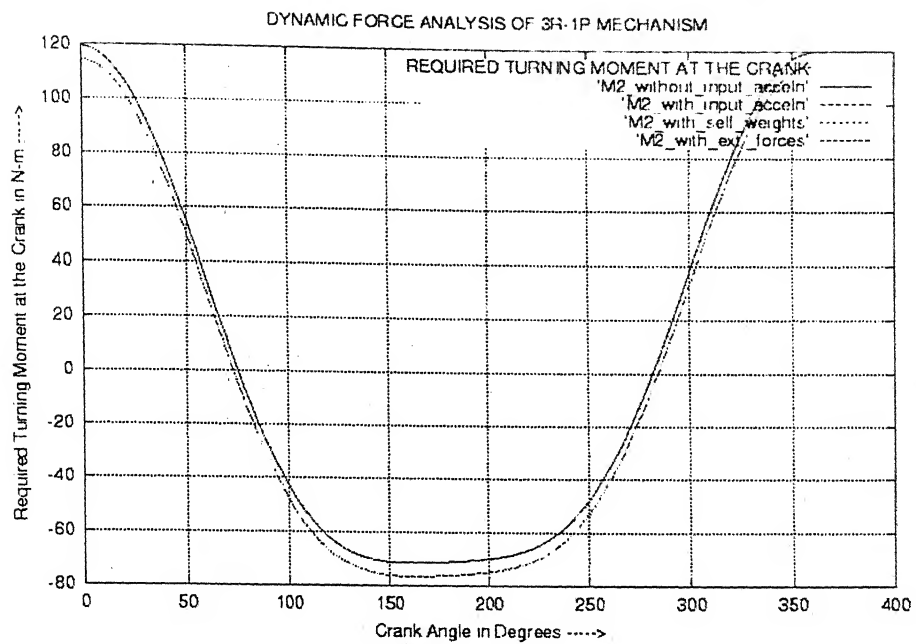


Figure 3.5.5 : Required Turning Moment at the Crank Vs Crank Angle.

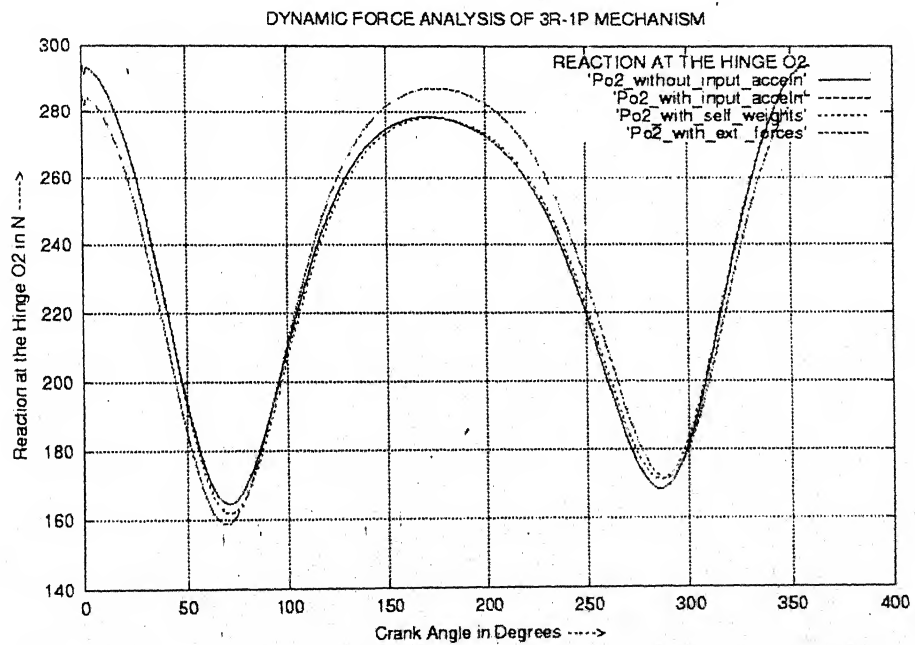


Figure 3.5.6 : Reaction at the hinge O₂ Vs Crank Angle.

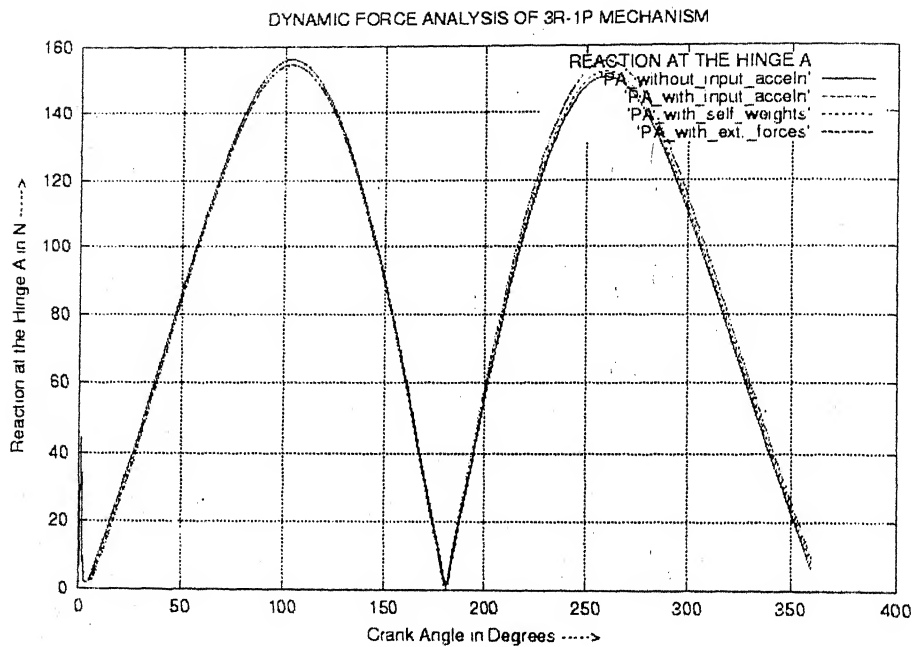


Figure 3.5.7 : Reaction at the hinge A Vs Crank Angle.

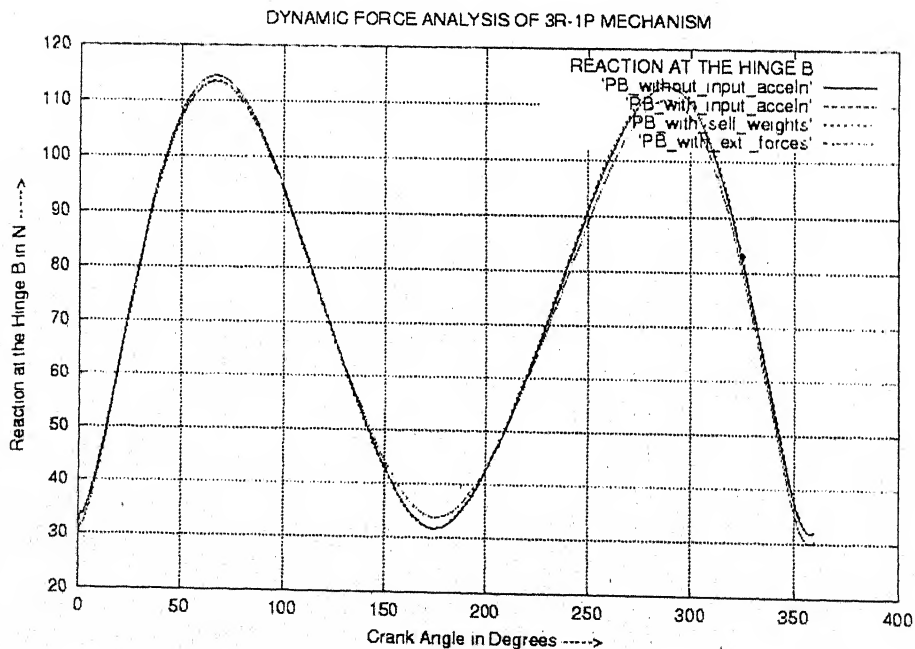


Figure 3.5.8 : Reaction at the hinge B Vs Crank Angle.

b) Dynamic motion analysis without friction

Example: -

A 3R-1P mechanism having crank length, $l_2 = 76.2$ mm, coupler length, $l_3 = 305$ mm, offset distance, $l_1 = 10$ mm and rotates at a speed of 100 rad/sec. Crank is having the following data: $g_2 = 25.4$ mm, $\gamma_2 = 15^\circ$, $m_2 = 0.125$ kg, $k_2 = 23$ mm, $M_2 = 0.5$ N-m. Coupler is having the following data: $g_3 = 102$ mm, $\gamma_3 = 14^\circ$, $m_3 = 0.25$ kg, $k_3 = 114$ mm. Slider is having the following data: $m_4 = 0.125$ kg, $F_4 = 5$ N. Determine the following when crank angle varies from 0° to 360° .

- 1) Acceleration of the crank.
- 2) Acceleration of the coupler.
- 3) Acceleration of the slider.

The following sample results are shown: -

- 1) Acceleration of the crank (fig.3.5.9)
- 2) Acceleration of the coupler (fig.3.5.10)
- 3) Acceleration of the slider (fig.3.5.11)

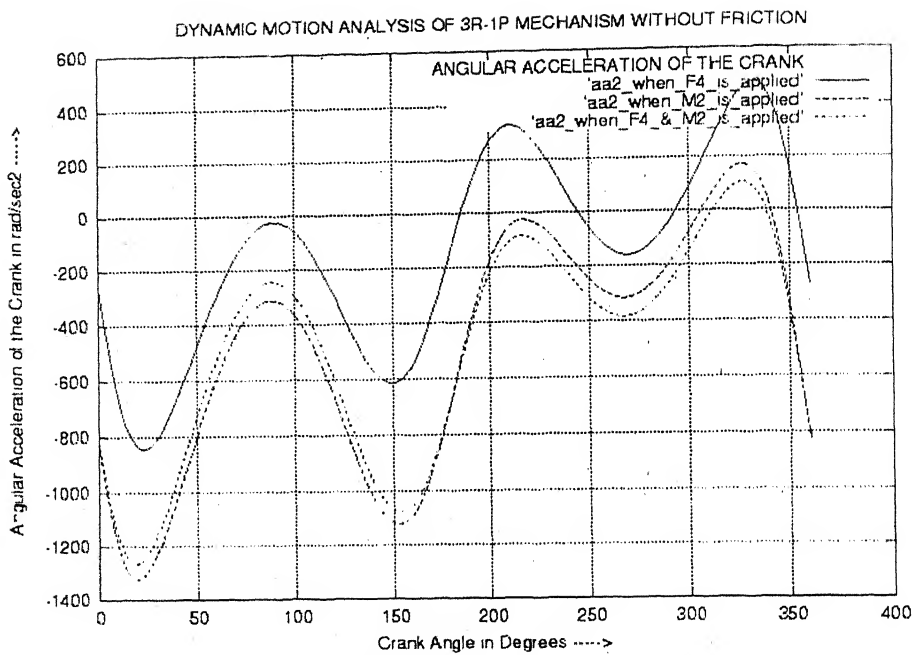


Figure 3.5.9 : Acceleration of the Crank Vs Crank Angle.

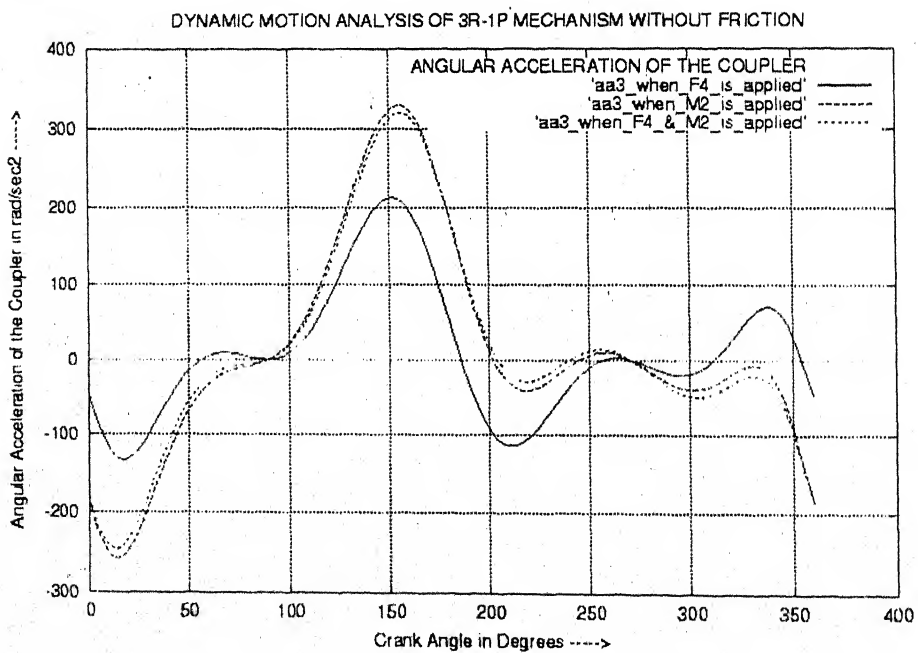


Figure 3.5.10 : Acceleration of the Coupler Vs Crank Angle.

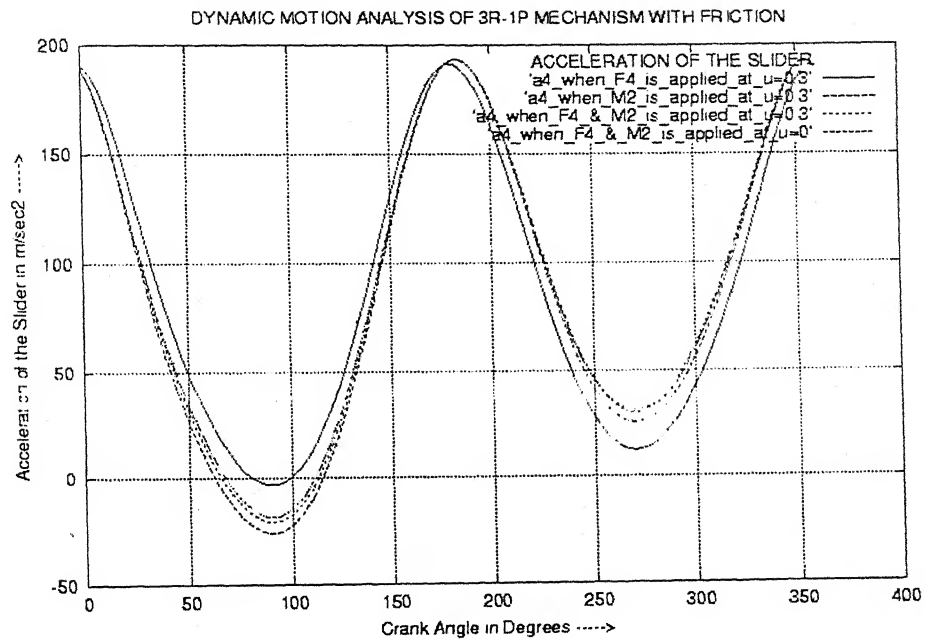


Figure 3.5.11 : Acceleration of the Slider Vs Crank Angle.

c) Dynamic motion analysis with friction

Example: -

A 3R-1P mechanism having crank length, $l_2 = 76.2$ mm, coupler length, $l_3 = 305$ mm, offset distance, $l_1 = 10$ mm and rotates at a speed of 100 rad/sec. Crank is having the following data: $g_2 = 25.4$ mm, $\gamma_2 = 15^\circ$, $m_2 = 0.125$ kg, $k_2 = 23$ mm, $M_2 = 0.5$ N-m. Coupler is having the following data: $g_3 = 102$ mm, $\gamma_3 = 14^\circ$, $m_3 = 0.25$ kg, $k_3 = 114$ mm. Slider is having the following data: $m_4 = 0.125$ kg, $F_4 = 5$ N. The coefficient of friction $\mu = 0.3$. Determine the following when crank angle varies from 0° to 360° .

- 1) Acceleration of the crank.
- 2) Acceleration of the coupler.
- 3) Acceleration of the slider.

The following sample results are shown: -

- 1) Acceleration of the crank (fig.3.5.12)
- 2) Acceleration of the coupler (fig.3.5.13)
- 3) Acceleration of the slider (fig.3.5.14)

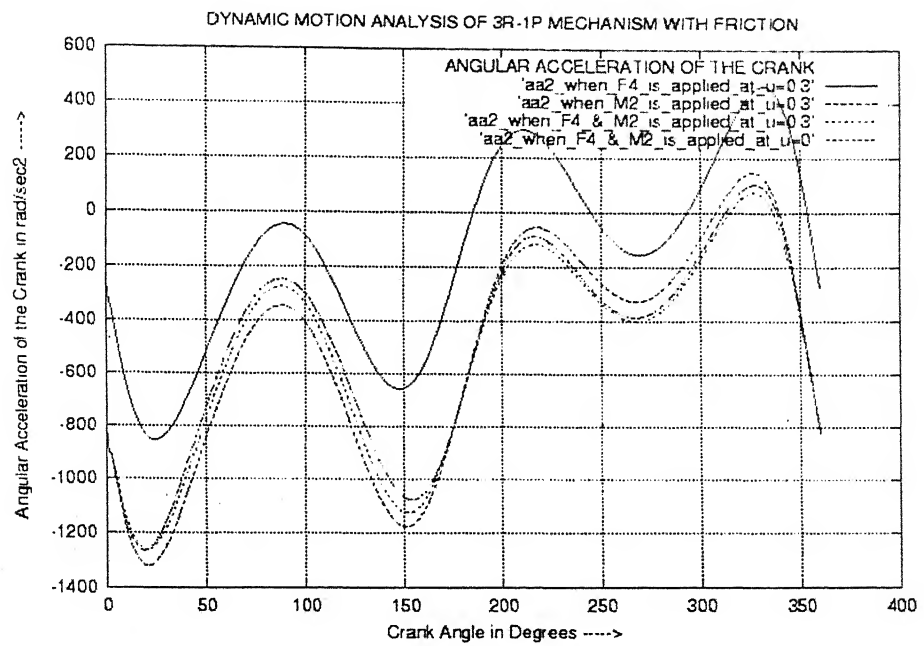


Figure 3.5.12 : Acceleration of the Crank Vs Crank Angle.

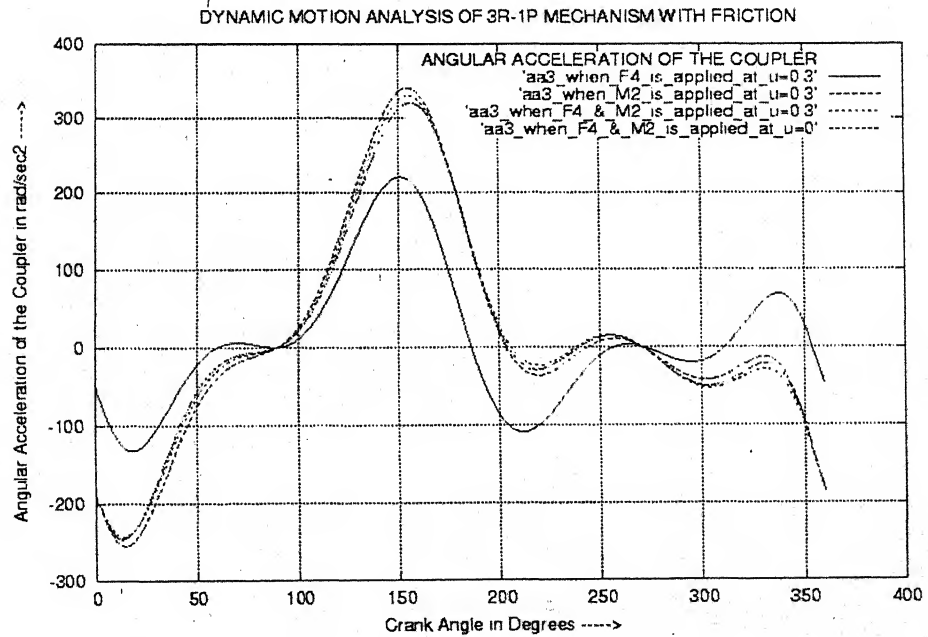


Figure 3.5.13 : Acceleration of the Coupler Vs Crank Angle.

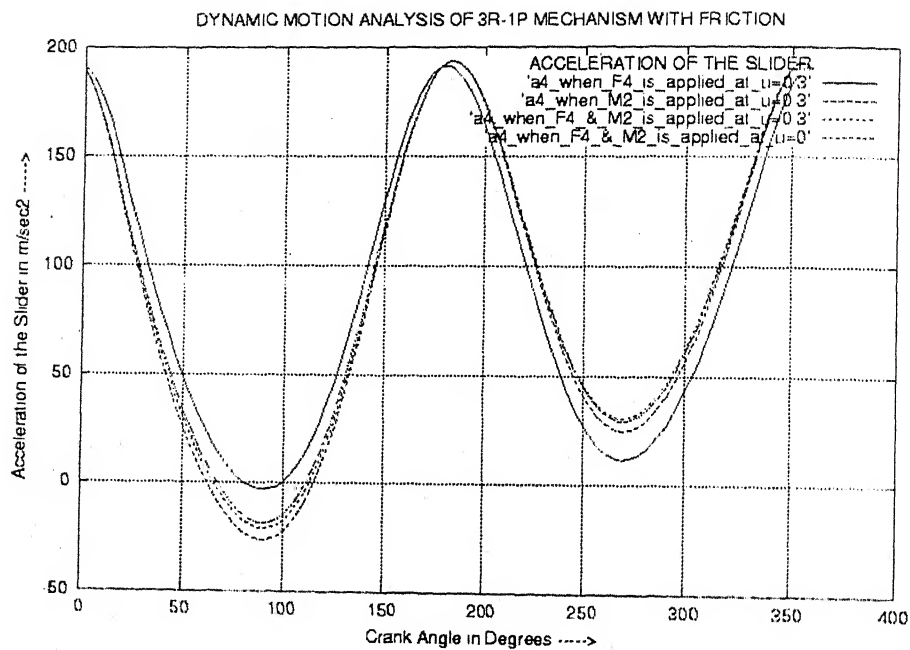


Figure 3.5.14 : Acceleration of the Slider Vs Crank Angle.

Chapter 4

2R-2P Mechanism

4.1 Introduction

There are two types of 2R-2P mechanisms, ordinary and crossed. The ordinary type is derived from the 3R-1P linkage by replacing the turning connection between the coupler and the slider with a sliding pair. Consequently, the ordinary 2R-2P mechanism has one member associated with two sliding pairs, two members with one sliding and one turning pair and one member with two turning pairs. In the crossed type, each link forms one turning and one sliding pair.

Examples of ordinary 2R-2P mechanism are *Elliptical Trammel*, *Scotch-Yoke* mechanism and *Oldham's coupling* and for crossed 2R-2P mechanism is *Rapson's slide*, occasionally used in the steering of ships [4].

Elliptical Trammel is an instrument used for drawing ellipses. This principle is also adopted in the elliptic chuck for the turning of elliptic sections and also in the machining and drilling of elliptic holes [3].

Scotch-Yoke mechanism is one that will give simple harmonic motion. Its early application was on steam pumps, but it is now used as a mechanism on a test machine to simulate vibrations. It is also used as a sine-cosine generator for computing machines [4].

In this chapter we are going to discuss the dynamic force and motion analysis of 2R-2P mechanisms. In *dynamic force analysis* we calculate the forces on various members of a mechanism for a known input motion which is usually determined by experimentation or analytical prediction based on *kinematic analysis* whereas for *dynamic motion analysis* we calculate the acceleration of various links of a mechanism for given forces on the mechanism [5].

4.2 Kinematic Analysis

1) 2R-2P Mechanism

A generalised 2R-2P mechanism for the *kinematic analysis* is shown in fig.4.2.1.1. Slider B is the input link, link 3 (BA) is the coupler and slider A is the output link.

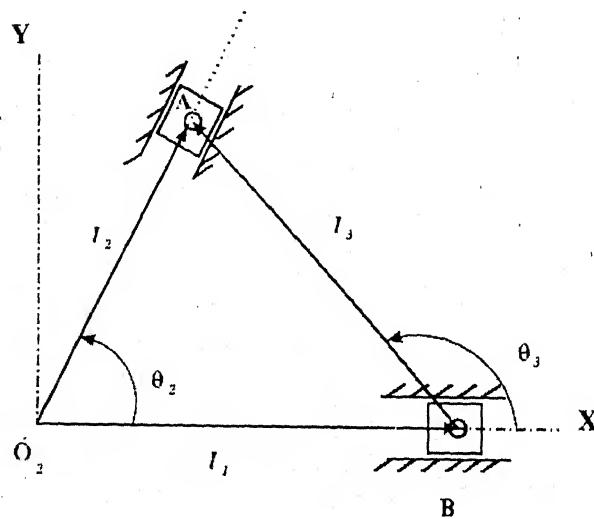


Figure 4.2.1.1 : Kinematic Analysis of a generalised 2R-2P Mechanism.

Using the symbols explained in fig. 4.2.1.1,
the governing loop-closure equation is given by,

$$\vec{l}_1 + \vec{l}_3 = \vec{l}_2 \quad (4.2.1.1)$$

or $\vec{l}_1 + \vec{l}_3 - \vec{l}_2 = 0$

or $l_1 + l_3 e^{i\theta_3} - l_2 e^{i\theta_2} = 0.$

Equating the real and imaginary parts of the above equation separately to zero, we get,

$$l_1 + l_3 \cos\theta_3 - l_2 \cos\theta_2 = 0$$

and $l_3 \sin \theta_3 - l_2 \sin \theta_2 = 0.$

From above equations, we get,

$$l_2 = l_1 \cos \theta_2 \pm \sqrt{l_1^2 \cos^2 \theta_2 - l_1^2 + l_3^2} \quad (4.2.1.2)$$

and $\theta_3 = \cos^{-1} \left(\frac{l_2^2 - l_1^2 - l_3^2}{2l_1 l_3} \right).$ (4.2.1.3)

Differentiating equations (4.2.1.2) and (4.2.1.3) with respect to time,

$$\dot{l}_2 = \dot{l}_1 \left(\frac{\cos \theta_3}{\cos(\theta_2 + \theta_3)} \right) \quad (4.2.1.4)$$

and $\dot{\theta}_3 = \frac{\dot{l}_2 \sin \theta_2}{l_3 \cos \theta_3}.$ (4.2.1.5)

Again differentiating equations (4.2.1.4) and (4.2.1.5) with respect to time,

$$\ddot{l}_2 = \frac{l_3 \dot{\theta}_3^2 + \ddot{l}_1 \cos \theta_3}{\cos(\theta_2 + \theta_3)} \quad (4.2.1.6)$$

and $\ddot{\theta}_3 = \frac{\ddot{l}_2 \sin \theta_2 + l_3 \dot{\theta}_3^2 \sin \theta_3}{l_3 \cos \theta_3}.$ (4.2.1.7)

2) Scotch-Yoke mechanism

The Scotch-Yoke mechanism for the *kinematic analysis* is shown in fig 4.2.2.1. Link 2 ($O_2 A$) is the input crank, link 3 (A) is the slider and l_1 is the offset distance.

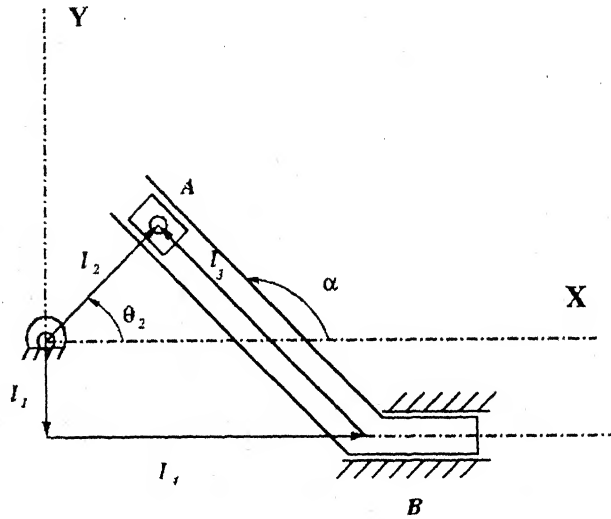


Figure 4.2.2.1 : Kinematic Analysis of a Scotch-Yoke Mechanism.

Using the symbols explained in fig. 4.2.2.1,
the governing loop-closure equation is given by,

$$\vec{l}_1 + \vec{l}_4 + \vec{l}_3 = \vec{l}_2 \quad (4.2.2.1)$$

or $\vec{l}_1 + \vec{l}_4 + \vec{l}_3 - \vec{l}_2 = 0$

or $l_1 e^{i\theta_1} + l_4 + l_3 e^{i\alpha} - l_2 e^{i\theta_2} = 0.$

Equating the real and imaginary parts of above equation separately to zero, we get,

$$l_1 \cos\theta_1 + l_4 + l_3 \cos\alpha - l_2 \cos\theta_2 = 0$$

and $l_1 \sin\theta_1 + l_3 \sin\alpha - l_2 \sin\theta_2 = 0.$

By putting $\theta_1 = -\pi/2$, we get,

$$l_3 = \frac{l_1 + l_2 \sin \theta_2}{\sin \alpha} \quad (4.2.2.2)$$

$$\text{and } l_4 = \frac{l_2 \sin(\alpha - \theta_2) - l_1 \cos \alpha}{\sin \alpha} . \quad (4.2.2.3)$$

Differentiating equations (4.2.2.2) and (4.2.2.3) w. R. T. Time,

$$\dot{l}_3 = \dot{\theta}_2 \left(\frac{l_2 \cos \theta_2}{\sin \alpha} \right) \quad (4.2.2.4)$$

$$\text{and } \dot{l}_4 = -l_2 \dot{\theta}_2 \left(\sin \theta_2 + \frac{\cos \theta_2}{\sin \alpha} \right) . \quad (4.2.2.5)$$

Again differentiating equations (4.2.2.4) and (4.2.2.5) w. R. T. Time,

$$\ddot{l}_3 = \frac{l_2 \ddot{\theta}_2 \cos \theta_2 - l_2 \dot{\theta}_2^2 \sin \theta_2}{\sin \alpha} \quad (4.2.2.6)$$

$$\text{and } \ddot{l}_4 = -l_2 \ddot{\theta}_2 \sin \theta_2 - l_2 \dot{\theta}_2^2 \cos \theta_2 - \ddot{l}_3 \cos \alpha . \quad (4.2.2.7)$$

4.3 Dynamic Force Analysis

1) 2R-2P mechanism

In *dynamic force analysis*, the motion is usually known either by experimentation or analytical predictions based on *kinematic analysis*, the forces at all the kinematic pairs are to be determined. Figure 4.3.1.1 shows a 2R-2P mechanism. The prismatic pairs are assumed to be frictionless.

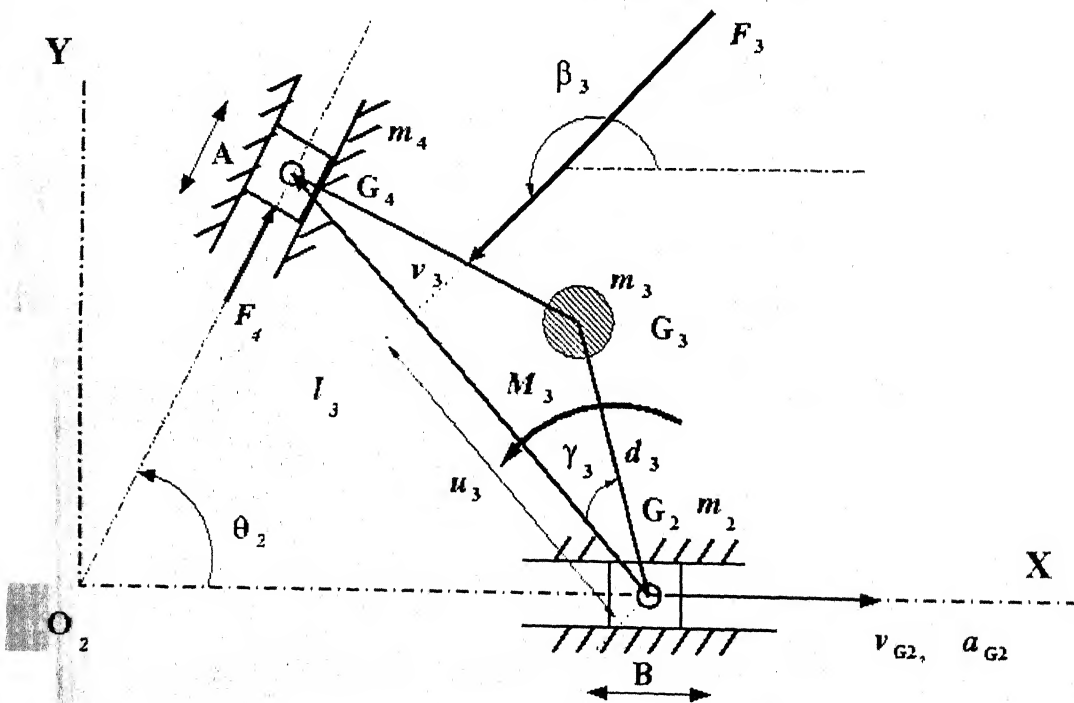


Figure 4.3.1.1 : Dynamic Force Analysis of a generalised 2R-2P Mechanism.

In fig. 4.3.1.1.

m_j = mass of the j -th link where $j = 2, 3, 4$.

G_j = location of the C.G. of the j -th link.

d_j = distance of G_j from a kinematic pair as indicated in fig. 4.3.1.1.

F_j = external force acting on the j -th link at an angle of β_j to the X -axis at a point with local coordination (u_j, v_j) .

$F_{j,x}$ = X -component of F_j .

$F_{j,y}$ = Y -component of F_j

F_j'' = normal force on the j -th link from the fixed link.

M_j = external moment on j -th link.

$P_{K,x}$ = force exerted at the hinge K in the x -direction where $K = B, A$

$P_{K,y}$ = force exerted at the hinge K in the y -direction.

k_j = radius of gyration of the j -th link.

The dynamic equations for each link can be obtained as discussed below :-

1. Slider B: -

Refer to fig.4.3.1.2 as the free-body-diagram of the slider B, with $K = B$ and $j = 2$

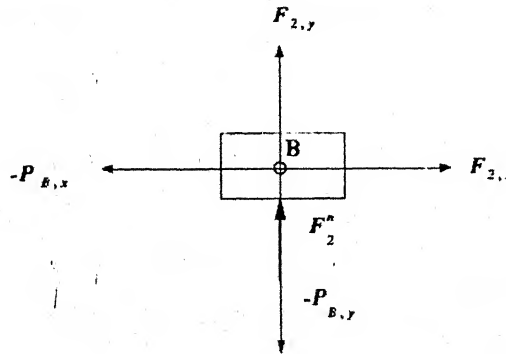


Figure 4.3.1.2 : Free-Body-Diagram of the Slider B for Force Analysis.

Equations of motion for the slider B are,

$$F_{2,x} - P_{B,x} = m_2 a_{G2,x} \quad (4.3.1.1)$$

$$\text{and } F_{2,y} - P_{B,y} = m_2 a_{G2,y} = 0. \quad (\because a_{G2,y} = 0)$$

or $F_{2,1} = F_2''$.

2. Coupler: -

Refer to fig.4.3.1.3 as the free-body-diagram of the coupler, with $K = A, B$ and $j = 3$.

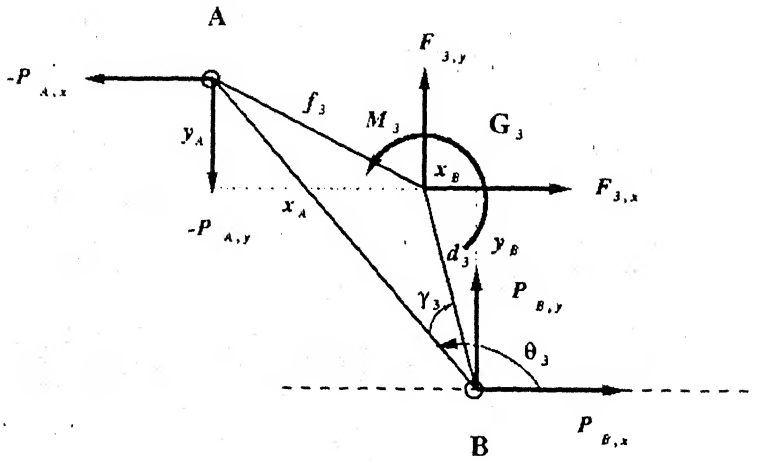


Figure 4.3.1.3 : Free-Body-Diagram of the Coupler for Force Analysis.

From the fig 4.3.1.3,

$$x_A = f_3 \sin(\theta_3 + \gamma'_3 - \pi/2),$$

$$y_A = f_3 \cos(\theta_3 + \gamma'_3 - \pi/2),$$

$$x_B = d_3 \sin(\theta_3 - \gamma_3 - \pi/2),$$

and $y_B = d_3 \cos(\theta_3 - \gamma_3 - \pi/2).$

Equations of motion for the coupler are,

$$\begin{Bmatrix} F_{3,x} \\ F_{3,y} \\ M_3 \end{Bmatrix} + \begin{bmatrix} 1 & 0 & -1 & 0 \\ 0 & 1 & 0 & -1 \\ y_B & x_B & y_A & x_A \end{bmatrix} \begin{Bmatrix} P_{B,x} \\ P_{B,y} \\ P_{A,x} \\ P_{A,y} \end{Bmatrix} = m_3 \begin{Bmatrix} a_{G3,x} \\ a_{G3,y} \\ \ddot{\theta}_3 k_3^2 \end{Bmatrix}. \quad (4.3.1)$$

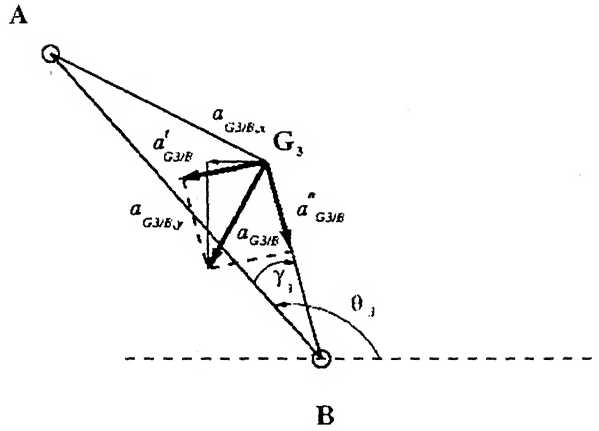


Figure 4.3.1.4 : Diagram of the Coupler for Acceleration Analysis.

Various components of acceleration of G_3 are explained in fig. 4.3.1.4 and the superscripts n , t refer to normal and tangential components, respectively.

From fig. 4.3.1.4,

$$a_{G3,x} = a_{B,x} + a_{G3/B,x} \quad (4.3.1.1)$$

$$\text{and } a_{G3,y} = a_{B,y} + a_{G3/B,y} \quad (4.3.1.2)$$

$$\text{where } a_{G3/B,x} = -a''_{G3/B} \cos(\pi - \theta_3 + \gamma_3) + a'_{G3/B} \sin(\pi - \theta_3 + \gamma_3)$$

$$\text{and } a_{G3/B,y} = a''_{G3/B} \sin(\pi - \theta_3 + \gamma_3) + a'_{G3/B} \cos(\pi - \theta_3 + \gamma_3) .$$

$$a''_{G3/B} = d_3 \dot{\theta}_3^2, a'_{G3/B} = d_3 \ddot{\theta}_3 .$$

Using equations (4.3.1.3) and (4.3.1.4), the right hand side of equation (4.3.1.2) turns out as,

$$m_3 \begin{Bmatrix} a_{G3,x} \\ a_{G3,y} \\ \ddot{\theta}_3 k_3^2 \end{Bmatrix} = m_3 \begin{Bmatrix} -d_3 \dot{\theta}_3^2 \cos(\pi - \theta_3 + \gamma_3) \\ d_3 \dot{\theta}_3^2 \sin(\pi - \theta_3 + \gamma_3) \\ 0 \end{Bmatrix} + m_3 \begin{Bmatrix} 0 & d_3 \sin(\pi - \theta_3 + \gamma_3) & 0 \\ 0 & d_3 \cos(\pi - \theta_3 + \gamma_3) & 0 \\ 0 & k_3^2 & 0 \end{Bmatrix} \begin{Bmatrix} a_{G2} \\ \ddot{\theta}_3 \\ a_{G4} \end{Bmatrix} \quad (4.3.1.5)$$

3. Slider A: -

Refer to fig.4.3.1.5 as the free-body-diagram of the slider A,
with $K = A$ and $j = 4$.

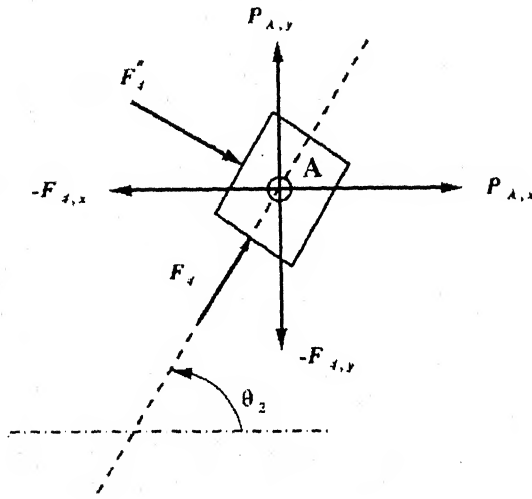


Figure 4.3.1.5 : Free-Body-Diagram of the Slider A for Force Analysis.

Equations of motion for the slider are,

$$\begin{Bmatrix} F_4'' \sin \theta_2 - F_{4,x} \\ -F_4'' \cos \theta_2 - F_{4,y} \end{Bmatrix} + \begin{bmatrix} 1 & 0 \\ 0 & 1 \end{bmatrix} \begin{Bmatrix} P_{A,x} \\ P_{A,y} \end{Bmatrix} = m_4 \begin{Bmatrix} a_{G4} \cos \theta_2 \\ a_{G4} \sin \theta_2 \end{Bmatrix} \quad (4.3.1.6)$$

Combining all equations (4.3.1.1), (4.3.1.2) and (4.3.1.6) one can write,

$$\{F\} + [Q]\{P\} = \{H\} \quad (4.3.1.7)$$

where ,

$$\{F\} = \begin{Bmatrix} F_{2,x} \\ F_{3,x} \\ F_{3,y} \\ M_3 \\ F_4'' \sin \theta_2 - F_{4,x} \\ -F_4'' \cos \theta_2 - F_{4,y} \end{Bmatrix}$$

$$[Q] = \begin{bmatrix} 0 & 0 & -1 & 0 \\ 1 & 0 & -1 & 0 \\ 0 & 1 & 0 & -1 \\ y_B & x_B & y_A & x_A \\ 0 & 0 & 1 & 0 \\ 0 & 0 & 0 & 1 \end{bmatrix}$$

$$\{P\} = \begin{Bmatrix} P_{B,x} \\ P_{B,y} \\ P_{A,x} \\ P_{A,y} \end{Bmatrix}$$

$$\{H\} = \begin{Bmatrix} m_2 a_{G2,x} \\ m_3 a_{G3,x} \\ m_3 a_{G3,y} \\ m_3 \ddot{\theta}_3 k_3^2 \\ m_4 a_{G4} \cos \theta_2 \\ m_4 a_{G4} \sin \theta_2 \end{Bmatrix}$$

But from equations (4.3.1.1), (4.3.1.5) and (4.3.1.6),

$$\{H\} = \{U\} + [\lambda] \{\ddot{\theta}\}, \quad (4.3.1.8)$$

where,

$$\{U\} = \begin{Bmatrix} 0 \\ -d_3 \dot{\theta}_3^2 \cos(\pi - \theta_3 + \gamma_3) \\ d_3 \dot{\theta}_3^2 \sin(\pi - \theta_3 + \gamma_3) \\ 0 \\ 0 \\ 0 \end{Bmatrix}$$

$$[\lambda] = \begin{bmatrix} m_2 [1 & 0 & 0] \\ m_3 \begin{bmatrix} 0 & d_3 \sin(\pi - \theta_3 + \gamma_3) & 0 \\ 0 & d_3 \cos(\pi - \theta_3 + \gamma_3) & 0 \\ 0 & k_3^2 & 0 \end{bmatrix} \\ m_4 \begin{bmatrix} 0 & 0 & \cos \theta_2 \\ 0 & 0 & \sin \theta_2 \end{bmatrix} \end{bmatrix}$$

$$\{\ddot{\theta}\} = \begin{Bmatrix} a_{G2} \\ \ddot{\theta}_3 \\ a_{G4} \end{Bmatrix}$$

From equation (4.3.1.7) we can evaluate the hinge reactions i.e. P_A and P_B for the given motion and external forces.

2) Scotch-Yoke Mechanism

In *dynamic force analysis*, the motion is usually known either by experimentation or analytical predictions based on *kinematic analysis*, the forces at all the kinematic pairs are to be determined [5]. Figure 4.3.2.1 shows a Scotch-Yoke mechanism. The prismatic pairs are assumed to be frictionless.

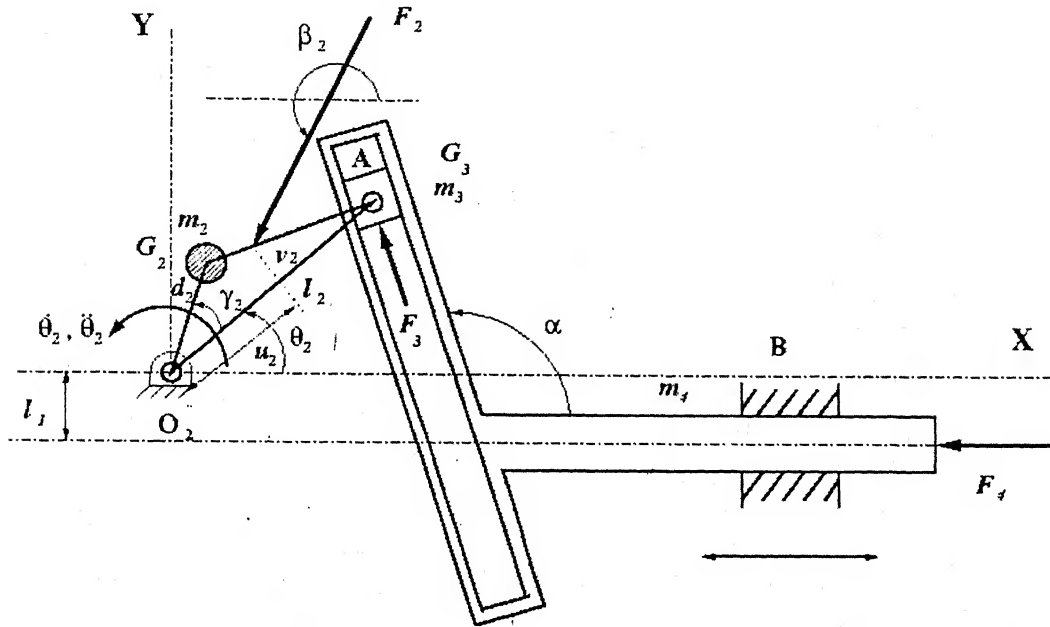


Figure 4.3.2.1 : Dynamic Force Analysis of Scotch-Yoke Mechanism.

In fig. 4.3.2.1,

m_j = mass of the j -th link where $j = 2, 3, 4$.

G_j = location of the C.G. of the j -th link.

d_j = distance of G_j from a kinematic pair as indicated in fig. 4.3.2.1.

F_j = external force acting on the j -th link at an angle of β_j to the X -axis at a point with local coordination (u_j, v_j) .

$F_{j,x}$ = X -component of F_j .

$F_{j,y}$ = Y -component of F_j .

F_j^u = normal force on the j -th link from the fixed link.

M_j = external moment on j -th link.

$P_{ij,x}$ = force exerted on the j -th link by the i -th link in the x -direction where, $i = 1, 2, 3$.

$P_{ij,y}$ = force exerted on the j -th link by the i -th link in the y -direction.

$P_{K,x}$ = force exerted at the hinge K in the x -direction where $K = O_2, A$

$P_{K,y}$ = force exerted at the hinge K in the y -direction.

k_j = radius of gyration of the j -th link.

The dynamic equations for each link can be obtained as discussed below :-

1. Crank:-

Refer to fig.4.3.2. 2 as the free-body-diagram of the crank,

with $i = 1, 3$, $j = 2$, $K = O_2, A$.

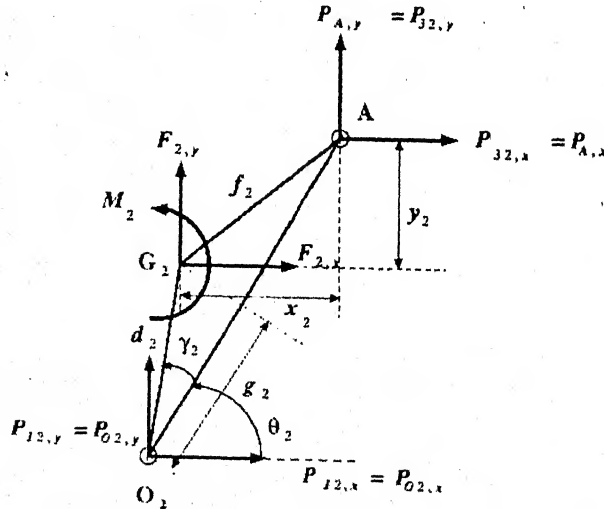


Figure 4.3.2.2 : Free-Body-Diagram of the Crank for Force Analysis.

From fig. 4.3.2.2,

$$x_2 = d_2 \sin \gamma_2 \sin \theta_2 + (l_2 - g_2) \cos \theta_2$$

and
$$y_2 = (l_2 - g_2) \sin \theta_2 - d_2 \sin \gamma_2 \cos \theta_2 .$$

Equations of motion for the crank are,

$$\begin{Bmatrix} F_{2,x} \\ F_{2,y} \\ M_2 \end{Bmatrix} + \begin{bmatrix} 1 & 0 & 1 & 0 \\ 0 & 1 & 0 & 1 \\ d_2 \sin(\theta_2 + \gamma_2) & -d_2 \cos(\theta_2 + \gamma_2) & -y_2 & x_2 \end{bmatrix} \begin{Bmatrix} P_{O2,x} \\ P_{O2,y} \\ P_{A,x} \\ P_{A,y} \end{Bmatrix} = m_2 \begin{Bmatrix} a_{G2,x} \\ a_{G2,y} \\ \ddot{\theta}_2 k_2^2 \end{Bmatrix} \quad (4.3.2.1)$$

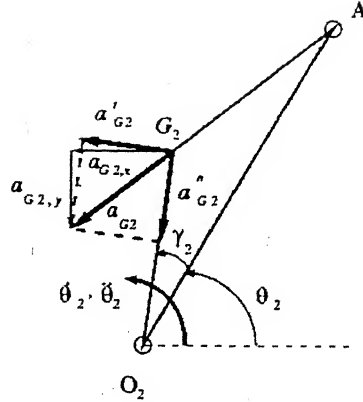


Figure 4.3.2.3 : Diagram of the Crank for Acceleration Analysis.

Various components of acceleration of G_2 are explained in fig. 4.3.2.3 and the superscripts n, t refer to normal and tangential components, respectively.

From fig. 4.3.2.3,

$$a_{G2,x} = a''_{G2} \cos(\theta_2 + \gamma_2) + a'_{G2} \sin(\theta_2 + \gamma_2) \quad (4.3.2.2)$$

$$\text{and } a_{G2,y} = a''_{G2} \sin(\theta_2 + \gamma_2) - a'_{G2} \cos(\theta_2 + \gamma_2) . \quad (4.3.2.3)$$

where $a''_{G2} = d_2 \dot{\theta}_2^2$, $a'_{G2} = d_2 \ddot{\theta}_2$.

Using equations (4.3.2.2) and (4.3.2.3), the right hand side of equation (4.3.2.1) turns out as,

$$m_2 \begin{Bmatrix} a_{G2,x} \\ a_{G2,y} \\ \ddot{\theta}_2 k_2^2 \end{Bmatrix} = m_2 \begin{Bmatrix} d_2 \dot{\theta}_2^2 \cos(\theta_2 + \gamma_2) \\ d_2 \dot{\theta}_2^2 \sin(\theta_2 + \gamma_2) \\ 0 \end{Bmatrix} + m_2 \begin{bmatrix} d_2 \sin(\theta_2 + \gamma_2) & 0 & 0 \\ -d_2 \cos(\theta_2 + \gamma_2) & 0 & 0 \\ k_2^2 & 0 & 0 \end{bmatrix} \begin{Bmatrix} \ddot{\theta}_2 \\ a_{G3} \\ a_{G4} \end{Bmatrix} \quad (4.3.2.4)$$

2. Slider: -

Refer to fig.4.3.2.4 as the free-body-diagram of the slider,
with $j = 3$, $K = A$.

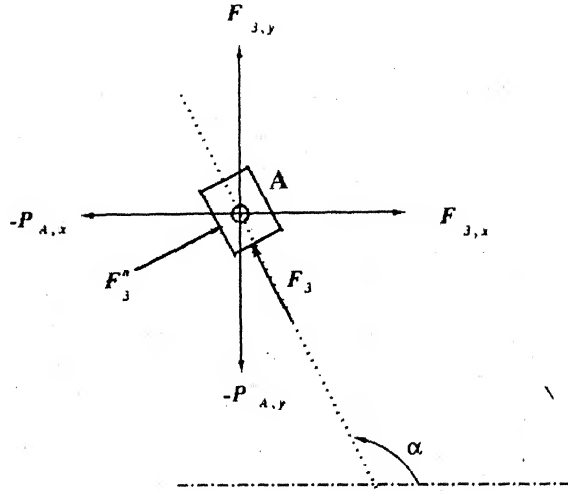


Figure 4.3.2.4 : Free-Body-Diagram of the Slider for Force Analysis.

Equations of motion for the slider are,

$$\begin{Bmatrix} F_{3,x} + F_3'' \sin \alpha \\ F_{3,y} + F_3'' \cos \alpha \end{Bmatrix} + \begin{bmatrix} -1 & 0 \\ 0 & -1 \end{bmatrix} \begin{Bmatrix} P_{A,x} \\ P_{A,y} \end{Bmatrix} = \begin{Bmatrix} m_3 a_{G3} \cos \alpha \\ m_3 a_{G3} \sin \alpha \end{Bmatrix} \quad (4.3.2.5)$$

3.Yoke: -

Refer to fig.4.3.2.5 as the free-body-diagram of the yoke,
with $j = 4$, $K = B$.

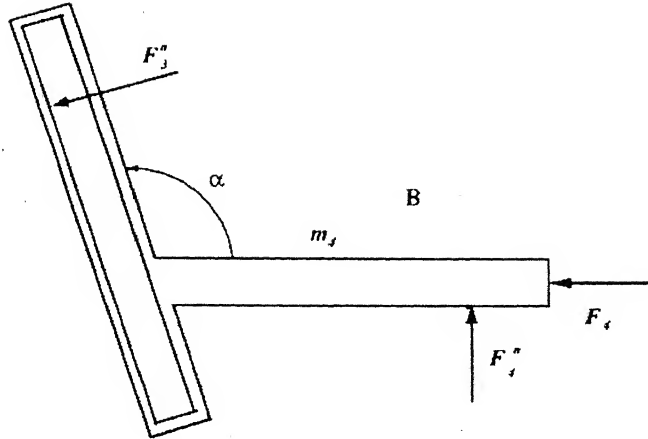


Figure 4.3.2.5 : Free-Body-Diagram of the Yoke for Force Analysis.

From fig. 4.3.2.5,

$$-F_4 - F_3^a \cos(\alpha - \pi/2) = m_4 a_{G4,x}$$

and $F_4^a - F_3^a \sin(\alpha - \pi/2) = m_4 a_{G4,y} = 0.$

By using the above equations, equation (4.3.2.5) becomes,

$$\begin{Bmatrix} F_{3,x} + F_4 \sin \alpha / \cos(\alpha - \pi/2) \\ F_{3,y} + F_4 \cos \alpha / \cos(\alpha - \pi/2) \end{Bmatrix} + \begin{bmatrix} -1 & 0 \\ 0 & -1 \end{bmatrix} \begin{Bmatrix} P_{A,x} \\ P_{A,y} \end{Bmatrix} = \begin{Bmatrix} m_3 a_{G3} \cos \alpha + m_4 a_{G4} \sin \alpha / \cos(\alpha - \pi/2) \\ m_3 a_{G3} \sin \alpha \end{Bmatrix} \quad (4.3.2.6)$$

Combining all equations (4.3.2.1) and (4.3.2.6) one can write,

$$\{F\} + [Q]\{P\} = \{H\} \quad (4.3.2.7)$$

where ,

$$\{F\} = \begin{Bmatrix} F_{2,x} \\ F_{2,y} \\ M_2 \\ F_{3,x} + F_3'' \sin \alpha \\ F_{3,y} + F_3'' \cos \alpha \end{Bmatrix}$$

$$[Q] = \begin{bmatrix} 1 & 0 & 1 & 0 \\ 0 & 1 & 0 & 1 \\ d_2 \sin(\theta_2 + \gamma_2) & -d_2 \cos(\theta_2 + \gamma_2) & -y_2 & -x_2 \\ 0 & 0 & -1 & 0 \\ 0 & 0 & 0 & -1 \end{bmatrix}$$

$$\{P\} = \begin{Bmatrix} P_{O2,x} \\ P_{O2,y} \\ P_{A,x} \\ P_{A,y} \end{Bmatrix}$$

But from the equations (4.3.2.1), (4.3.2.4) and (4.3.2.5),

$$\{H\} = \{U\} + [\lambda] \{\ddot{\theta}\}. \quad (4.3.2.8)$$

where,

$$\{U\} = \begin{Bmatrix} m_2 d_2 \dot{\theta}_2^2 \cos(\theta_2 + \gamma_2) \\ m_2 d_2 \dot{\theta}_2^2 \sin(\theta_2 + \gamma_2) \\ 0 \\ 0 \\ 0 \end{Bmatrix}$$

$$[\lambda] = \begin{bmatrix} \begin{matrix} d_2 \sin(\theta_2 + \gamma_2) & 0 & 0 \\ m_2 [-d_2 \cos(\theta_2 + \gamma_2) & 0 & 0] \\ k_2^2 & 0 & 0 \end{matrix} \\ \begin{matrix} 0 & m_3 \cos \alpha & m_4 \sin \alpha / \cos(\alpha - \pi/2) \\ m_3 [0 & \sin \alpha & 0] \end{matrix} \end{bmatrix}$$

$$\{\ddot{\theta}\} = \begin{Bmatrix} \ddot{\theta}_2 \\ a_{G3} \\ a_{G4} \end{Bmatrix}$$

From the above equation (4.3.2.6) we can evaluate the driving torque and the hinge reactions i.e. M_2 and P_{O2} , P_A for the given motion and external forces. Also we can evaluate F_4 for a given torque M_2 .

4.4 Dynamic Motion Analysis

In *dynamic motion analysis*, the acceleration behaviour of each member of a mechanism is to be determined for a prescribed input force and moment and instantaneous velocities. The *Rate-of-change-of-energy Method* is used for motion analysis. It is based directly on the instantaneous energy balance [5].

a) Dynamic Motion Analysis without friction

Figure 4.4.1 shows a generalised 2R-2P mechanism.

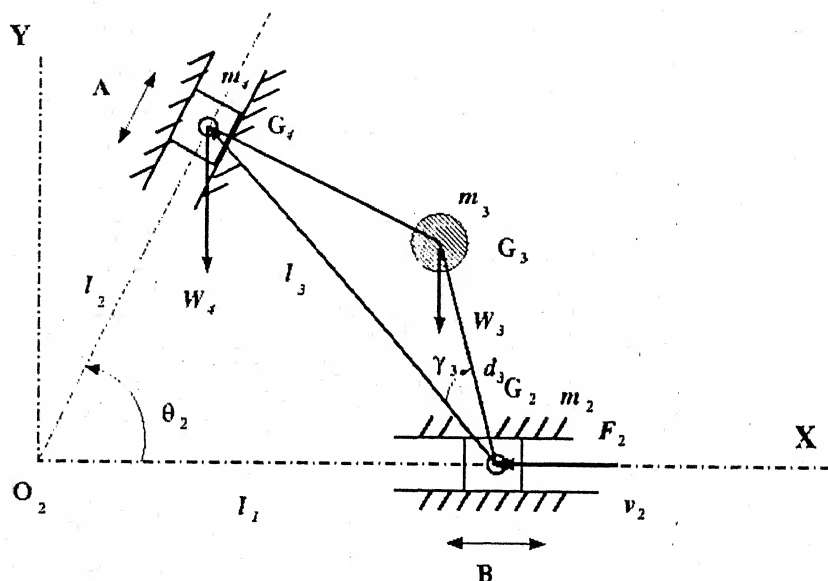


Figure 4.4.1 : Dynamic Motion Analysis of 2R-2P Mechanism without friction.

In fig.4.4.1,

m_j = mass of the j -th link where $j = 2, 3, 4$.

G_j = location of the C.G. of the j -th link.

d_j = distance of G_j from a kinematic pair as indicated in fig. 4.4.1

M_j = external moment on j -th link

W_j = weight of the j -th link.

k_j = radius of gyration of the j -th link.

The total K.E. of a mechanism can be expressed as,

$$T = \frac{1}{2} \sum^r J_o \omega^2 + \frac{1}{2} \sum^s m V^2 + \frac{1}{2} \sum^f m V_G^2 + \frac{1}{2} \sum^f J_G \omega^2. \quad (4.4.1)$$

where, r , s , and f refer to rotating, sliding, and floating links; J_o is the moment of inertia of a rotating link about an axis passing through the hinge; V_G the velocity of the C.G. of a floating link; and J_G the moment of inertia of the floating link about the axis passing through the C.G [5].

The time rate of change of the total kinetic energy of the mechanism is equal to the power input of the force system acting on it [7].

It is expressed mathematically by,

$$\sum \dot{\phi} = \frac{dT}{dt} = \sum^r J_o \omega \alpha + \sum^s m V_a + \sum^f m V_G (a_G)_t + \sum^f J_G \omega \alpha. \quad (4.4.2)$$

where, $(a_G)_t$ is the tangential component of the acceleration of G , i.e., the component of a_G in the direction of V_G

From Goodman transformation equations (J. Hirschhorn [4], p.123) in the form applicable to mechanisms with a sliding input link,

$$a_l = a_{l''} + \frac{v_l}{v_i} a_i \quad (4.4.3)$$

$$\alpha_l = \alpha_{l''} + \frac{\omega_l}{v_i} a_i \quad (4.4.4)$$

$$\text{and } (a_G)_t = (a_{G''})_t + \frac{v_G}{v_i} a_i. \quad (4.4.5)$$

where, α_l = angular acceleration of the link l .

a_i = acceleration of the input link i .

$\alpha_{l''}$ = angular acceleration of the link l obtained from an auxiliary acceleration analysis based on actual velocities but with zero input acceleration.

ω_l = angular velocity of the link l .

v_l = velocity of the link l .

v_i = velocity of the input link i .

$(a_G)_t$ = component of acceleration a_G in the direction of v_G .

$(a_{G''})_t$ = component of acceleration a_G in the direction of v_G from the auxiliary acceleration diagram.

The method of solution involves the construction of the velocity diagram and of the auxiliary acceleration diagram, based on the actual velocities and an arbitrarily assumed zero input acceleration.

The velocity diagram is constructed as shown in fig.4.4. 2,

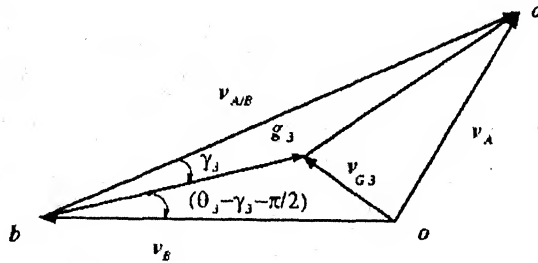


Figure 4.4.2 : Velocity diagram of a 2R-2P Mechanism.

From equations (4.2.1.4) and (4.2.1.5),

$$l_2 = v_4 = l_1 \left(\frac{\cos \theta_3}{\cos(\theta_2 + \theta_3)} \right)$$

and $\dot{\theta}_3 = \omega_3 = \frac{l_2 \sin \theta_2}{l_3 \cos \theta_3}.$

From fig.4.4.2,

$$v_{G3} = \overline{og_3} = \overline{oh} + \overline{hg_3}$$

$$\therefore v_{G3} = \sqrt{v_B^2 + (hg_3)^2 - 2v_B hg_3 \cos(\theta_3 - \gamma_3 - \pi/2)} \quad (4.4.6)$$

The auxiliary acceleration diagram is constructed as shown in fig. 4.4.3,

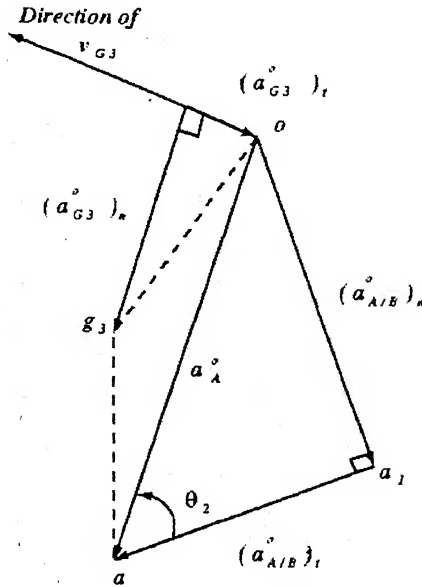


Figure 4.4.3 : Auxiliary acceleration diagram of a 2R-2P Mechanism

From fig 4.4.3,

$$(a_{A/B})_n = l_3 \omega_3^2$$

$$(a_{G3})_t = \overline{bo} = \overline{bg_3} - \overline{og_3}$$

$$\alpha_{3''} = \frac{(a_{BA})_t}{l_3} \quad (4.4.7)$$

But from the Goodman transformation equations (4.5.3), (4.5.4) and (4.5.5), with $i=2$, yield:

Link 2:

$$a_2 = a_{2''} + \frac{v_2}{v_2} a_2 = a_{G2} \quad (4.4.8)$$

Link 3:

$$\alpha_3 = \alpha_3 + \frac{\omega_3}{v_2} a_{G2} \quad (4.4.9)$$

$$(a_{G3})_t = (a_{G3}^o)_t + \frac{v_{G3}}{v_2} a_{G2} \quad (4.4.10)$$

Link 4:

$$a_{G4} = a_4^o + \frac{v_4}{v_2} a_{G2} \quad (4.4.11)$$

The corresponding time rates of change of kinetic energy are:

For link 2: $m_2 v_2 a_{G2}$

For link 3: $m_3 v_{G3} (a_{G3})_t + J_{G3} \omega_3 \alpha_3$

For link 4: $m_4 v_4 a_{G4}$

Equation (4.4.2) becomes,

$$\frac{dT}{dt} = m_2 v_2 \dot{a}_{G2} + m_3 v_{G3} (a_{G3})_t + J_{G3} \omega_3 \alpha_3 + m_4 v_4 a_{G4} \quad (4.4.12)$$

The power input of the force system in the phase considered is,

$$\sum \dot{W} = F_2 v_2 + (W_3)_t v_{G3} + W_4 v_4 \quad (4.4.13)$$

a_{G2} can be evaluated by equating equations (4.4.12) and (4.4.13).

From equations (4.4.9) and (4.4.11), we can evaluate the value of α_3 and a_{G4} .

b) Dynamic motion Analysis with friction

The effect of friction in hinged joints is negligibly small, whereas that of sliding connections may be quite appreciable. Consideration of friction is thus complicated by a feedback effect: while the friction forces are a function of the accelerations, they themselves affect the accelerations by virtue of their power input, which is equal to the negative product of the force magnitude and the relative speed of the moving parts [5]. Figure 4.4.4 shows a 2R-2P mechanism

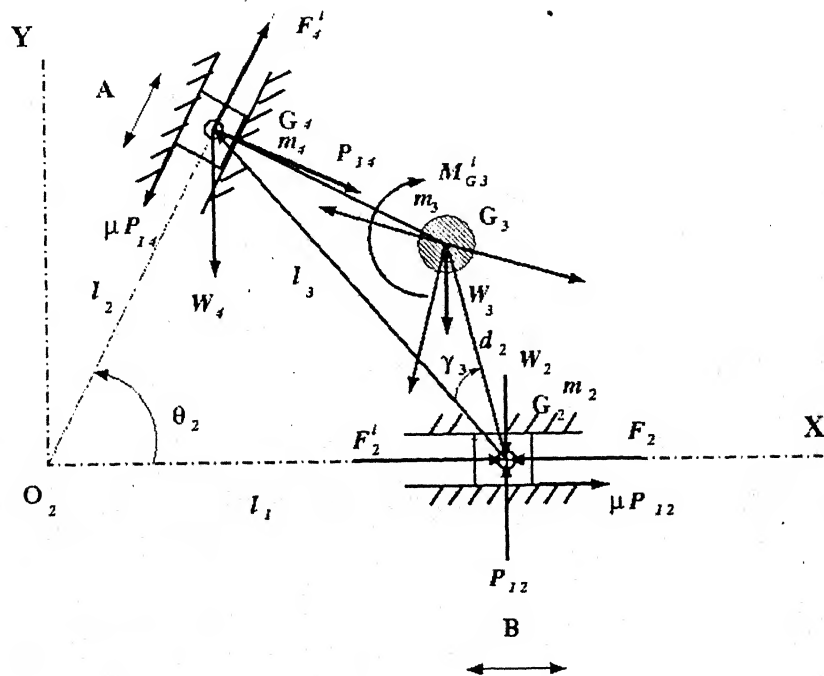


Figure 4.4.4 : Dynamic Motion Analysis of 2R-2P Mechanism with friction.

In fig.4.4.4,

m_j = mass of the j -th link where $j = 2,3,4$.

G_j = location of the C.G. of the j -th link.

d_j = distance of G_j from a kinematic pair as indicated in fig. 4.4.1.

M_j = external moment on j -th link

W_j = weight of the j -th link.

k_j = radius of gyration of the j -th link.

M_{Gj}^i = inertial moment of the j -th link

F_{Gj}^i = inertial force of the j -th link.

$(F_{Gj}^i)_n$ = normal component of inertial force of the j -th link.

$(F_{Gj}^i)_t$ = component of inertial force in the direction of v_{Gj} of the j -th link.

where, superscript i represents the inertia.

From equations (4.4.12) and (4.4.13),

$$\frac{dT}{dt} = m_2 v_2 a_{G2} + m_3 v_{G3} (a_{G3})_t + J_{G3} \omega_3 \alpha_3 + m_4 v_4 a_{G4}$$

$$\sum \phi = F_2 v_2 + (W_3)_t v_{G3} + W_4 v_4$$

After equating these equations,

$$a_2 = f(\sum \phi) \quad (4.4.1)$$

Since the static loads and the normal components of the inertia forces are independent of the input acceleration, while the inertia torques and tangential components of the inertia forces are linear functions of it, P_{12} , P_{14} and the frictional power loss $\Delta \sum \phi$ are also linear functions of a_2 [7],

$$\therefore \Delta \sum \phi = f(a_2) \quad (4.4.2)$$

The normal side reaction P_{12} and P_{14} is determined by considering the equilibrium of the subassembly consisting of the coupler and the slider and taking moments about A and B as shown in fig 4.5.4.

$$\therefore \Delta \sum \phi = -\mu_2 P_{12} v_2 - \mu_4 P_{14} v_4 \quad (4.4.3)$$

The power input of the force system in the phase considered without friction is,

$$\sum \phi_{ph} = F_2 v_2 + (W_3)_t v_{G3} + W_4 v_4 \quad (4.4.4)$$

$$\therefore a_2 = f(\sum \phi_{ph} + \Delta \sum \phi) \quad (4.4.1)$$

By plotting equations,

$$\alpha_2 = f(\sum \phi) \quad (1)$$

and

$$\alpha_2 = f(\sum \phi_{ph} + \Delta \sum \phi) \quad (2)$$

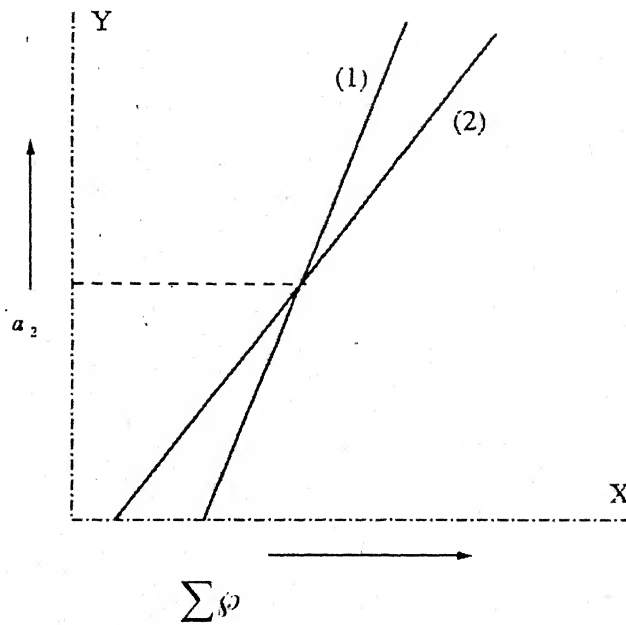


Figure 4.4.5 : Acceleration of the Slider B Vs Power input of the system.

a_2 is obtained graphically, at the intersection of two lines, as shown in fig. 4.4.5.

4.5 Numerical Examples and Results

Computer programs in C language have been developed for solving the problems. This section illustrates some examples giving the results generated by those programs.

a) Kinematic Analysis

1. 2R-2P mechanism

Example: -

A 2R-2P mechanism having coupler length, $l_3 = 76.2\text{mm}$, $\theta_2 = 60^\circ$ and slider B moves at a speed of 0.5 m/sec and an acceleration of 0.5 m/sec^2 . Determine the following when slider B moves at $x = 0$ to $x = l_3$.

- 1) Velocities of the coupler and slider
- 2) Accelerations of the coupler and slider.

The following sample results are shown: -

- 1) Angular velocity of the coupler (fig.4.5.1)
- 2) Velocity of the slider A (fig.4.5.2)
- 3) Angular acceleration of the coupler (fig.4.5.3)
- 4) Acceleration of the slider A (fig.4.5.4).

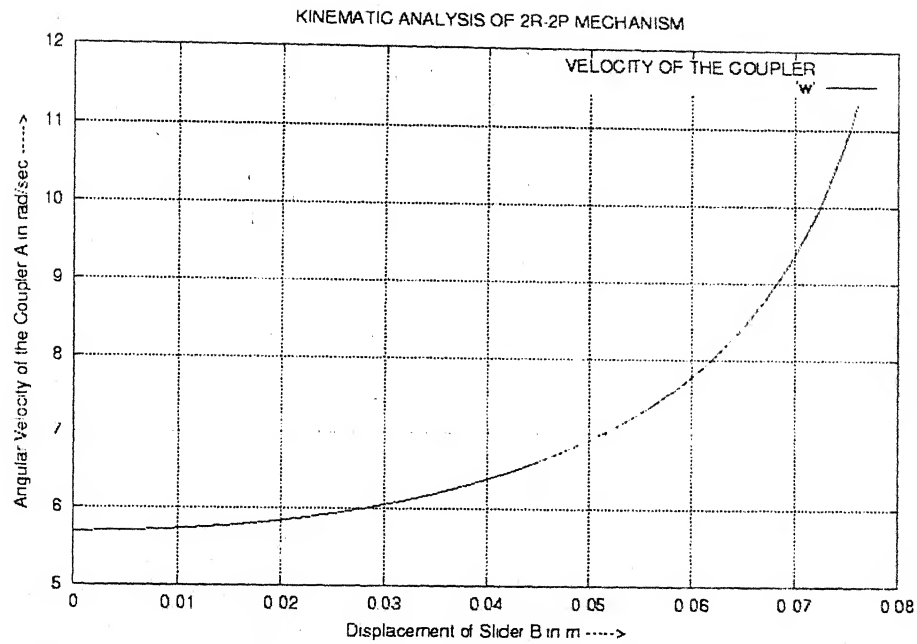


Figure 4.5.1 : Angular velocity of the coupler Vs Displacement of the Slider B.

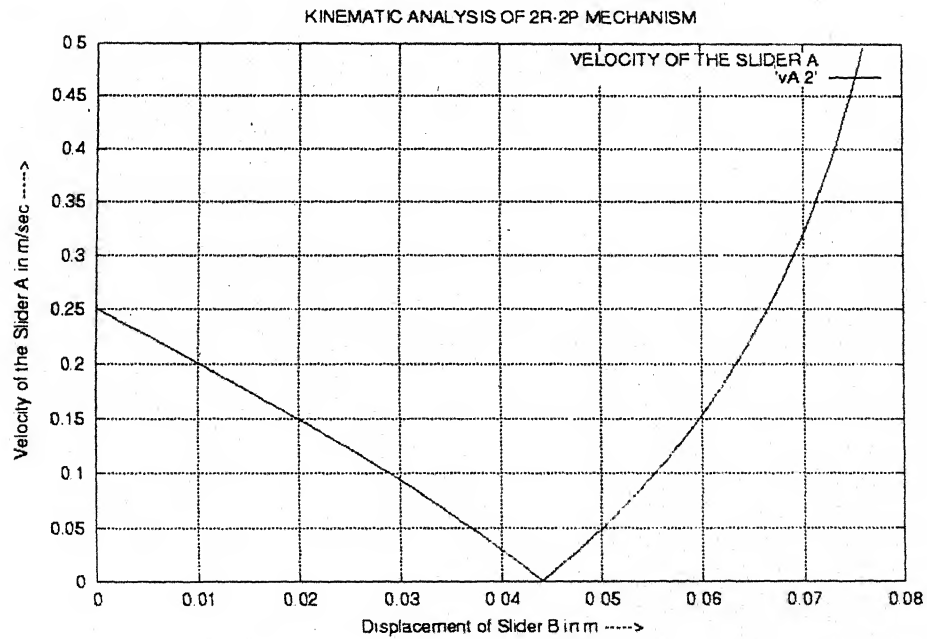


Figure 4.5.2 : Velocity of the slider A Vs Displacement of the Slider B.

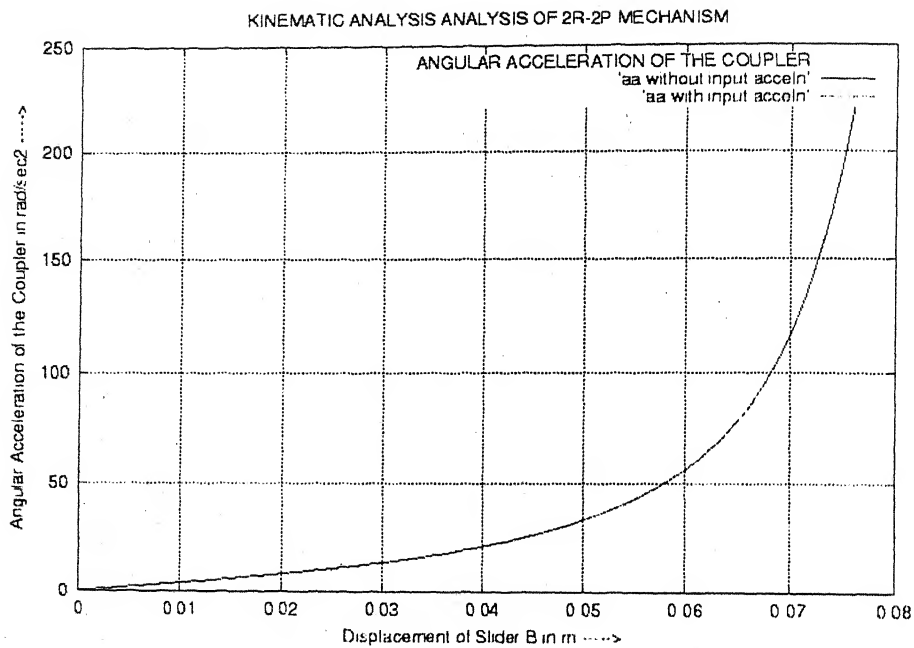


Figure 4.5.3 : Angular acceleration of the coupler Vs Displacement of the Slider B.

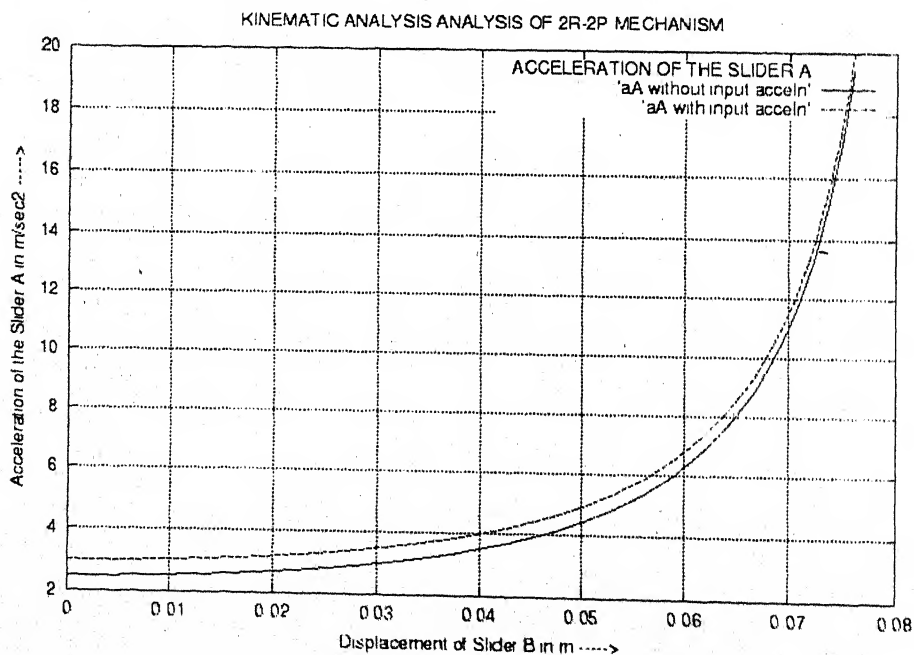


Figure 4.5.4 : Acceleration of the slider A Vs Displacement of the Slider B.

2. Scotch-Yoke mechanism

Example: -

A Scotch-Yoke mechanism having crank length, $l_2 = 76.2$ mm, offset distance, $l_1 = 10$ mm, $\alpha = 120^\circ$ and rotates at a speed of 100 rad/sec and an acceleration of 25 rad/sec^2 .

Determine the following when crank angle varies from 0° to 360° .

- 3) Displacements of the coupler and slider
- 4) Velocities of the coupler and slider
- 5) Accelerations of the coupler and slider.

The following sample results are shown: -

- 1) Displacement of the slider and yoke (fig.4.5.5)
- 2) Velocity of the slider and yoke (fig.4.5.6)
- 3) Acceleration of the slider and yoke (fig.4.5.7)

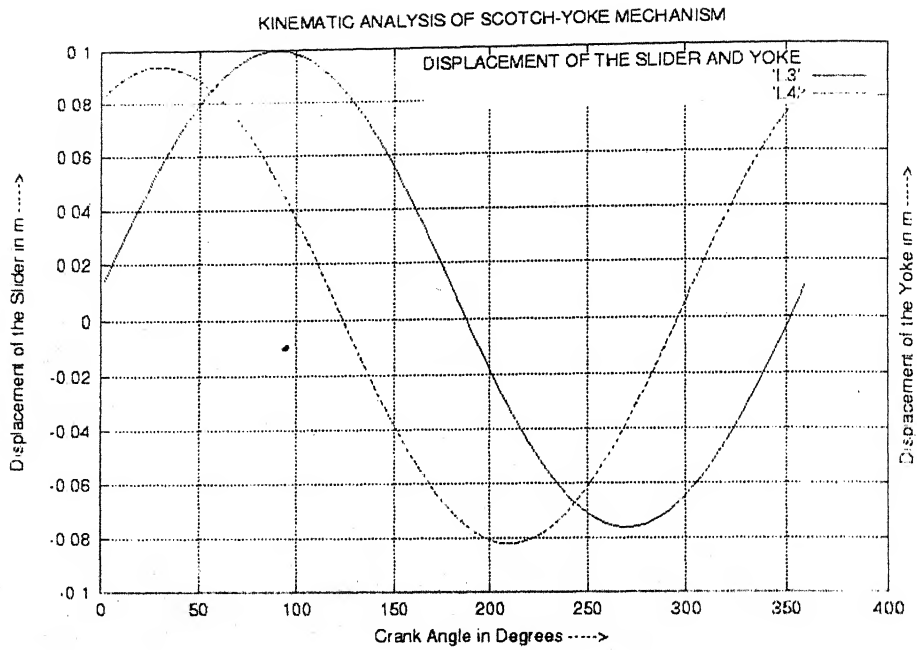


Figure 4.5.5 : Displacement of the Slider and Yoke Vs Crank Angle.

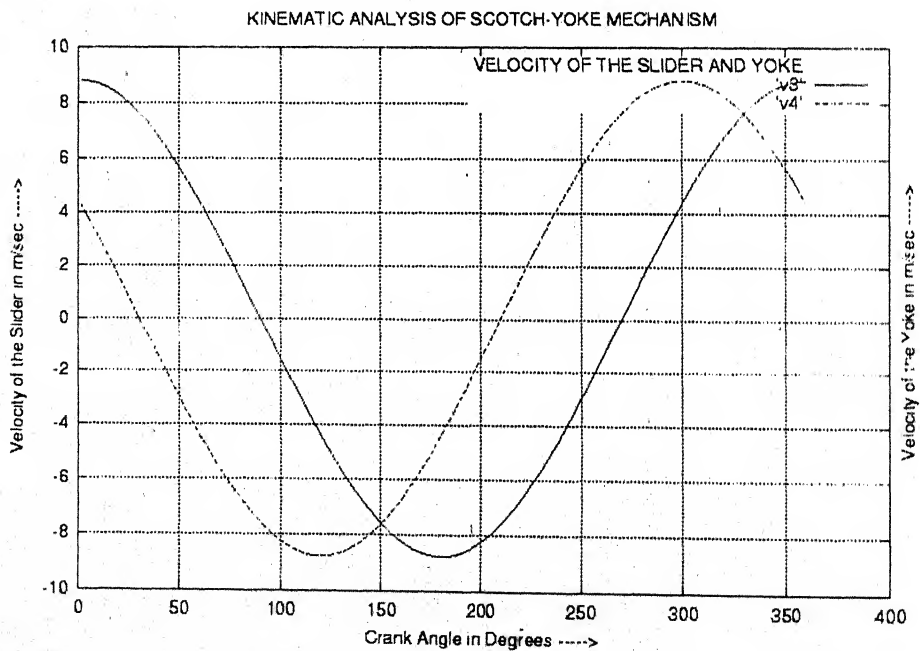


Figure 4.5.6 : Velocity of the Slider and Yoke Vs Crank Angle.

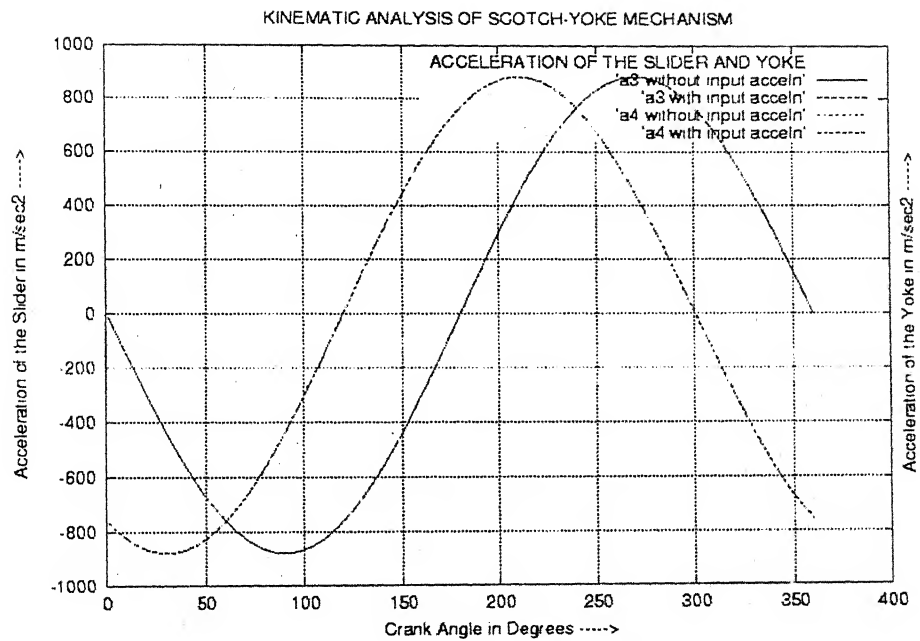


Figure 4.5.7 : Acceleration of the Slider and Yoke Vs Crank Angle.

b) Dynamic Force Analysis

1. 2R-2P mechanism

Example: -

A 2R-2P mechanism having coupler length, $l_3 = 76.2$ mm and slider B moves at a speed of 0.5 m/sec and an acceleration of 0.5 m/sec^2 . Coupler is having the following data: $g_3 = 25.4$ mm, $\gamma_3 = 15^\circ$, $m_3 = 0.25$ kg, $k_3 = 23$ mm, $F_3 = 2$ N, $\beta_3 = 10^\circ$. Sliders are having the following data: $m_2 = m_4 = 0.125$ kg, $F_4 = 2$ N. $\theta_2 = 60^\circ$. Determine the following when slider B moves at $x = 0$ to $x = l_3$.

- 1) Reaction at the hinge A, P_A .
- 2) Reaction at the hinge B, P_B .

The following sample results are shown: -

- 1) Reaction at the hinge B (fig.4.5.8)
- 2) Reaction at the hinge A (fig.4.5.9)

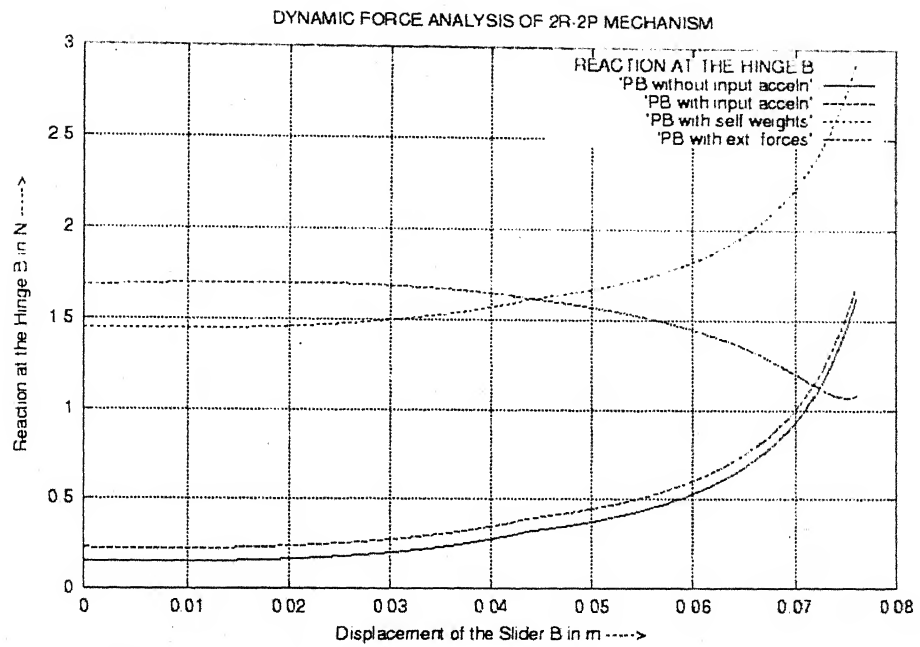


Figure 4.5.6 : Reaction at the hinge B Vs Displacement of the Slider B.

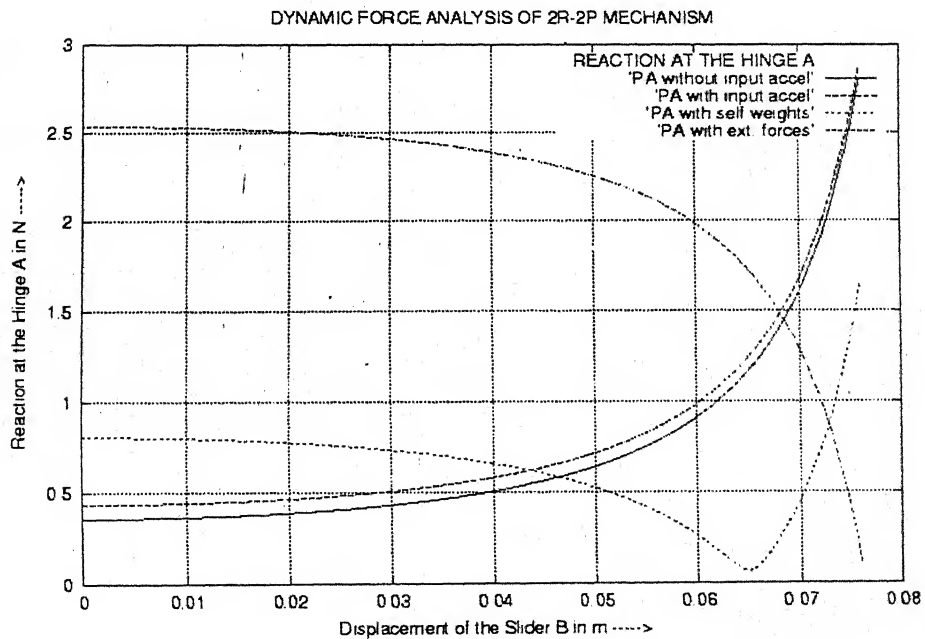


Figure 4.5.7 : Reaction at the hinge A Vs Displacement of the Slider B.

2. Scotch-Yoke mechanism

Example: -

A Scotch-Yoke mechanism having crank length, $l_2 = 76.2$ mm, offset distance, $l_1 = 10$ mm, $\alpha = 120^\circ$ and rotates at a speed of 100 rad/sec and an acceleration of 25 rad/sec^2 . Crank is having the following data: $g_2 = 25.4$ mm, $\gamma_2 = 15^\circ$, $m_2 = 0.125$ kg, $k_2 = 23$ mm, $F_2 = 2$ N, $\beta_2 = 10^\circ$. Slider is having the following data: $m_3 = 0.25$ kg, $F_3 = 2$ N. Yoke is having the following data: $m_4 = 0.125$ kg, $F_4 = 5$ N. Determine the following when crank angle varies from 0° to 360° .

- 1) Required turning moment at the crank, M_2 .
- 2) Reaction at the hinge O_2 , P_{O_2} .
- 3) Reaction at the hinge A, P_A .

The following sample results are shown: -

- 1) Required turning moment at the crank (fig.4.5.10)
- 1) Reaction at the hinge O_2 (fig.4.5.11)
- 2) Reaction at the hinge A (fig.4.5.12)

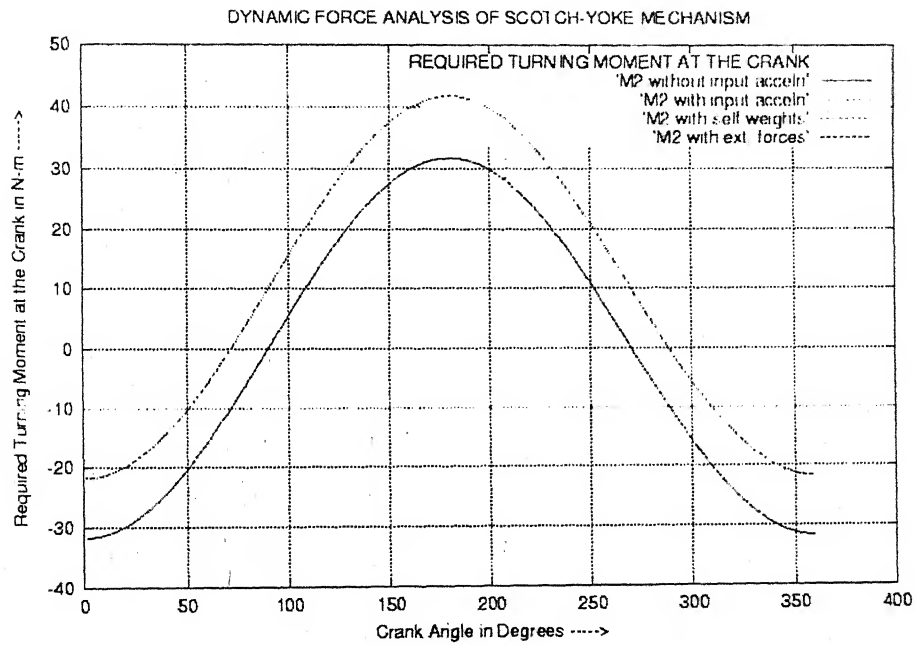


Figure 4.5.8 : Required Turning Moment at the Crank Vs Crank Angle.

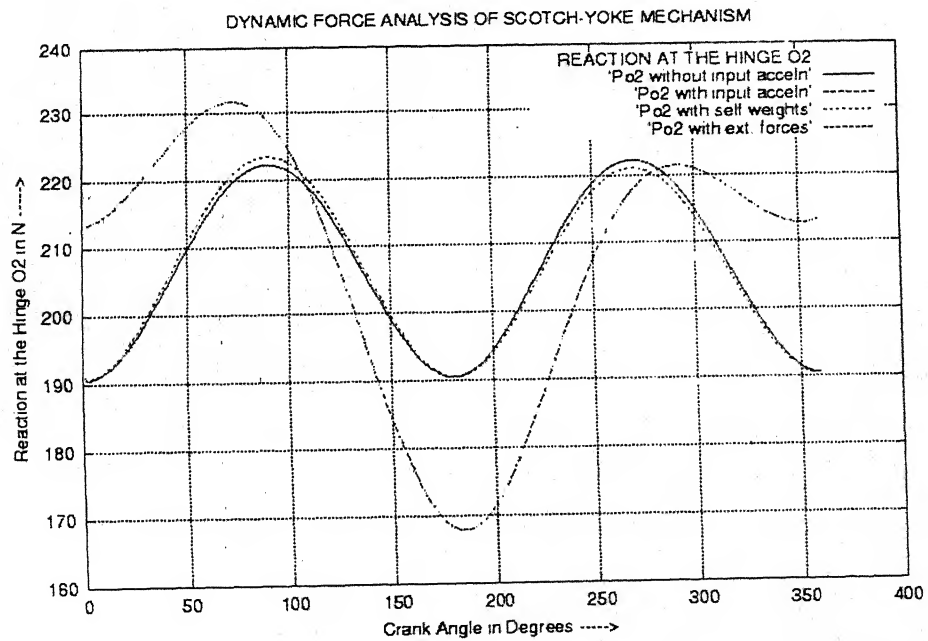


Figure 4.5.9 : Reaction at the hinge O₂ Vs Crank Angle.

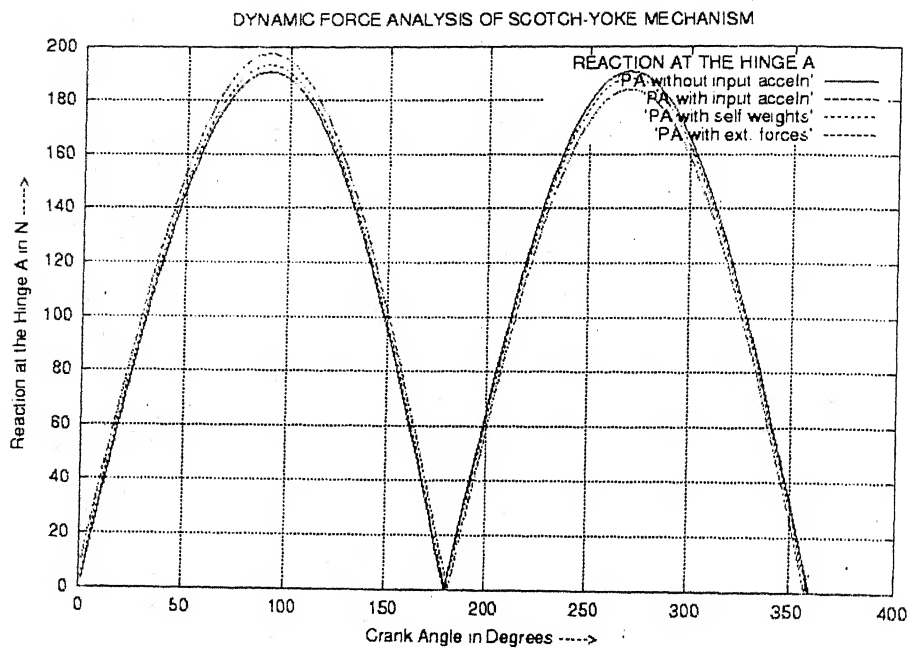


Figure 4.5.10 : Reaction at the hinge A Vs Crank Angle.

c) Dynamic motion analysis without friction

Example: -

A 2R-2P mechanism having coupler length, $l_3 = 398.7$ mm and slider B moves at a speed of 1 m/sec and Coupler is having the following data: $g_3 = 199.38$ mm, $\gamma_3 = 0^\circ$, $m_3 = 20$ kg, $J_{G_3} = 0.265 \text{ kg} \cdot \text{m}^2$, Sliders are having the following data: $m_2 = m_4 = 10$ kg, and $\theta_2 = 90^\circ$, force is applied at the slider B having magnitude of 294 N in the direction of velocity.

Determine the following when slider B moves at $x = 0$ to $x = l_3$.

- 1) Acceleration of the slider B.
- 2) Acceleration of the coupler.
- 3) Acceleration of the slider A.

The following sample results are shown: -

- 1) Acceleration of the slider B (fig. 4.5.13)
- 2) Acceleration of the coupler (fig. 4.5.14)
- 3) Acceleration of the slider A (fig. 4.5.15).

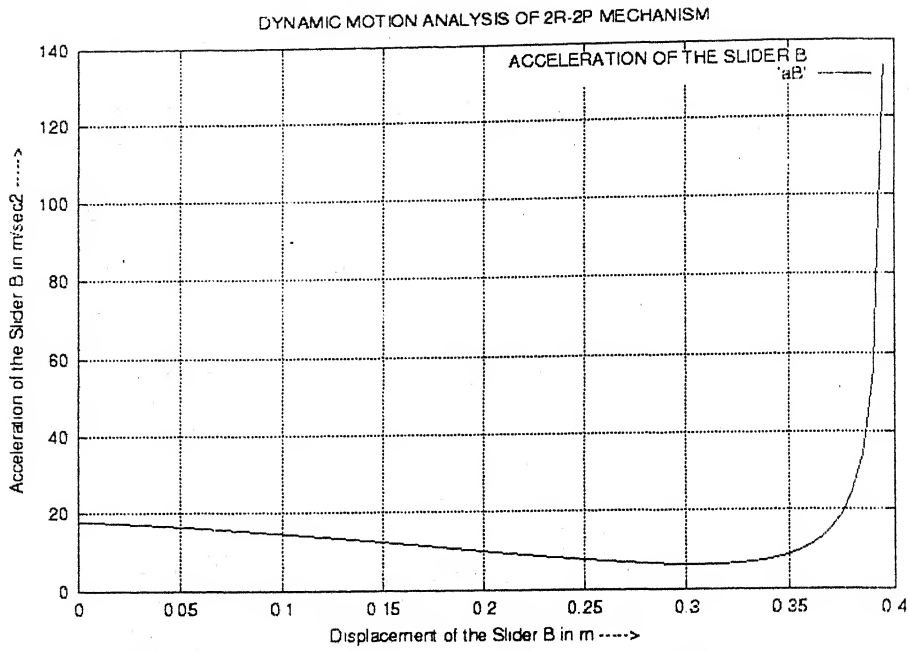


Figure 4.5.13 : Acceleration of the Slider B Vs Displacement of the Slider B.

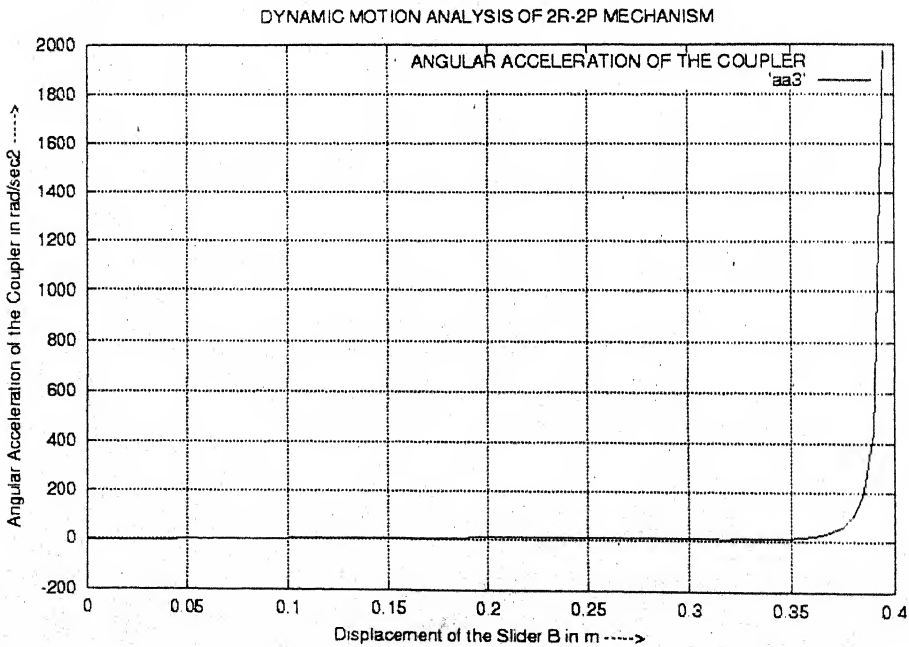


Figure 4.5.14 : Acceleration of the Coupler Vs Displacement of the Slider B.

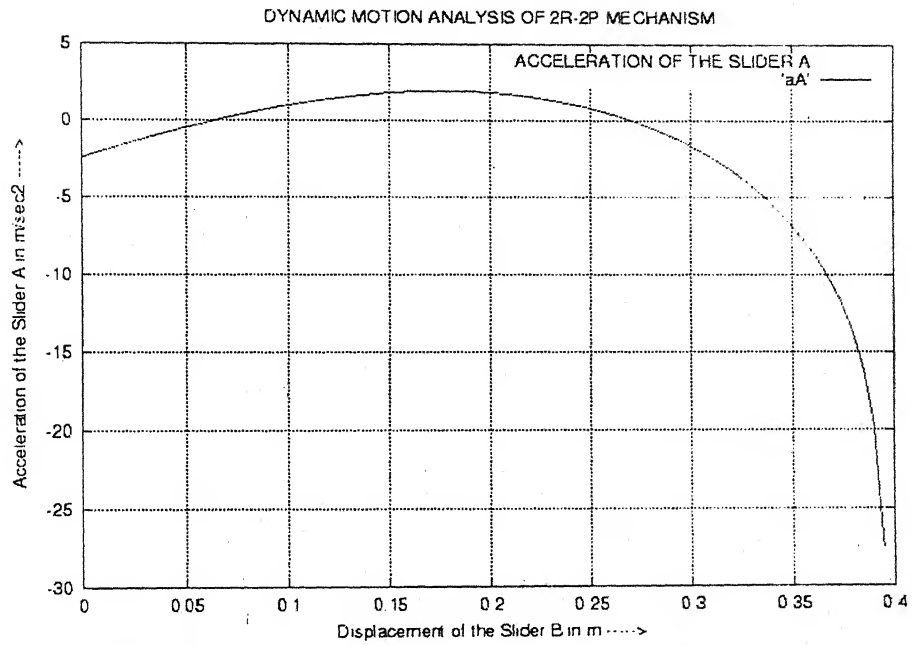


Figure 4.5.15 : Acceleration of the slider A Vs Displacement of the Slider B.

l) Dynamic motion analysis with friction

sample: -

A 2R-2P mechanism having coupler length, $l_3 = 398.7$ mm and slider B moves at speed of 1 m/sec and Coupler is having the following data: $g_3 = 199.38$ mm, $\gamma_3 = 0^\circ$, $m_3 = 0$ kg, $J_{G_3} = 0.265 \text{ kg-m}^2$. Sliders are having the following data: $m_2 = m_4 = 10$ kg, and $\theta_2 = 90^\circ$, $\mu_A = 0.3$, $\mu_B = 0.3$, force is applied at the slider B having magnitude of 294 N in the direction of velocity.

Determine the following when slider B moves at $x = 0$ to $x = 0.3$ m,

- 1) Acceleration of the slider B.
- 2) Acceleration of the coupler.
- 3) Acceleration of the slider A.

The following sample results are shown: -

- 1) Acceleration of the slider B (fig.4.5.16)
- 2) Acceleration of the coupler (fig. 4.5.17)
- 3) Acceleration of the slider A (fig. 4.5.18).

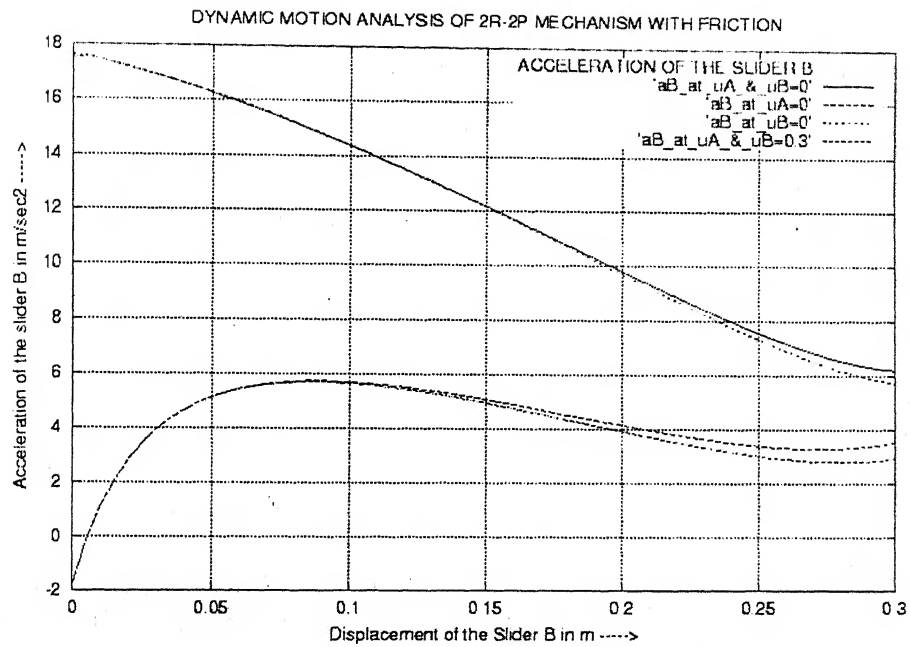


Figure 4.5.16 : Acceleration of the Slider B Vs Displacement of the Slider B.

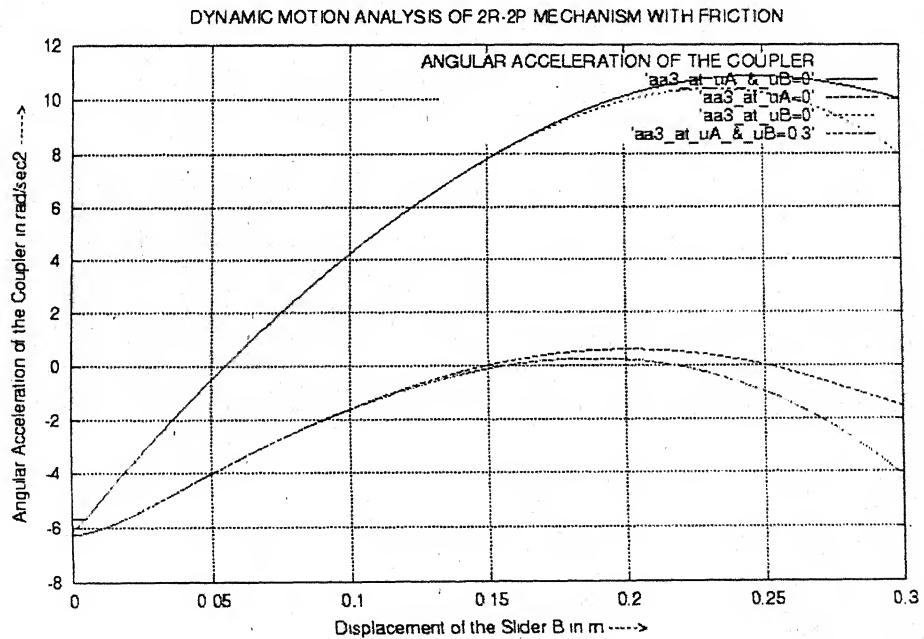


Figure 4.5.17 : Acceleration of the Coupler Vs Displacement of the Slider B.

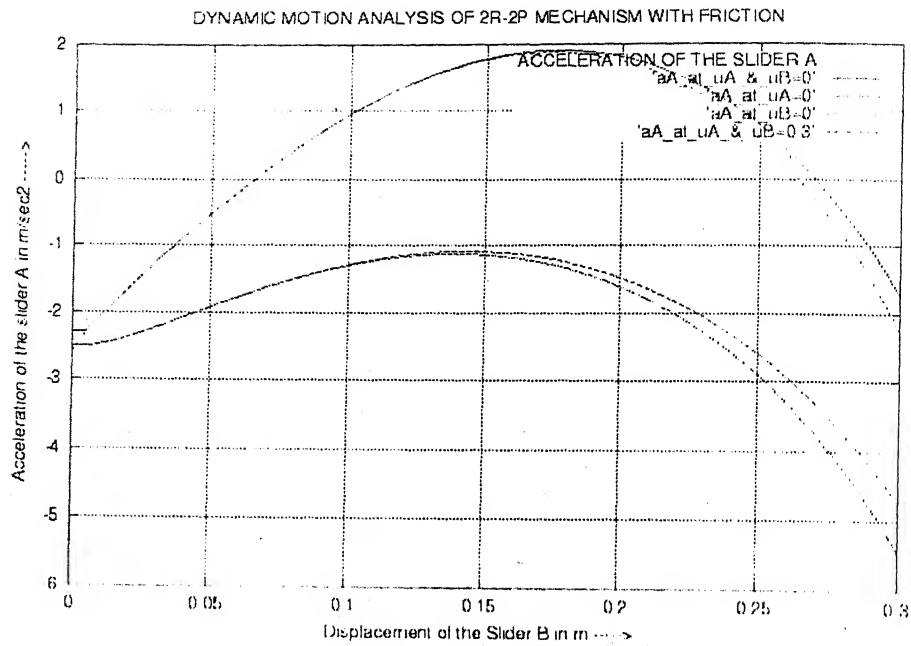


Figure 4.5.18 : Acceleration of the slider A Vs Displacement of the Slider B.

Chapter 5

Conclusion and Suggestions for Future Work

5.1 Conclusion

In the present work, a software package for the kinematic analysis, dynamic force analysis, dynamic motion analysis without and with friction of four-link mechanisms and balancing of 4R mechanism, has been developed.

With prescribed kinematic dimensions, from this package we can evaluate the displacements, velocities and accelerations of various members of the mechanism for a given input motion. The hinge reactions and the driving torque or force can also be evaluated for given external forces on the mechanism. In dynamic motion analysis, we can evaluate the accelerations of various members of a mechanism for a given input motion without and with friction. In case of balancing of 4R mechanism, we can evaluate the counterweights and its positions for force balance and moment of inertia of the counterweights for the shaking moment balance and also the required turning moment at the crank after force and shaking moment balancing have been achieved. This package supplements an earlier package developed for kinematic synthesis.

5.2 Suggestions for Future Work

The following directions may be taken up to extend the work carried out in the present thesis:

This work can be extended to include flexible links and / or connections, spatial four-link mechanisms and robot manipulators.

This package should be ported to windows environment, so as to have all the facilities and tools of a commercially available software package.

Bibliography

- [1] Dukkupati R. V., and Rao J. S., "Mechanism and Machine Theory", WEL Press, 1989.
- [2] Erdman A. G., "Computer Aided Design of Mechanisms: 1984 and beyond", Mechanism and Machine Theory, Vol. 20, 1985, pp. 225-49.
- [3] Rattan S. S., "Theory of Machines", Tata McGraw-Hill, 1994.
- [4] Green W. G., "Theory of machines", Blackie and Son, 1963.
- [5] Ghosh A., and Mallik A. K., "Theory of Mechanisms and machines", AEW Press, 1998.
- [6] Erdman A.G., and Sandor G.N., "Mechanism Design", Vol. I and II, Prentice Hall, 1984.
- [7] Hirschhorn J., "Kinematics and Dynamics of plane mechanism", McGraw-Hill, 1962.
- [8] Berkof R. S., "Complete Force and Moment Balancing of Inline Four-Bar Linkages", Mechanism and Machine Theory, Vol. 8, 1973, pp. 397-410.
- [9] Wiederrich J. L., and Roth B., "Momentum Balancing of Four-Bar Linkages", Journal of Engineering for Industry, 1976, pp.1289-95.
- [10] Berkof R. S., "The Input Torque in Linkages", Mechanism and Machine Theory, Vol. 14, 1979, pp. 61-73.
- [11] Shigley J.E., and Uicker J. J., "Theory of machines and Mechanisms", McGraw-Hill, 1980.
- [12] Williams R. J., and Rupperecht S., "Dynamic Force Analysis of Planer Mechanisms", Mechanism and Machine Theory, Vol. 16, 1981, pp. 425-40.

- [13] Paul B., "Analytical Dynamics of Mechanisms-A Computer Oriented Overview", Mechanism and Machine Theory, Vol. 10, 1975, pp. 481-507.
- [14] Miguel A. S., Rafael A., and Javier G. J., "Dynamic Analysis of plane mechanisms with lower pairs in basic coordinates", Mechanism and Machine Theory, Vol. 17, 1982, pp. 397-403.
- [15] Haug E. J., "Computer Aided Kinematics and Dynamics of mechanical systems", AAB Series, 1989.
- [16] Berkof R. S., Lowen G. G., and Tepper F. R., "Balancing of Linkages-An Update", Mechanism and Machine Theory, Vol. 18, 1983, pp. 213-20.
- [17] Kochev I. S., and Gourav G., "General criteria for optimum balancing of combined shaking force and shaking moment in planer linkages", Mechanism and Machine Theory, Vol. 23, 1988, pp. 481-89.
- [18] Niu Ming Qi, and Pennestri E., "Optimum Balancing of Four-Bar Linkages", Mechanism and Machine Theory, Vol. 26, 1991, pp. 337-48.
- [19] Arakelian V. H., and Smith M. R., "Complete Shaking Force and Shaking Moment Balancing of Linkages", Mechanism and Machine Theory, Vol. 34, 1999, pp. 1141-53.